A Finite-Rate Surface Reaction Model for the Data-Parallel Line Relaxation (DPLR) Computational Fluid Dynamics Code

Jochen Marschall
SRI International
jochen.marschall@sri.com

Matthew MacLean
CUBRC, Inc.
maclean@cubrc.org

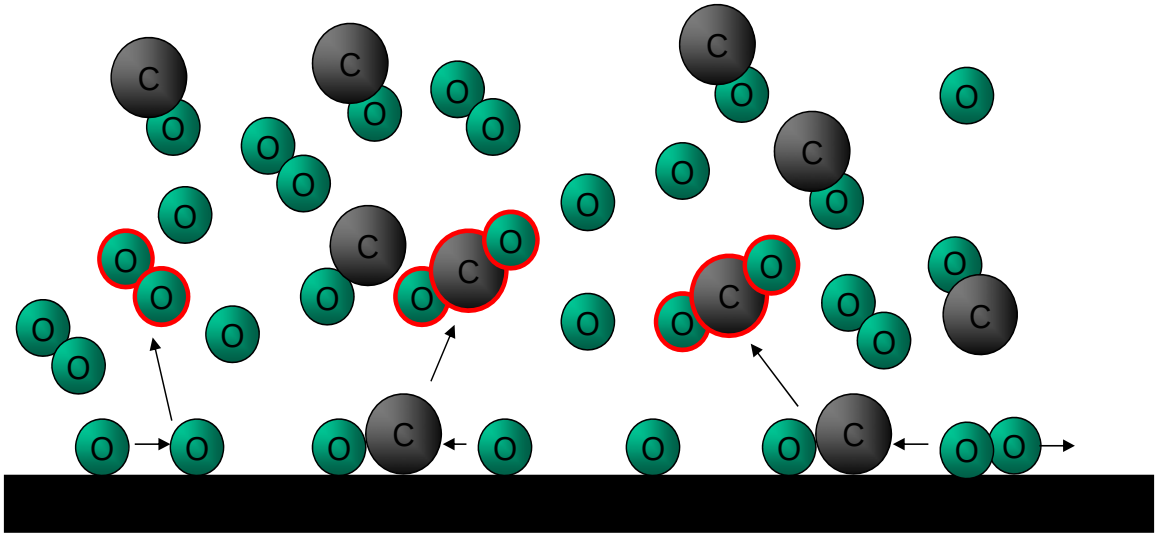

June 30, 2011

Table of Contents

Table of Figures

Executive Summary

This manual summarizes the formulation of a general finite-rate surface reaction framework and its implementation into the NASA data-parallel line relaxation (DPLR) computational fluid dynamics (CFD) code. The DPLR CFD code is one of the main simulation tools currently used by NASA to investigate hypersonic flows around flight vehicles and test components.

DPLR currently implements several simple surface catalysis models. The non-catalytic wall enforces a boundary condition in which gradients of species densities are set to zero. This boundary condition results in the minimum level of heating that could be delivered to the vehicle surface, and as such is not practical for realistic thermal protection system (TPS) design. The constant γ catalysis is a better option for design calculations, and DPLR allows for either a user-specified γ at runtime or material-specific values for certain recombination reactions. These values can be functions of the wall temperature and typically come from curve-fitting experimental data from arc-jets or elsewhere for specific materials. The so-called "super-catalytic" boundary condition sets the surface mass fractions to the state that results in maximum energy reclamation and therefore maximizes the heat delivered to the vehicle TPS. This is done without regard to kinetics or species availability. The super-catalytic boundary is often employed for mission design since it guarantees a conservative prediction, but it will result in an overly conservative TPS that limits scientific payload, constrains trajectory and landing options, and otherwise increases the stress placed on the design of other systems on the vehicle. Some complex reaction systems for air and CO_2 environments have been incorporated into the code, but they are essentially hard-wired on a case by case basis. It difficult for developers to build new models as new needs arise.

Therefore, a general finite-rate surface-chemistry framework has been developed and incorporated into the DPLR CFD code to enhance DPLR's surface-reaction modeling capability. This model enables DPLR users to implement problem-specific surface reaction mechanisms as species boundary conditions in gas environments, without the need for hard-wired code modifications.

The basic modeling approach is to represent surface chemistry by competing finite-rate kinetic processes operating at sets of active sites on the surface. Both catalytic and surface-altering (e.g., oxidation, nitridation, sublimation) reactions can be modeled within this framework. Forward reaction-rate coefficients can be specified by Arrhenius functions or by kinetics-based expressions for specific processes like adsorption, sublimation, Eley-Rideal recombination, and Langmuir-Hinshelwood recombination. Backward rate coefficients are computed from available thermodynamic data for gas and bulk species, together with transition-state approximations for thermal desorption and adsorption/desorption equilibrium constants. A rudimentary form of blowing is included for pyrolysis, in-depth ablation, or transpiration simulation.

This manual is divided into 7 Chapters.

Chapter 1 gives a detailed overview of the model formulation, defines basic quantities and conventions, and gives expressions for the various forward rate coefficients, equilibrium constants, and production rates in the model.

Chapter 2 describes how the model formulation is implemented in a stand-alone code that allows the user to develop and test specific surface reaction models prior to implementing them into a full DPLR CFD computation.

Chapter 3 discusses the implementation of the model formulation into DPLR. The general mass and energy balance control volumes for ablating surfaces are described and the tightly-coupled implicit surface boundary condition for DPLR is derived.

Chapter 4 gives the analytic derivatives of various model quantities that are needed for the construction of the Jacobian for implicit solutions of the surface reaction model within the stand-alone code and DPLR.

Chapter 5 details the format of various input files required to run a specific surface reaction model using the stand-alone code and DPLR.

Chapter 6 presents some examples of surface reaction computations with the stand-alone code.

Chapter 7 presents some examples of surface reaction computations with DPLR.

Acknowledgements

We acknowledge useful advice and helpful feedback from numerous colleagues, including Michael Barnhardt, Michael Wright, Ioana Cozmuta, and David Driver of NASA Ames Research Center, and Tom Schwartzentuber, Cory Sorensen, and Paolo Valentini of the University of Minnesota.

This work was supported by NASA Ames Research Center through grant NNX08AR52G and by NASA's Fundamental Aeronautics Hypersonics Project through grant NNX09AK38A.

Nomenclature

A_v	Avogadro number, 6.0221×10^{23} mol^{-1}
a_k	activity of species k
C_k	concentration of gas species k, mol m^{-3}
C_y	char yield (ratio of char density over virgin ablator density)
D_k	diffusion coefficient of gas species k, m^2 s^{-1}
E_a	Arrhenius equation energy barrier, J mol^{-1}
E_{ad}	energy barrier for adsorption, J mol^{-1}
E_{des}	energy barrier for desorption, J mol^{-1}
E_{er}	energy barrier for Eley-Rideal recombination, J mol^{-1}
E_{lh}	energy barrier for Langmuir-Hinshelwood recombination, J mol^{-1}
E_m	energy barrier for surface diffusion, J mol^{-1}
E_{sub}	energy barrier for sublimation, J mol^{-1}
$G_k^o(T)$	Gibb's energy, J mol^{-1}
$H_k^o(T)$	enthalpy, J mol^{-1}
h	Planck constant, 6.6261×10^{-34} J s
I	total number of surface reactions
i	surface reaction index ($i = 1\cdots I$)
K	total number of species
K_b	total number of bulk species
K_g	total numbers of gas species
K_s	total number of surface species
K_{ns}	number of species on surface phase ns
$K_{ns,na}$	number of species in active site set na on surface phase ns
K_{nb}	number of species in bulk phase nb

K_a	activity-based equilibrium constant
K_c	concentration-based equilibrium constant, units vary
k	species index ($k = 1 \cdots K$)
k_{bi}	backward reaction rate for reaction i, units vary
k_{fi}	forward reaction rate for reaction i, units vary
N	total number of phases
N_b	number of bulk phases
N_g	number of gas phases (always 1)
N_s	number of surface phases
$N_{ns,a}$	number of active site sets in surface phase ns
N_a	number of active site sets
N_{blw}	number of blowing gas mixtures
na	active site set index $\left(na = 1 \cdots N_{ns,a}\right)$
nb	bulk phase index $\left(nb = 1 \cdots N_b\right)$
$nblw$	blowing gas mixture index $\left(nblw = 1 \cdots N_{blw}\right)$
ns	surface phase index $\left(ns = 1 \cdots N_s\right)$
P	pressure, Pa
P_k	partial pressure of gas species k , Pa
R	universal gas constant, 8.3145 J mol^{-1} K^{-1}
$r_{i,ns}$	reaction flux of reaction i on surface phase ns , mol m^{-2} s^{-1}
$S_k^o(T)$	entropy, J mole^{-1} K^{-1}
S, S_0	sticking coefficients
T	temperature, K
t	time, s
$\bar{v}_k$	thermal speed $\left(\sqrt{8RT/\pi M_k}\right)$ of species k , m s^{-1}
ν'_{ki}	reactant stoichiometric coefficient for species k in reaction i

ν''_{ki}	product stoichiometric coefficient for species k in reaction i
ν_{ki}	net stoichiometric coefficient for species k in reaction i, $\left(\nu''_{ki} - \nu'_{ki}\right)$
ν_s	site exponent
ν_w	gas velocity at the wall, m s^{-1}
$\dot{w}_{ki}$	production rate of species k in reaction i, moles m^{-2} s^{-1}
$\dot{w}_k$	production rate of species k in all reactions, moles m^{-2} s^{-1}
X_k	generalized concentration of species k , moles m^{-3} in the gas phase, moles m^{-2} on a surface phase dimensionless in a bulk phase
y_k	mass fraction of species k
δ	control volume thickness, m
Γ_k	impingement flux of gas species k $\left[C_k \bar{v}_k / 4\right]$, m^{-2} s^{-1}
γ_{er}, γ_0	Eley-Rideal reaction efficiency
Δ_{ns}	average distance between active sites on surface phase ns , m
$\theta_{ns,k}$	fraction of active sites occupied by species k on surface phase ns
ν	attempt frequency s^{-1}
ρ_b	mass density of bulk environment kg m^{-3}
ρ_{nb}	mass density of bulk phase nb kg m^{-3}
ρ_w	gas mass density at the wall kg m^{-3}
Φ_{total}	total active site density on the surface moles m^{-2}
Φ_{ns}	active site density on surface phase ns moles m^{-2}
$\Phi_{ns,k}$	concentration of species k on surface phase ns moles m^{-2}
ϕ_b	porosity of bulk environment
ϕ_{nb}	porosity of bulk phase nb
χ_k	mole fraction of species k

$\chi_{nb,k}$	mole fraction of bulk species k in bulk phase nb
$\chi_{nblw,k}$	mole fraction of gas species k in blowing gas mixture $nblw$
Ω_{ns}	surface fraction occupied by phase ns

Chapter 1: Finite-Rate Model Formulation

1.1 The System

The model system consists of three environments: the gas environment, the surface environment, and the bulk environment. Each environment is comprised of one or more "phases" that are meant to represent physically distinct regions of each environment.

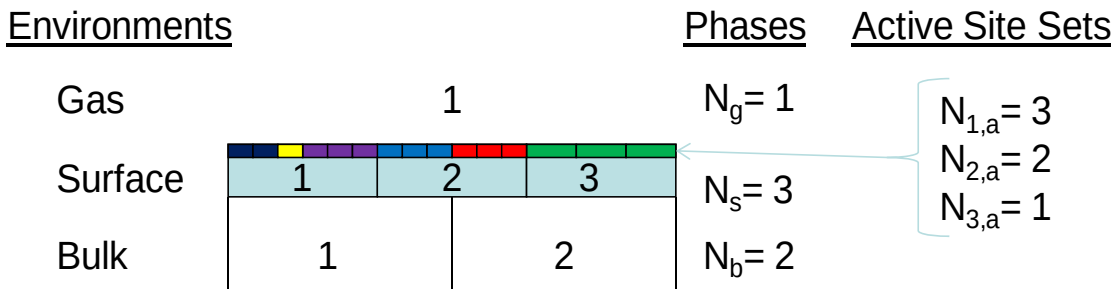

Figure 1.1.1 Surface Reaction Model System Consisting of Environments, Phases and Sets of Active Sites.

By definition, the gas environment is a single phase ($N_g = 1$) containing $k = 1 \ldots K_g$ chemically distinct gas-phase species. All gas-phase species must be either reactants or products involved in surface reactions or species blown into the gas phase by gas injection, transpiration, or in-depth pyrolysis.

The surface environment can have multiple phases ($ns = 1 \ldots N_s$), each occupying a fraction Ω_{ns} of the total surface. Each surface phase can contain multiple sets of active sites ($na = 1 \ldots N_{ns.a}$) where surface reactions can take place.

Each set of active sites has a site density $\Phi_{ns,na}$ (moles m^{-2}) and an associated set of chemically-distinct surface species $k = 1 \ldots K_{ns,na}$. Thus, each surface species is uniquely associated with a single set of active sites and each set of active sites is uniquely associated with a single surface phase.

One surface species in each active site set is defined as an empty site, while all other species in that active site set represent an adsorbed atom or molecule. The concentration of surface species k associated with the active site set na on phase ns in designated by $\Phi_{ns,na,k}$.

The bulk environment can also be made up of several phases ($nb = 1 \ldots N_b$), each occupying a volume fraction v_{nb} of bulk. Each bulk phase contains a unique set of species $k = 1 \ldots K_{nb}$.

The total number of phases in our system is:

$$N = 1 + N_s + N_b \quad . \tag{1.1.1}$$

The total number of active site sets is:

$$N_a = \sum_{ns=1}^{N_s} N_{ns,a} \quad . \tag{1.1.2}$$

The total number of species in our system is:

$$K = K_g + \sum_{ns=1}^{N_s} \sum_{na=1}^{N_{ns,a}} K_{ns,na} + \sum_{nb=1}^{N_b} K_{nb} \quad . \tag{1.1.3}$$

Note that with this definition, a particular atom (say atomic oxygen) is considered a different species if it is in the gas phase or in a particular active site set in a particular surface phase or in a particular bulk phase.

This formulation is similar to that of Surface Chemkin.[1-2]

1.2 Active Site and Phase Conventions

All surface reactions take place at active sites. The number of active sites is conserved (no active sites are created, destroyed or converted), and each surface species occupies only a single surface site at one time.

Individual surface reactions must take place within a single surface phase but can involve more than one set of active sites in that surface phase.

All active sites in a single surface phase are pictured as homogenously distributed over the surface of that phase and are treated as an ideal mixture of sites. The total site density on a given surface phase is, therefore:

$$\Phi_{ns} = \sum_{na=1}^{N_{ns,a}} \Phi_{ns,na} \quad . \tag{1.2.1}$$

Because multiple sets of active sites on a single surface phase are treated as an ideal mixture, the concentration of surface species k on surface phase ns is $\Phi_{ns,k} = \Phi_{ns,na,k}$.

Multiple surface phases are treated as segregated areas on the surface. Therefore, the effective (or average) active site density over the entire surface is:

$$\Phi_a = \sum_{ns=1}^{N_s} \Omega_{ns} \Phi_{ns} \quad . \tag{1.2.2}$$

The fraction of active sites in phase ns belonging to active site set na is:

$$\theta_{ns,na} = \frac{\Phi_{ns,na}}{\Phi_{ns}} \quad . \tag{1.2.3}$$

The fraction of active sites in phase n_s that are occupied by species k is:

$$\theta_{ns,k} = \frac{\Phi_{ns,k}}{\Phi_{ns}} = \frac{\Phi_{ns,na,k}}{\Phi_{ns}} \quad . \tag{1.2.4}$$

Figure 1.2.1 shows a conceptual example of a surface reaction model with two surface phases, three sets of active sites, and four adsorbed surface species.

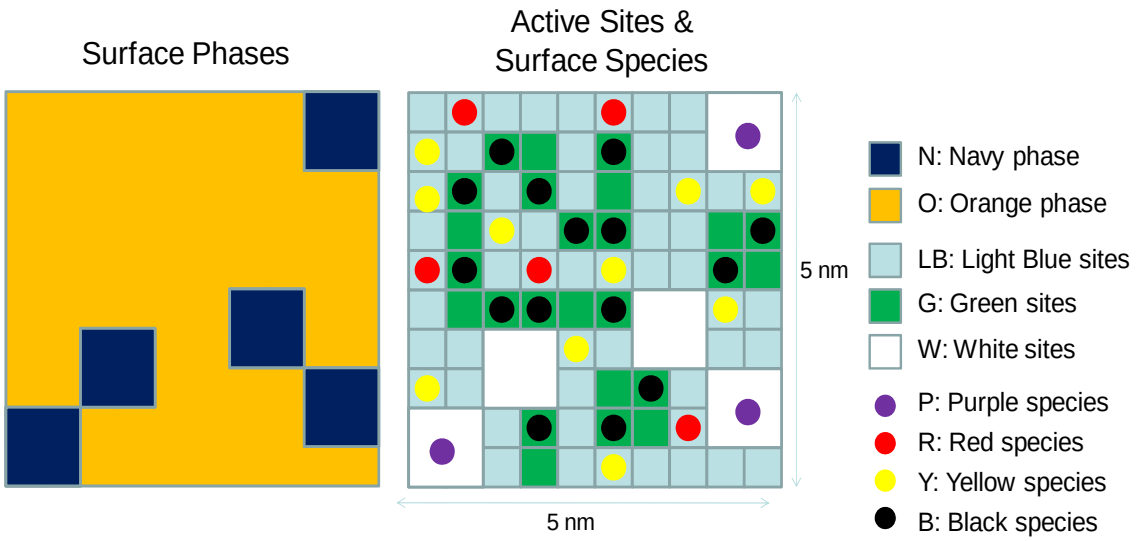

Figure 1.2.1 Example with Two Phases (Orange and Navy), Three Active Site Sets (Light Blue, Green, and White), and Four Adsorbed Species (Red, Yellow, Black, and Purple).

Phases:

$N_s = 2 \qquad \Omega_N = 5/25 = 0.2 \qquad \Omega_O = 20/25 = 0.8$

Active sites:

$N_{N,A} = 1 \qquad \Phi_{N,W} = 5/5 = 1\ \text{nm}^{-2}$

$N_{O,A} = 2 \qquad \Phi_{O,LB} = 55/20 = 2.75\ \text{nm}^{-2} \qquad \Phi_{O,G} = 25/20 = 1.25\ \text{nm}^{-2}$

$\Phi_N = \Phi_{N,W} = 1\ \text{nm}^{-2} \qquad \Phi_O = \Phi_{O,LB} + \Phi_{O,G} = 2.75 + 1.25 = 4\ \text{nm}^{-2}$

$\Phi_a = 0.2(1) + 0.8(4) = 3.4\ \text{nm}^{-2}$

Surface species:

$K_{N,W} = 2 \qquad K_{O,LB} = 3 \qquad K_{O,G} = 2$

$\Phi_{N,W,empty} = 2/5\ \text{nm}^{-2} \qquad \Phi_{N,W,P} = 3/5\ \text{nm}^{-2}$

$\Phi_{O,G,empty} = 10/20\ \text{nm}^{-2} \qquad \Phi_{O,G,B} = 15/20\ \text{nm}^{-2}$

$\Phi_{O,LB,empty} = 40/20\ \text{nm}^{-2} \qquad \Phi_{O,LB,R} = 5/20\ \text{nm}^{-2} \qquad \Phi_{O,LB,Y} = 10/20\ \text{nm}^{-2}$

Fractional species coverage in surface phases:

$\theta_{N,W,empty} = (2/5)/1 = 2/5 \qquad \theta_{N,W,P} = (3/5)/1 = 3/5$

$\theta_{O,G,empty} = (10/20)/4 = 10/80 \qquad \theta_{O,G,B} = (15/20)/4 = 15/80$

$\theta_{O,LB,empty} = (40/20)/4 = 40/80 \qquad \theta_{O,LB,R} = (5/20)/4 = 5/80 \qquad \theta_{O,LB,Y} = (10/20)/4 = 10/80$

Fractional site coverage in surface phases:

$\theta_{N,W} = 1/1 = 1 \qquad \theta_{O,G} = (1.25/4) = 5/16 \qquad \theta_{O,LB} = (2.75/4) = 11/16$

The average distance between active sites in a surface phase is:

$$\Delta_{ns} = \frac{1}{\sqrt{A_v \Phi_{ns}}} \tag{1.2.5}$$

A portion of the surface that is inert or porous can be specified as a surface phase with no active sites ($N_{ns,a} = 0$). Such a phase will not participate directly in any surface chemistry but will influence the conversion of local production rates to global values, since the total area fraction occupied by the chemically active surface phases will be less than one.

Bulk phases are pictured as physically distinct volumes of the bulk environment with their individual chemical compositions, densities, and porosities. Multiple bulk phases can be used to model a composite material in a way consistent with known physical and chemical characteristics of the composite. Similar to inert areas on the surface, inert components in the bulk can be modeled as phases with no chemically active species ($K_{nb} = 0$).

The density and the porosity of the bulk environment are given by:

$$\rho_b = \sum_{nb=1}^{N_b} \nu_{nb} \rho_{nb} \tag{1.2.6}$$

$$\phi_b = \sum_{nb=1}^{N_b} \nu_{nb} \phi_{nb} \tag{1.2.7}$$

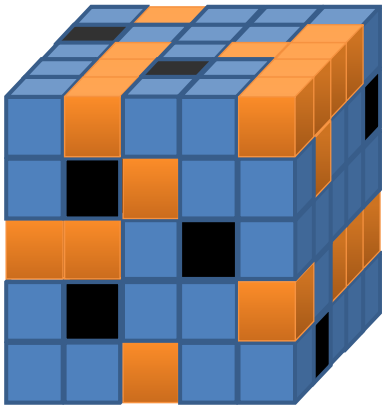

$$N_b = 3$$

$$\nu_{blue} = 0.72 \quad \rho_{blue} = 10000\,\text{kg/m}^3 \quad \phi_{blue} = 0$$
$$\nu_{orange} = 0.18 \quad \rho_{orange} = 3000\,\text{kg/m}^3 \quad \phi_{orange} = 0$$
$$\nu_{black} = 0.10 \quad \rho_{black} = 0\,\text{kg/m}^3 \quad \phi_{black} = 1$$

$$\rho_b = 0.72(10000) + 0.18(3000) + 0.10(0) = 7740\,\text{kg/m}^3$$
$$\phi_b = 0.72(0) + 0.18(0) + +0.10(1) = 0.10$$

Figure 1.2.2 Example of a Porous Composite: Three Bulk Phases (Blue, Orange, and Black) with the Blue and Orange Phases Representing Different Solid Constituents and the Black Phase Representing Pore Space.

1.3 Generalized Species Concentrations

Generalized species concentrations X_k are used to describe the amount of each species *k* in the different phases.

In the gas phase, the generalized species concentration (moles m^{-3}) is related to its partial pressure:

$$X_k \equiv C_k = \frac{P_k}{RT} = \chi_k \frac{P}{RT} \tag{1.3.1}$$

Each surface reaction takes place within a single surface phase. Therefore, the generalized concentration for a surface species is its surface concentration (moles m^{-2}) in the relevant surface phase:

$$X_k \equiv \Phi_{ns,k} = \theta_{ns,k}\Phi_{ns} \tag{1.3.2}$$

This is consistent with treating each surface phase as an independent physical/chemical entity and treating multiple sets of active sites in a given surface phase as an ideal mixture of active sites.

In a bulk phase, the generalized species concentration is dimensionless and equals the mole fraction:

$$X_k \equiv \chi_{nb,k} \tag{1.3.3}$$

This is consistent with treating each reacting bulk phase as an ideal mixture of species.

This formulation is similar to Surface Chemkin.[1-2]

1.4 Surface Reaction Formulation and Rate Expressions

Consider a system with *K* species and *I* surface reactions. The general form for reaction *i* can be written as:

$$\sum_{k=1}^{K} \nu'_{ki} A_k \leftrightarrow \sum_{k=1}^{K} \nu''_{ki} A_k \qquad (1.4.1)$$

where A_k is the chemical symbol, and ν'_k and ν''_k are the stoichiometric coefficients for species *k* on the reactant and product sides of the equation. Each reaction takes place on a specific surface phase and can involve one or more sets of active sites on that phase.

The following conventions are adopted for writing surface reaction equations:

- At least one surface species must appear on each side of every reaction.
- An adsorption reaction is required for every adsorbed species.
- No more than 3 different reactants and 3 different products per reaction.
- No more than one gas and one bulk species on each side of a reaction.
- Chemical elements must balance on both sides of a reaction.
- The number of like active sites must balance on both sides of a reaction.
- The number of surface species must balance on both sides of a reaction.
- The order of species on both sides of a reaction should be written as: gas species, mobile surface species, immobile surface species, and bulk species.
- No non-integer stoichiometric coefficients or arbitrary reaction orders.

Some examples of different surface reactions according to these conventions are given below:
Adsorption (thermal desorption)

$$O + [s] \leftrightarrow [O]_s$$
$$N + [s] \leftrightarrow [N]_s$$
$$CO + [s] \leftrightarrow [CO]_s$$

Eley-Rideal recombination (dissociative with partial-adsorption)

$$N + [N]_s \leftrightarrow N_2 + [s]$$
$$O + [O]_s \leftrightarrow O_2 + [s]$$
$$N + [O]_s \leftrightarrow NO + [s]$$
$$O + [N]_s \leftrightarrow NO + [s]$$
$$O + [CO]_s \leftrightarrow CO_2 + [s]$$
$$CO + [O]_s \leftrightarrow CO_2 + [s]$$

Langmuir-Hinshelwood recombination (dissociative adsorption)

$$2[N]_s \leftrightarrow N_2 + 2[s]$$
$$2[O]_s \leftrightarrow O_2 + 2[s]$$
$$[O]_s + [N]_s \leftrightarrow NO + 2[s]$$
$$[N]_s + [O]_s \leftrightarrow NO + 2[s]$$
$$[O]_s + [CO]_s \leftrightarrow CO_2 + 2[s]$$
$$[CO]_s + [O]_s \leftrightarrow CO_2 + 2[s]$$

Carbon sublimation (condensation)

$$[s] + [C]_b \leftrightarrow C + [s]$$
$$2[s] + 2[C]_b \leftrightarrow C_2 + 2[s]$$
$$3[s] + 3[C]_b \leftrightarrow C_3 + 3[s]$$

Various carbon oxidation (coking) mechanisms

$$O + [s] + [C]_b \leftrightarrow CO + [s]$$
$$[O]_s + [C]_b \leftrightarrow CO + [s]$$
$$O + [O]_s + [C]_b \leftrightarrow CO_2 + [s]$$
$$2[O]_s + [C]_b \leftrightarrow CO_2 + 2[s]$$
$$O_2 + [s] + [C]_b \leftrightarrow CO + [O]_s$$
$$O_2 + 2[s] + 2[C]_b \leftrightarrow 2CO + 2[s]$$
$$2[CO]_s \leftrightarrow CO_2 + 2[s] + [C_b]$$

The reaction flux, $r_{i,ns}$, for reaction *i* on phase ns is given by:

$$r_{i,ns} = k_{fi} \prod_{k=1}^{K} X_k^{v'_{ki}} - k_{bi} \prod_{k=1}^{K} X_k^{v''_{ki}} \quad . \tag{1.4.2}$$

where k_{fi} and k_{bi} are the forward and backward reaction rates for reaction *i* at a given temperature.

The reaction flux gives the number of reaction events in moles m^{-2} s^{-1}. A variety of chemical species production rates can be computed from the reaction flux.

The *reaction-specific local* production rate of species *k* via reaction *i* on surface phase ns is:

$$\dot{w}_{ki,ns} = v_{ki} r_{i,ns} \quad . \tag{1.4.3}$$

where $\nu_{ki} = \left(\nu''_{ki} - \nu'_{ki}\right)$.

The *net local* production rate of species *k* on surface phase n_s is the sum of production from all reactions operating in phase n_s:

$$\dot{w}_{k,ns} = \sum_{i}^{I} \dot{w}_{ki,ns} \quad . \tag{1.4.4}$$

The *reaction-specific global* production rate of species *k* via reaction *i* is:

$$\dot{w}_{ki} = \Omega_{ns} \dot{w}_{ki,ns} \quad . \tag{1.4.5}$$

The *net global* production rate of species *k* by all reactions is:

$$\dot{w}_{k} = \sum_{i}^{I} \dot{w}_{ki} \quad . \tag{1.4.6}$$

For a gas species, the net global production rate is the rate that surface reactions are adding (positive) or removing (negative) that species from the gas environment. It is these net global production rates that couple the surface environment to the gas environment through the diffusive and convective mass flux boundary conditions.

For a bulk species, the net global production rate is the rate that surface reactions are adding (positive) or removing (negative) that species from the bulk environment. In the absence of a materials response model, these rates do not change the compositions of the bulk phases. Mass removed from the bulk environment is added to the gas environment and vice versa. It is this net mass transfer between the bulk and gas environments that produces a non-zero convective mass-flux boundary condition.

For a surface species, the net global species production rate is the rate that surface reactions are augmenting or depleting the population of that species when averaged over the entire surface. This is a less useful quantity than the net local species production rate.

Since each surface species is uniquely associated with a particular set of active sites, the net local chemical production rate of a surface species is the rate that surface reactions are augmenting (positive) or depleting (negative) the population of that species on its surface phase:

$$\dot{w}_{k,ns} = \frac{\partial \Phi_{ns,na,k}}{\partial t} \quad . \tag{1.4.7}$$

Because multiple surface species are competing for the same active sites and because surface species may transfer between different sets of active sites, the surface species populations in a

given phase are highly coupled. For steady-state conditions species surface coverage is determined by the solution of the coupled equation set:

$$\dot{w}_{k,ns} = 0 \quad . \tag{1.4.8}$$

Both steady-state and transient surface populations are constrained by the requirement that the population of all species associated with a given active site set must sum to the total site density of that active site set:

$$\Phi_{ns,na} = \sum_{k=1}^{K_{ns,na}} \Phi_{ns,na,k} \quad . \tag{1.4.9}$$

1.5 Equilibrium Constants

The *activity-based* equilibrium constant for reaction *i* is defined:

$$K_{ai} = \prod_{k=1}^{K} (a_k)^{\nu_{ki}} \quad . \tag{1.5.1}$$

Activity of ideal gas-phase species is its partial pressure divided by a reference pressure:

$$a_k = \left(\frac{P_k}{P_{ref}} \right) = \chi_k \left(\frac{P}{P_{ref}} \right) \quad . \tag{1.5.2}$$

This is the same as the species mole fraction times the ratio of the total gas pressure to the reference pressure. This ratio will generally be different than 1. The reference pressure used by the CEA and DPLR codes is 1 bar (10^5 Pa).

Activity of a pure solid or liquid phase is taken as 1:

$$a_k = 1 \quad . \tag{1.5.3}$$

The activity of a species in an ideal solid or liquid solution in phase nb is taken as its concentration divided by a reference concentration:

$$a_k = \left(\frac{C_k}{C_{nb,ref}} \right) = \chi_k \left(\frac{C_{nb}}{C_{nb,ref}} \right) \quad . \tag{1.5.4}$$

If the total collection of potential sites available to a solute species in bulk phase nb remains fixed, $C_{nb} / C_{nb,ref} = 1$.

The activity of a species adsorbed to surface phase ns is taken as its surface concentration divided by a reference surface concentration:

$$a_k = \left(\frac{\Phi_k}{\Phi_{ns,ref}} \right) = \theta_{ns,k} \left(\frac{\Phi_{ns}}{\Phi_{ns,ref}} \right) \quad . \tag{1.5.5}$$

If the total number of potential active sites available for an adsorbant species on surface phase ns remains constant, $\Phi_{ns} / \Phi_{ns,ref} = 1$.

The *activity-based* equilibrium constant is related to changes in the Gibbs energy of formation at temperature *T* in going from reactants to products:

$$K_{ai} = \exp\left[\frac{-\Delta G_i^o(T)}{RT} \right] = \exp\left[\frac{-\sum_{k=1}^{K} \nu_{ki} G_k^o(T)}{RT} \right] \quad . \tag{1.5.6}$$

The *activity-based* equilibrium constant can be calculated directly if the necessary thermodynamic functions are available for each species in the reaction:

$$\frac{G_k^o(T)}{RT} = \frac{H_k^o(T)}{RT} - \frac{S_k^o(T)}{R} \quad . \tag{1.5.7}$$

Values are generally available for gases, pure liquids, and pure solids, but not for solutions or surface phases.

The *concentration-based* equilibrium constant is related to the *activity-based* equilibrium constant by the following general relationship:

$$K_{ci} = K_{ai} \left(\frac{P_{ref}}{RT} \right)^{\nu_{gi}} \prod_{ns=1}^{N_s} \left(\Phi_{ns,ref} \right)^{\nu_{si}} \quad , \tag{1.5.8}$$

where the net stoichiometric exponents ν_{gi} and ν_{si}, run separately over the gas species and the surface species in each phase involved in the reaction, respectively:

$$\nu_{gi} = \sum_{k=1}^{K_g} \left(\nu''_{ki} - \nu'_{ki} \right) \quad \text{and} \quad \nu_{si} = \sum_{k=1}^{K_s} \left(\nu''_{ki} - \nu'_{ki} \right) \; . \tag{1.5.9}$$

Because of the convention that the number of like active sites must balance on both sides of every surface reaction, $\nu_{si} = 0$ for all surface reactions, and the conversion of *activity-based* to *concentration-based* equilibrium constants is simplified to only the gas phase factor in Eq. 1.5.8, or:

$$K_{ci} = K_{ai}\left(\frac{P_{ref}}{RT}\right)^{\nu_{gi}} \quad . \tag{1.5.10}$$

The *concentration based* equilibrium constant for reaction *i* is related to the forward and backward reaction rate coefficients by the relationship:

$$K_{ci} = \frac{k_{fi}}{k_{bi}} \quad . \tag{1.5.11}$$

Calculation of the reaction flux $r_{i,ns}$ requires numerical values for two of three quantities, k_{fi}, k_{bi}, and K_{ci}.

The relationship between reaction-rate coefficients and equilibrium constants is illustrated for various characteristic surface reactions below:

Adsorption of species *A*:

$$A + [s] \leftrightarrow [A]_s \qquad K_a = \exp\left[\frac{-G^o_{[A]_s}(T) + G^o_{[s]}(T) + G^o_A(T)}{RT}\right]$$

$$r = r_f - r_b = k_f \Phi_{s,e} C_A - k_b \Phi_{s,A}$$

k_f in m^3 $mole^{-1}$ s^{-1} $\qquad$ k_b in s^{-1} $\qquad$ K_c in m^3 $mole^{-1}$

$$K_c = \frac{k_f}{k_b} = \frac{\Phi_{s,A}}{\Phi_{s,e} C_A} = \left[\frac{\left(\Phi_{s,A}/\Phi_s\right)}{\left(\Phi_{s,e}/\Phi_s\right)\left(C_A/C_{ref}\right)}\right]\left(\frac{\Phi_s}{\Phi_s C_{ref}}\right) = K_a\left(\frac{P_{ref}}{RT}\right)^{-1}$$

Check: $\nu_{gi} = 0 - 1 = -1$ and $\nu_{si} = (0-1) + (1-0) = 0$.

Condensation of species *A*:

$$A + [s] \leftrightarrow [s] + [A]_b \qquad K_a = \exp\left[\frac{G^o_A(T) - G^o_{[A]_b}(T)}{RT}\right]$$

$$r = r_f - r_b = k_f \Phi_{s,e} C_A - k_b \chi_{b,A} \Phi_{s,e}$$

k_f in m^3 $mole^{-1}$ s^{-1} k_b in s^{-1} K_c in m^3 $mole^{-1}$

$$K_c = \frac{k_f}{k_b} = \frac{\Phi_{s,e}\chi_{b,A}}{\Phi_{s,e}C_A} = \left[\frac{\chi_{b,A}}{\left(C_A/C_{ref}\right)}\right]\left(C_{ref}\right)^{-1} = K_a\left(\frac{P_{ref}}{RT}\right)^{-1}$$

Check: $\nu_{gi} = 0-1 = -1$ and $\nu_{si} = (1-1) = 0$.

Eley-Rideal recombination of species *A* and *B*:

$$A + [B]_s \leftrightarrow AB + [s] \qquad K_a = \exp\left[\frac{-G^o_{AB}(T) - G^o_{[s]}(T) + G^o_A(T) + G^o_{[B]_s}(T)}{RT}\right]$$

$$r = r_f - r_b = k_f \Phi_{s,B} C_A - k_b \Phi_{s,e} C_{AB}$$

k_f in m^3 $mole^{-1}$ s^{-1} k_b in m^3 $mole^{-1}$ s^{-1} K_c is dimensionless

$$K_c = \frac{k_f}{k_b} = \frac{\Phi_{s,e}C_{AB}}{\Phi_{s,B}C_A} = \left[\frac{\left(\Phi_{s,A}/\Phi_s\right)\left(C_{AB}/C_{ref}\right)}{\left(\Phi_{s,e}/\Phi_s\right)\left(C_A/C_{ref}\right)}\right]\left(\frac{\Phi_s C_{ref}}{\Phi_s C_{ref}}\right) = K_a$$

Check: $\nu_{gi} = (0-1)+(1-0) = 0$ and $\nu_{si} = (0-1)+(1-0) = 0$.

Langmuir-Hinshelwood recombination of *A* and *B* on one active site set:

$$[A]_s + [B]_s \leftrightarrow AB + 2[s] \qquad K_a = \exp\left[\frac{-G^o_{AB}(T) - 2G^o_{[s]}(T) + G^o_{[A]_s}(T) + G^o_{[B]_s}(T)}{RT}\right]$$

$$r = r_f - r_b = k_f \Phi_{s,B}\Phi_{s,A} - k_b \Phi^2_{s,e} C_{AB}$$

k_f in m^2 $mole^{-1}$ s^{-1} k_b in m^5 $mole^{-2}$ s^{-1} K_c in mole m^{-3}

$$K_c = \frac{k_f}{k_b} = \frac{\Phi^2_{s,e}C_{AB}}{\Phi_{s,A}\Phi_{s,B}} = \left[\frac{\left(\Phi_{s,e}/\Phi_s\right)^2\left(C_{AB}/C_{ref}\right)}{\left(\Phi_{s,A}/\Phi_s\right)\left(\Phi_{s,A}/\Phi_s\right)}\right]\left(\frac{\Phi^2_s C_{ref}}{\Phi_s\Phi_s}\right) = K_a\left(\frac{P_{ref}}{RT}\right)$$

Check: $v_{gi} = (1-0) = 1$ and $v_{si} = (0-1)+(0-1)+(2-0) = 0$.

Langmuir-Hinschelwood recombination of *A* and *B* on two sets of active sites:

$[A]_{s1} + [B]_{s2} \leftrightarrow AB + [s1] + [s2]$

$$K_a = \exp\left[\frac{-G^o_{AB}(T) - G^o_{[s1]}(T) - G^o_{[s2]}(T) + G^o_{[A]_{s1}}(T) + G^o_{[B]_{s2}}(T)}{RT}\right]$$

$r = r_f - r_b = k_f \Phi_{s2,B} \Phi_{s1,A} - k_b \Phi_{s1,e} \Phi_{s2,e} C_{AB}$

k_f in m^2 $mole^{-1}$ s^{-1} $\quad$ k_b in m^5 $mole^{-2}$ s^{-1} $\quad$ K_c in mole m^{-2}

$$K_c = \frac{k_f}{k_b} = \frac{\Phi_{s1,e}\Phi_{s2,e}C_{AB}}{\Phi_{s1,A}\Phi_{s2,B}} = \left[\frac{(\Phi_{s1,e}/\Phi_s)(\Phi_{s2,e}/\Phi_s)(C_{AB}/C_{ref})}{(\Phi_{s1,A}/\Phi_s)(\Phi_{s2,B}/\Phi_s)}\right]\left(\frac{\Phi_s \Phi_s C_{ref}}{\Phi_s \Phi_s}\right) = K_a\left(\frac{P_{ref}}{RT}\right)$$

Check: $v_{gi} = (1-0) = 1$, $v_{s1i} = (0-1)+(1-0) = 0$ and $v_{s2i} = (0-1)+(1-0) = 0$.

Oxidation of *A*:

$[O]_s + [A]_b \leftrightarrow AO + [s]$ $\qquad$ $K_a = \exp\left[\frac{-G^o_{AO}(T) - G^o_{[s]}(T) + G^o_{[A]_b}(T) + G^o_{[O]_s}(T)}{RT}\right]$

$r = r_f - r_b = k_f \chi_{b,A} \Phi_{s,O} - k_b \Phi_{s,e} C_{AO}$

k_f in s^{-1} $\quad$ k_b in m^3 $mole^{-1}$ s^{-1} $\quad$ K_c in mole m^{-3}

$$K_c = \frac{k_f}{k_b} = \frac{\Phi_{s,e} C_{AO}}{\Phi_{s,O}\chi_{b,A}} = \left[\frac{(\Phi_{s,e}/\Phi_s)(C_{AO}/C_{ref})}{(\Phi_{s,O}/\Phi_s)\chi_{b,A}}\right]\left(\frac{\Phi_s C_{ref}}{\Phi_s}\right) = K_a\left(\frac{P_{ref}}{RT}\right)$$

Check: $v_{gi} = (1-0) = 1$ and $v_{si} = (0-1)+(1-0) = 0$.

1.6 Surface Equilibrium Constants and Thermodynamics

Thermochemical data have been carefully and extensively determined for most important gas-phase and solid-phase species. The uncertainties associated with these thermodynamic data are typically less than the uncertainties associated with chemical reaction rate data, so that it is preferable to specify only one of the reaction rates (usually the forward rate) and to calculate the other (backward) rate using the equilibrium constant.

However, the calculation of the equilibrium constants for surface reactions requires thermodynamic data for each surface species in the reaction, and those data are usually not available. The missing data appear in the formulae for activity-based surface equilibrium constants as the difference between the Gibbs energy of formation of occupied and vacant surface sites for each adsorbed species:

$$G^o_{[A]_s}(T) - G^o_{[s]}(T) \quad . \tag{1.6.1}$$

One approach is to create (empirically or through *ab initio* methods) temperature-dependent enthalpy and entropy functions for the various surface species so that the Gibbs energies of formation can be computed as a function of temperature. However, this is a time-consuming procedure with hard-to-quantify uncertainties.

An alternate procedure is to specify, in addition to k_{fi} for each adsorption reaction, either the backward rate constant k_{bi} for the corresponding desorption reaction, or the concentration-based equilibrium constant K_{ci} for adsorption reaction. Both can be specified using statistical thermodynamic or kinetic theory based expressions.

If k_{bi} is specified, the concentration-based equilibrium constant can be calculated directly from Eq. (1.5.11), and then can be converted to an activity-based equilibrium constant by inverting relation (1.5.10). Since ν_{gi} will always equal -1 for an adsorption reaction, the combination of these procedures yields:

$$K_{ai} = \frac{k_{fi}}{k_{bi}}\left(\frac{P_{ref}}{RT}\right) \quad . \tag{1.6.2}$$

If K_{ci} is specified, inverting relationship (1.5.10) directly yields:

$$K_{ai} = K_{ci}\left(\frac{P_{ref}}{RT}\right) \quad . \tag{1.6.3}$$

The activity-based equilibrium constant can then be used to compute the missing thermochemical data:

$$G^o_{[A]_s}(T) - G^o_{[s]}(T) = G^o_A(T) - RT\ln(K_{ai}) \quad . \tag{1.6.4}$$

In either case, the calculated difference in Gibbs formation energy can be used together with tabulated thermodynamic data for solid-phase and gas-phase species to evaluate the equilibrium constants for other surface reactions; i.e., Eley-Rideal and Langmuir-Hinschelwood recombination, oxidation, etc.

To simplify programming logic, we adopt the following convention:

For each individual surface phase, either thermodynamic data must be supplied for all surface species in all active site sets, or theory-based expressions for desorption or equilibrium must be supplied for all adsorbed species.

In the latter case, so long as the formation energies are only used to compute equilibrium constants (where only the difference $G^o_{[A]_s}(T) - G^o_{[s]}(T)$ is important), one can arbitrarily assign: $G^o_{[s]}(T) = 0$ and $G^o_{[A]_s}(T) = G^o_A(T) - RT\ln(K_{ai})$.

1.7 Thermal Desorption Rate Expressions

A general expression for the thermal desorption rate of species A is:

$$r_{des} = k_{des}\Phi^{\eta}_{s,A} = \nu \exp\left(-\frac{E_{des}}{RT}\right)\Phi^{\eta}_{s,A} \ , \tag{1.7.1}$$

where η is the reaction order.

In our surface reaction model, we limit thermal desorption to first order ($\eta = 1$) kinetics, which is consistent with the constraint that adsorbed species (whether atomic or molecular) only occupy a single surface site.

The attempt frequency ν (s^{-1}) and the desorption energy E_{des} (J mol^{-1}) can both depend on surface coverage, but in our surface reaction model we take ν and E_{des} as independent of surface coverage because the correct functional forms for surface coverage-dependence are uncertain. Moreover, experimental data for systems of interest are scarce, and most aerothermal applications will take place at high surface temperatures, where adsorbed species coverage will be low and the surface-coverage dependence of ν and E_{des} should be weak.

Several different approaches to modeling and specifying the desorption rate constant are possible. Typically, E_{des} is specified as a constant value, but different choices exist for specifying the attempt frequency ν. The simplest approach is to take ν as a constant value, usually in the range 10^{12} -10^{15} s^{-1}.[3-5] Then:

$$k_{des} = \nu \exp\left(-\frac{E_{des}}{RT}\right) . \tag{1.7.2}$$

Another approach is to use approximations for ν based on different levels of transition state theory. Transition state theory predicts that:

$$\nu = \left(\frac{RT}{A_v h}\right)\frac{q'_{sA}}{q_{sA}} , \tag{1.7.3}$$

where q_{sA} and q'_{sA} are the partition functions for the adsorbed surface complex and the activated adsorbed surface complex without the vibrational degree of freedom normal to the surface, respectively.[6-7]

With the common assumption that the ratio, $q'_{sA}/q_{sA} = 1$, the desorption rate constant becomes[8-10]

$$k_{des} = \left(\frac{RT}{A_v h}\right)\exp\left(-\frac{E_{des}}{RT}\right) . \tag{1.7.4}$$

One can also expand the partition function of the surface complex into a surface contribution and translational, vibrational (both with respect to the surface and internally), and rotational contributions of the adsorbed species, so that:

$$\nu = \left(\frac{RT}{A_v h}\right)\frac{\left(q_{se}q_{sA,t}q^2_{sA,v//}q_{sA,v\,\mathrm{int}}q_{sA,r}\right)'}{\left(q_{se}q_{sA,t}q_{sA,v\perp}q^2_{sA,v//}q_{sA,v\,\mathrm{int}}q_{sA,r}\right)} . \tag{1.7.5}$$

Here the subscripts " // " and " ⊥ " indicate vibration parallel and perpendicular to the surface, respectively. If we assume, after Daiß et al.,[11-12] that the surface complex and its activated counterpart have the same degrees of freedom (i.e., that partition functions describing the same types of contributions are identical in the surface and activated surface species):

$$\nu = \left(\frac{RT}{A_v h}\right)\frac{1}{q_{sA,v\perp}} , \tag{1.7.6}$$

where the partition function for the vibrational degree of freedom normal to the surface has the Boltzmann form:

$$q_{sA,v\perp} = \frac{\exp\left(-\frac{hA_v v_{sA,\perp}}{2RT}\right)}{1-\exp\left(-\frac{hA_v v_{sA,\perp}}{RT}\right)} \ . \qquad (1.7.7)$$

The theoretical expression for the desorption rate constant is then:

$$k_{des,sA} = \left(\frac{RT}{A_v h}\right)\frac{1-\exp\left(-\frac{hA_v v_{sA,\perp}}{RT}\right)}{\exp\left(-\frac{hA_v v_{sA,\perp}}{2RT}\right)}\exp\left(-\frac{E_{des}}{RT}\right) \ . \qquad (1.7.8)$$

Note that in the high temperature limit ($T >> hA_v v_{sA,\perp}/R$) the entire pre-exponential term reduces back to $v_{sA,\perp}$, so the temperature variation of the attempt frequency is very mild.

To allow for general scaling and the adjustment of the temperature dependence (for example, to account for the imperfect cancellation of partition functions for like degrees of freedom), the program computes the desorption rate constant as:

$$k_{des,sA} = A_{des} T'^{\beta} \nu \exp\left(-\frac{E_{des}}{RT}\right) \ , \qquad (1.7.9)$$

where T' is a dimensionless temperature ($T' \equiv T/1\,\mathrm{K}$) and the approximation for ν must be specified by a "form:"

Form 0, Arrhenius Desorption: $\nu = 1$ (1.7.10)

Form 1, Constant Frequency: $\nu = v_{sA,\perp}$ (1.7.11)

Form 2, Simple TST Desorption: $\nu = \left(\frac{RT}{A_v h}\right)$ (1.7.12)

and

Form 3, Complex TST Desorption: $\nu = \left(\frac{RT}{A_v h}\right)\frac{1-\exp\left(-\frac{hA_v v_{sA,\perp}}{RT}\right)}{\exp\left(-\frac{hA_v v_{sA,\perp}}{2RT}\right)}$ (1.7.13)

The numerical values that must be specified to the program are A_{des}, β, $\nu_{sA,\perp}$, and E_{des}. The units of $\nu_{sA,\perp}$ are s^{-1}, the units of $E_{des,s,A}$ are J $mole^{-1}$; β and A_{des} are dimensionless. In the absence of other information the values, $A_{des} = 1$ and $\beta = 0$ should be used. A pure Arrhenius formulation is recovered by specifying Form 0 and values for A_{des}, β, and E_{des}.

1.8 Surface Equilibrium Constant Expressions

The concentration-based equilibrium constant for the adsorption of species A from the gas phase is given by the transition-state theory expression:

$$K_c = \frac{k_f}{k_b} = \frac{\Phi_{s,A}}{\Phi_{s,e} N_A} = \frac{q_{sA}}{q_{se} q_A} \exp\left(\frac{E_{des} - E_{ad}}{RT} \right) , \tag{1.8.1}$$

where the partition functions for the adsorbed complex, the surface and the gas-phase species are q_{sA}, q_{se}, and q_A. We further assume that we can expand the partition function of the surface complex into a surface contribution with the translational, vibrational, and rotational contributions of the adsorbed species ($q_{sA} = q_{se} q_{sA,t} q_{sA,v} q_{sA,r}$) and the partition function for the gas-phase species into translational, vibrational, and rotational contributions ($q_A = q_{A,t} q_{A,v} q_{A,r}$). Then:

$$K_c = \frac{q_{sA,t} q_{sA,v} q_{sA,r}}{q_{A,t} q_{A,v} q_{A,r}} \exp\left(\frac{E_{des} - E_{ad}}{RT} \right) . \tag{1.8.2}$$

In the gas phase, the translational partition function is:

$$q_{A,t} = \left(\frac{2\pi M_A RT}{(A_v h)^2} \right)^{3/2} . \tag{1.8.3}$$

For immobile surface adsorption:

$$q_{sA,t} = 1 \tag{1.8.4}$$

while for mobile surface adsorption (modeled as two dimensional gas):

$$q_{sA,t} = \left(\frac{2\pi M_A RT}{(A_v h)^2} \right) . \tag{1.8.5}$$

A common approximation is to substitute in the expressions for the translational energy partition functions and assume that the remaining ratio of vibrational and rotational partition functions cancel; i.e., $q_{sA,v}q_{sA,r}/q_{A,v}q_{A,r}=1$. Then for immobile adsorption:

$$K_{c,im}=\left(\frac{2\pi\ M_A RT}{(A_v h)^2}\right)^{-3/2}\exp\left(\frac{E_{des}-E_{ad}}{RT}\right) \tag{1.8.6}$$

and for mobile adsorption:

$$K_{c,m}=\left(\frac{2\pi\ M_A RT}{(A_v h)^2}\right)^{-1/2}\exp\left(\frac{E_{des}-E_{ad}}{RT}\right)\ . \tag{1.8.7}$$

Another approach is to expand the vibrational partition function of the surface species into internal and surface vibrational contributions and assume the ratio: $q_{sA,v\,\mathrm{int}}q_{sA,r}/q_{A,v}q_{A,r}=1$ [11-12].

For immobile adsorption, the adsorbed species has no translational degrees of freedom and three vibrational degrees of freedom so:

$$q_{sA,v\perp}=\frac{\exp\left(-\frac{hA_v\nu_{sA,\perp}}{2RT}\right)}{1-\exp\left(-\frac{hA_v\nu_{sA,\perp}}{RT}\right)}\quad\text{and}\quad q_{sA,v//}=\frac{\exp\left(-\frac{hA_v\nu_{sA,//}}{2RT}\right)}{1-\exp\left(-\frac{hA_v\nu_{sA,//}}{RT}\right)}\ . \tag{1.8.8}$$

For mobile adsorption, the adsorbed species has full two-dimensional freedom of motion on the surface and no vibrational modes parallel to the surface:

$$q_{sA,v\perp}=\frac{\exp\left(-\frac{hA_v\nu_{sA,\perp}}{2RT}\right)}{1-\exp\left(-\frac{hA_v\nu_{sA,\perp}}{RT}\right)}\quad\text{and}\quad q_{sA,v//}=1\ . \tag{1.8.9}$$

The general theoretical expressions for immobile and mobile adsorption equilibrium are:

$$K_{c,im}=\left(\frac{2\pi\ M_A RT}{(A_v h)^2}\right)^{-3/2}\left(\frac{\exp\left(-\frac{hA_v\nu_{sA,\perp}}{2RT}\right)}{1-\exp\left(-\frac{hA_v\nu_{sA,\perp}}{RT}\right)}\right)\left(\frac{\exp\left(-\frac{hA_v\nu_{sA,//}}{2RT}\right)}{1-\exp\left(-\frac{hA_v\nu_{sA,//}}{RT}\right)}\right)^2\exp\left(\frac{E_{des}-E_{ad}}{RT}\right) \tag{1.8.10}$$

and,

$$K_{c,m} = \left(\frac{2\pi\, M_A RT}{(A_v h)^2} \right)^{-1/2} \left(\frac{\exp\left(-\frac{hA_v \nu_{sA,\perp}}{2RT} \right)}{1 - \exp\left(-\frac{hA_v \nu_{sA,\perp}}{RT} \right)} \right) \exp\left(\frac{E_{des} - E_{ad}}{RT} \right) \quad . \tag{1.8.11}$$

In the program, we make the simplification $\nu_{sA} = \left(\nu_{sA,\perp} \nu_{sA,//}^2 \right)^{1/3}$ in the above expression for immobile absorption, which leads to the correct values in the high temperature limit $T >> hA_v \nu_{sA,\perp} / R$, and we add parameters to allow for general scaling and the adjustment of the temperature dependence.

The general equation used in the program has the form:

$$K_c = A_{eq} T'^{\beta} K_0 \exp\left(\frac{E_{des} - E_{ad}}{RT} \right) \ , \tag{1.8.12}$$

where the form of adsorption-desorption equilibrium must be specified:

Form 0, Arrhenius: $K_0 = 1$ (1.8.13)

Form 1, Simple Immobile TST: $K_0 = \left(\frac{2\pi\, M_A RT}{(A_v h)^2} \right)^{-3/2}$ (1.8.14)

Form 2, Complex immobile TST: $K_0 = \left(\frac{2\pi\, M_A RT}{(A_v h)^2} \right)^{-3/2} \left(\frac{\exp\left(-\frac{hA_v \nu_{sA}}{2RT} \right)}{1 - \exp\left(-\frac{hA_v \nu_{sA}}{RT} \right)} \right)^3$ (1.8.15)

Form 3, simple mobile TST: $K_0 = \left(\frac{2\pi\, M_A RT}{(A_v h)^2} \right)^{-1/2}$ (1.8.16)

Form 4, complex mobile TST: $$K_0 = \left(\frac{2\pi\, M_A RT}{(A_v h)^2} \right)^{-1/2} \left(\frac{\exp\left(-\frac{hA_v \nu_{sA,\perp}}{2RT} \right)}{1 - \exp\left(-\frac{hA_v \nu_{sA,\perp}}{RT} \right)} \right) \tag{1.8.17}$$

The numerical values that must be specified are A_{eq}, β, ν_{sA}, and E_{des}. The units of ν_{sA} are s^{-1}, the units of E_{des} are J $mole^{-1}$; β and A_{eq} are dimensionless. In the absence of other information, $A_{eq} = 1$ and $\beta = 0$. A pure Arrhenius formulation is recovered by specifying Form 0 and values for A_{eq}, β, and E_{des}.

1.9 Forward Reaction Rate Coefficients

Reaction-rate coefficients can be specified in several different ways. The most general is an Arrhenius expression as used in Surface Chemkin:

Type 0: Arrhenius:

$$k_{fi} = A_i T'^{\beta_i} \exp\left(\frac{-E_{ai}}{RT}\right) \qquad (1.9.1)$$

The required inputs are the pre-exponential factor A_i, the temperature exponent β_i, and the activation energy E_{ai}. Here, and in all reaction rate equations that follow, T' is again the dimensionless temperature defined by $T' \equiv T/1\,\mathrm{K}$.

The units of E_{ai} are J mole^{-1}, and β_i is dimensionless. The units of A_i depend on the particular reaction; the units of A_i must ultimately yield a reaction flux in moles m^{-2} s^{-1} when multiplied by the generalized concentrations used in the reaction equation.

The disadvantage of this approach is that the magnitudes of A_i and β_i are difficult to relate to physical, chemical, or kinetic processes.

A more insightful way to specify surface reaction rates is through a kinetics-based formulation for the forward reaction rate between a gas-phase or mobile surface-phase reactant, and an immobile surface species:

Some examples of kinetic-based forward reaction rates are given below:

Adsorption of *A* on phase *ns*:

$$A + [s] \leftrightarrow [A]_s$$

The forward reaction flux is the product of the sticking coefficient, the impingement flux of species *A* on the surface, and the fraction of available active sites that are empty:

$$r_f = S\,\Gamma_A \theta_{s,e}$$

where the sticking coefficient: $$S = S_0 \exp\left(-\frac{E_{ad}}{RT}\right) \qquad (1.9.2)$$

the impingement flux: $$\Gamma_A = \frac{\bar{v}_A}{4} C_A \qquad (1.9.3)$$

the thermal velocity: $$\bar{v}_A = \sqrt{\frac{8RT}{\pi M_A}} \qquad (1.9.4)$$

and the open site fraction in phase n_s: $$\theta_{s,e} = \frac{\Phi_{s,e}}{\Phi_s} \qquad (1.9.5)$$

These can be combined to yield:

$$r_f = \left[\frac{\bar{v}_A}{4\Phi_s} S_0 \exp\left(-\frac{E_{ad}}{RT}\right)\right] \Phi_{s,e} C_A \qquad (1.9.6)$$

so that the forward reaction rate coefficient is:

$$k_f = \left(\frac{\bar{v}_A}{4\Phi_s}\right) S_0 \exp\left(-\frac{E_{ad}}{RT}\right) \qquad (1.9.7)$$

This reaction rate constant has units of (m^3 $mole^{-1}$ s^{-1}). The quantity in the leading brackets of Eq. (1.9.7) can be calculated directly from gas species and surface phase inputs.

For dissociative adsorption reactions, the site density is raised to the power ν_s equal to the sum of the stoichiometric coefficients of all surface reactants, and the units of the reaction-rate coefficient change accordingly. For example, for the reaction:

$$A_2 + 2[s] \leftrightarrow 2[A]_s$$

ν_s equals 2, so,

$$k_f = \left(\frac{\bar{v}_A}{4\Phi_s^2}\right) S_0 \exp\left(-\frac{E_{ad}}{RT}\right)$$

and the units of the reaction rate constant are (m^5 $mole^{-2}$ s^{-1}).

For a more general formulation of inputs to the program, we include a parameter for imposing a temperature dependence:

Type 1: Adsorption:

$$k_f = \left(\frac{\bar{v}_A}{4\Phi_s^{\nu_s}}\right) S_0 T'^{\beta} \exp\left(-\frac{E_{ad}}{RT}\right) \qquad (1.9.8)$$

The required inputs are S_0, E_{ad}, and β. The energy barrier for adsorption, E_{ad}, is specified in J mole^{-1} and usually taken as 0 for atomic adsorption.

In a pure kinetic formulation, $\beta = 0$ and S_0 is the dimensionless initial sticking coefficient for input within the range 0 to 1. To retain the meaning of the pre-factor to the exponential as a sticking coefficient, the program limits the maximum value of the product $S_0 T'^{\beta}$ to 1.

Eley-Rideal recombination of gas-phase *A* with surface *B* on phase *ns*:

$$A + [B]_s \leftrightarrow AB + [s]$$

The forward reaction flux is product of the Eley Rideal reaction efficiency, the impingement flux of species *A* on the surface, and the fraction of active sites that are occupied by adsorbed species *B*:

$$r_f = \gamma_{er} \Gamma_A \theta_{s,B} \tag{1.9.9}$$

The Eley Rideal reaction efficiency is: $$\gamma_{er} = \gamma_0 \exp\left(-\frac{E_{er}}{RT}\right) \tag{1.9.10}$$

The reaction flux can be rewritten as:

$$r_f = \left[\frac{\bar{v}_A}{4\Phi_s}\gamma_0 \exp\left(-\frac{E_{er}}{RT}\right)\right]\Phi_{s,B}\, C_A \tag{1.9.11}$$

with the forward reaction rate coefficient:

$$k_f = \left(\frac{\bar{v}_A}{4\Phi_s}\right)\gamma_0 \exp\left(-\frac{E_{er}}{RT}\right) \quad . \tag{1.9.12}$$

This reaction rate constant has units of (m^3 mole^{-1} s^{-1}). The quantity in the leading brackets can be calculated directly from gas species and surface-phase input.

For Eley-Rideal reactions involving multiple surface sites, the site density is raised to the power v_s equal to the sum of the stoichiometric coefficients of all surface reactants, and the units of the reaction rate coefficient change accordingly. For example, C_3 (carbon vapor) condensation mediated by available empty active sites on the surface is written as:

$$C_3 + 3[s] \leftrightarrow 3[s] + 3[C]_b$$

so ν_s equals 3 and the units of the reaction rate constant are (m^7 $mole^{-3}$ s^{-1}).

For a more general formulation of inputs to the program, we include a parameter for adjusting the wall temperature dependence:

Type 2: Eley-Rideal Recombination:

$$k_f = \left(\frac{\bar{v}_A}{4\Phi_s^{\nu_s}} \right) \gamma_0 T'^{\beta} \exp\left(-\frac{E_{er}}{RT} \right) \tag{1.9.13}$$

The required inputs are γ_0, E_{er}, and β. The energy barrier for Eley-Rideal recombination, E_{er}, is specified in J $mole^{-1}$.

In a pure kinetic formulation, $\beta = 0$ and γ_0 is the reaction probability to be input within the range 0 to 1. To retain the meaning of the pre-factor to the exponential as a reaction probability coefficient, the program limits the maximum value of the product $\gamma_0 T'^{\beta}$ to 1.

Langmuir-Hinshelwood reaction of mobile *A* and immobile *B* on two sets of active sites :

$$[A]_{s1} + [B]_{s2} \leftrightarrow AB + [s1] + [s2]$$

The forward reaction flux is the product of the Langmuir-Hinshelwood reaction frequency, the total site density in phase *ns*, and the fractions of active sites in phase *ns* that are occupied by adsorbed species *A* and *B*:

$$r_f = \nu_{lh} \Phi_s \theta_{s,1,A} \theta_{s,2,B} \tag{1.9.14}$$

The Langmuir-Hinshelwood reaction frequency is:

$$\nu_{lh} = \frac{C_{lh}}{\Delta} \bar{v}_{2D,A} \exp\left(-\frac{E_{lh}}{RT} \right) \tag{1.9.15}$$

where the activation energy is computed by,

$$E_{lh} = \max\left(E_{mA}, E_{s1,des,A} + E_{s2,des,B} - E_{s2,dis,AB} \right) \tag{1.9.16}$$

the mean thermal speed of *A* in a 2-D gas, $$\bar{v}_{2D,A} = \sqrt{\frac{\pi RT}{2M_A}} \tag{1.9.17}$$

the average spacing between sites, $$\Delta = \frac{1}{\sqrt{A_v \Phi_s}} \tag{1.9.18}$$

and C_{lh} is a dimensionless constant.

The forward reaction flux can then be written as:

$$r_f = \left[\left(\bar{v}_{2D,A} \sqrt{\frac{A_v}{\Phi_s}} \right) C_{lh} \exp\left(-\frac{E_{lh}}{RT} \right) \right] \Phi_{s,1,A} \Phi_{s,2,B} \tag{1.9.19}$$

and the forward rate coefficient as,

$$k_f = \left(\bar{v}_{2D,A} \sqrt{\frac{A_v}{\Phi_s}} \right) C_{lh} \exp\left(-\frac{E_{lh}}{RT} \right) \tag{1.9.19}$$

For this example, the site density exponent is 2 and the reaction rate constant has units of (m^2 $mole^{-1}$ s^{-1}).

For a more general formulation of inputs to the program, we include a parameter for adjusting the wall temperature dependence and show the site density exponent explicitly:

Type, 3: Langmuir-Hinshelwood:

$$k_f = \left(\bar{v}_{2D,A} \sqrt{A_v} \right) \Phi_s^{(1.5-\nu_s)} C_{lh} T'^{\beta} \exp\left(-\frac{E_{lh}}{RT} \right) \tag{1.9.20}$$

The required inputs are the dimensionless scaling coefficient C_{lh} and the activation energy for surface diffusion, E_{mA} in J $mole^{-1}$. The quantity in the leading brackets can be calculated directly from species and phase information input separately, as long as the LH equation type is specified.

Sublimation of C_3 from bulk phase *nb* via empty active sites on surface phase *ns*:

$$3[s] + 3[C]_b \leftrightarrow C_3 + 3[s]$$

The forward reaction flux is the product of the evaporation/condensation coefficient, the impingement flux of species C_3 on surface phase *ns* under saturated vapor pressure conditions, and the fraction of empty active sites on surface phase *ns*:

$$r_f = \alpha \Gamma_{C_3} \theta_{s,e}^3 \chi_{nb,C}^3 \tag{1.9.21}$$

where the evaporation coefficient can be temperature dependant, but must lie in the range 0 to 1:

$$\alpha = \alpha_0 \exp\left(-\frac{E_\alpha}{RT}\right) \quad . \tag{1.9.22}$$

The C_3 impingement flux is given by:

$$\Gamma_{C_3} = \frac{\bar{v}_{C_3}}{4} C_{eq,C_3} = \frac{\bar{v}_{C_3}}{4} \frac{P_{eq,C_3}}{RT} = \frac{\bar{v}_{C_3}}{4} \frac{P_0}{RT} \exp\left(-\frac{E_{vap}}{RT}\right) \tag{1.9.23}$$

The forward reaction flux can be expressed as:

$$r_f = \left[\frac{\bar{v}_{C_3}}{4\Phi_s^3} \frac{\alpha_0 P_0}{RT} \exp\left(-\frac{E_{vap} + E_\alpha}{RT}\right)\right] \Phi_{s,e}^3 \chi_{nb,C}^3 \tag{1.9.24}$$

or

$$k_f = \left[\frac{\bar{v}_{C_3}}{4\Phi_s^3} \frac{\gamma_{sub}}{RT} \exp\left(-\frac{E_{sub}}{RT}\right)\right] \tag{1.9.25}$$

where $\gamma_{sub} = \alpha_0 P_0$ and $E_{sub} = E_{vap} + E_\alpha$. In this example, the site density exponent is 3, and the reaction-rate constant has units of (m^4 $mole^{-2}$ s^{-1}).

For a more general formulation of inputs to the program, we include a parameter for adjusting the wall temperature dependence and show the site density exponent explicitly:

Type 4: Sublimation:

$$k_f = \left[\frac{\bar{v}_{C_3}}{4\Phi_s^{\nu_s} RT}\right] \gamma_{sub} T'^{\beta} \exp\left(-\frac{E_{sub}}{RT}\right) \tag{1.9.26}$$

Finally, we note there are many reaction processes that can be specified according to our rules (see section 1.4), but they do not fit neatly into the categories given above; for example:

$$[A]_s + [B]_b \leftrightarrow AB + [s]$$
$$A + [s] + [B]_b \leftrightarrow AB + [s]$$
$$A + [A]_s + [B]_b \leftrightarrow BA_2 + [s]$$
$$A + [BC]_s \leftrightarrow AB + [C]_s$$

It is always possible to specify the forward reaction rate for any of these processes using the basic Arrhenius formulation, Eq. (1.9.1).

Although the classic definition of an Eley-Rideal reaction is the reaction of a gas-phase reactant with an adsorbed reactant to form a gas-phase product ($A + [B]_s \leftrightarrow AB + [s]$), it is also possible to use the gas-kinetic Eley-Rideal rate formulation, Eq. (1.9.13) to represent any process that involves the impingement of a gas phase reactant on the surface (for example, the last three reactions listed directly above.)

1.10 Species Production Rates, Loss Efficiencies, and Branching Fractions

For a gas-phase reactant *k*, the *global* loss efficiency is defined as the fraction of collisions with the surface that result in its permanent removal from the gas environment:

$$\gamma_k = \frac{-\dot{w}_k}{\Gamma_k} \quad . \tag{1.10.1}$$

The *local* loss efficiency of gas phase species *k* on surface phase n_s is defined as the fraction of collisions with the surface phase n_s that result in the permanent removal of *k* from the gas phase:

$$\gamma_{k,n_s} = \frac{-\dot{w}_{k,n_s}}{\Gamma_k} \quad . \tag{1.10.2}$$

The two efficiencies are the same if the surface is modeled with a single surface phase. The negative sign appears because the loss efficiency is a positive number for the loss of a gas species at the wall (i.e., a negative production of a species at the wall.)

Often, a gas-phase species can participate in more than one surface reaction. The individual contribution of each surface reaction to the net production rate of a particular species is given by the *reaction-specific global* production rate of Eq. (1.4.5). Sometimes, it is convenient to characterize the contributions of different reaction pathways by branching fractions defined as the ratio of the *reaction-specific global* production rates to the *net global* production rate,

$$f_{k,i} = \frac{\dot{w}_{ki}}{\dot{w}_k} \quad . \tag{1.10.3}$$

Branching fractions are most useful for gas-phase reactants (products) that undergo loss (production) by multiple pathways. In these cases, the branching fractions will all be positive and indicate directly the fraction of loss (production) due to a particular reaction.

It is possible that a gas species is lost by some pathways and produced by others. In such a case, some branching fractions will be negative, indicating that the production rate of a particular

reaction acts in opposition to the *net global* production rate. Branching fractions will still sum to one for that species, but the interpretation of numerical values is less intuitive (for example, the magnitudes of individual branching fractions could exceed one.) Obviously, in instances where the *net global* production rate is zero, branching fractions have no meaning.

1.11 Mass Transfer to the Gas Phase and Blowing Species Production Rates

The total mass flux (kg m^{-2} s^{-1}) between the bulk and gas environments *due to surface reactions* can be computed by summing the global mass production rates of all bulk species in all bulk phases:

$$\dot{m}_c = -\sum_{nb=1}^{N_b} \sum_{k=1}^{K_{nb}} M_k \dot{w}_k \quad . \tag{1.11.1}$$

For ablating materials, $\dot{m}_c$ is usually termed the "char" mass flux and contains contributions from any surface reactions that transport mass between the bulk and gas environments. The negative sign appears in Eq. (1.11.1) because we want $\dot{m}_c$ to be a positive number for mass transfer into the gas phase.

It is often necessary to consider the flow of gases passing into the boundary layer from beneath the material surface. Such gas flow may result from deliberate gas injection (transpiration cooling) or in-depth pyrolysis (thermal decomposition). Although the present finite-rate reaction model does not compute in-depth chemical reactions, blowing species may still influence the balance of mass and energy that is enforced at the gas/surface interface. These blowing sources are considered in addition to the blowing that occurs from bulk phase mass loss.

In the present implementation of the code, blowing species can be incorporated in one of two ways. Both methods require that all blowing gas species (whether they participate in surface chemistry or not) be included in the gas phase species set $k = 1 \ldots K_g$.

The first approach is to specify the molar composition and mass flow rate, $\dot{m}_g$, (kg m^{-2} s^{-1}) of one or more blowing gas mixtures. The molar production rate of species *k* by N_{blw} blowing gas mixtures is then given by:

$$\dot{w}_{blw,k} = \sum_{n=1}^{N_{blw}} \left[\frac{\chi_{n,k} \dot{m}_{g,n}}{\sum_{k=1}^{K_g} \chi_{n,k} M_k} \right] \quad . \tag{1.11.2}$$

The energies fluxes carried by blowing gas species can be computed from the blowing production rates using tabulated enthalpy functions in the Lewis thermodynamic database evaluated at the temperature of the surface.

The second approach is to use a "steady-state ablation" approximation. In this approximation, the locations of the char front, the pyrolysis front, and the boundary between heated and unheated ablator material, all remain constant in time with respect to the surface, and the temperature and density profiles within the heated material remain constant (see section 3.1 for a full derivation).

With these simplifications, the pyrolysis gas mass flux is constrained by the relationship:

$$\dot{m}_g = \dot{m}_c \left[\frac{1}{C_y} - 1 \right] \quad , \tag{1.11.3}$$

where the char yield, C_y, is the ratio of the char density to the density of the virgin ablator.

The char mass flux is computed by the finite-rate surface reaction model through Eq. (1.11.1). The required inputs are the char yield, the enthalpy of the virgin ablator at the temperature of the unheated ablator, and the molar composition of the pyrolysis gas.

The molar production rate of species *k* in the pyrolysis gas mixtures is given by Eq. (1.11.2) with $N_{blw} = 1$. The energies carried by blowing gas species can be computed from these blowing production rates using tabulated enthalpy functions in the Lewis/Glenn thermodynamic database evaluated at the temperature of the surface.

Chapter 2. Stand-Alone Code Implementation

This chapter describes numerical implementations of the finite-rate surface chemistry formulation in a stand-alone code. This implementation of the finite-rate surface chemistry formulation is built with the same source code used in DPLR.

The stand-alone code was developed for testing specific surface reaction models and checking their consistency with thermochemical equilibrium. This code solves for a variety of steady-state solutions of the finite-rate surface chemistry model given an initial state of the system. Convection and diffusion processes are neglected in the stand-alone code, and the rate of change of each surface and gas species is computed as the finite-rate surface production term of that species. The code provides time-integrated solutions of the finite-rate equations for constant gas-phase, constant volume, and constant pressure boundary conditions.

The code also computes the steady-state surface species populations for the constant gas-phase boundary condition by solving a coupled algebraic equation set. For the constant volume and constant pressure boundary conditions, the stand-alone code also computes the corresponding thermochemical equilibrium states using free-energy minimization for the same initial state of the system.

The three types of solutions–time-integration to steady-state, algebraic solution for steady-state surface populations, and thermochemical equilibrium by free-energy minimization–are described in the three sections below. In this chapter, we use the subscripts *g*, *s*, and *b* to indicate gas, surface, and bulk species, and the bracket notation, [ ], to indicate vector quantities.

2.1 Time-Integrated Steady-State Solutions

Given an initial state–the temperature, pressure, and starting concentrations of all species–the finite-rate surface-reaction model can be iterated to steady-state in several different ways. We imagine a control volume extending a distance δ above a fixed area (1 m^2) of the surface and apply the divergence theorem, which relates the rate of change of each concentration within the volume to the flux passing through the single surface. This volume contains all surface and gas species, and, since the gas contained within the volume is considered uniform, only the ratio of the volume to the initial volume is important to the system (δ/δ^0). The equations for the rates of change of the surface and gas species in this volume are:

$$\frac{d[\mathrm{X}]_s}{dt} = [\dot{w}]_s \tag{2.1.1}$$

and

$$\frac{d\delta[\mathrm{X}]_g}{dt} = [\mathrm{X}]_g \frac{d\delta}{dt} + \delta \frac{d[\mathrm{X}]_g}{dt} = [\dot{w}]_g \ , \tag{2.1.2}$$

where the brackets indicate vectors. The concentrations of bulk species are assumed constant, so their rates of change are zero and no equation is needed.

Three types of steady-state solutions can be computed using the stand-alone code by integrating the finite-rate equations in time: fixed gas phase, constant volume, and constant pressure. The temperature is fixed at its initial value in all three cases.

The fixed gas phase solution is obtained by holding pressure, volume, and composition at their initial values. In this case, only Eq. (2.1.1) needs to be solved. The surface species populations adjust until they come into steady state with the fixed gas environment. However, the resulting steady-state combination surface coverage, temperature, pressure, volume, and gas composition *is not a thermodynamic equilibrium state, in general*.

The constant volume solution is obtained by setting $\delta = 1\,\mathrm{m}$ and $d\delta/dt = 0$ in Eq. (2.1.2) and solving it together with Eq. (2.1.1). Both the surface and gas-phase species populations are allowed to adjust until steady state is reached. The gas pressure at steady state will differ from the initial pressure because the gas-phase concentrations are allowed to change, but the system volume and temperature are kept constant. The steady-state pressure can be computed from the ideal gas law and the steady-state gas species concentrations. This solution of the finite-rate surface chemistry model should be equivalent to the thermodynamic equilibrium state obtained by minimizing the free energy of the system at constant temperature and volume in most cases, but this can differ from equilibrium if no finite-rate reaction pathway exists to equilibrate the gas concentrations.

A constant pressure, solution is obtained by adding the additional constraint that the sum of all gas-phase concentrations must remain constant, or that:

$$\sum_{g=1}^{N_g} \frac{d\mathrm{X}_g}{dt} = 0 \quad . \tag{2.1.3}$$

The steady-state volume of the system will differ from the initial volume, since the gas-phase concentrations are allowed to change but the system pressure is kept constant. An expression for the volume change, $d\delta/dt$, can be obtained by summing Eq. (2.1.2) and inserting the constraint Eq. (2.1.3):

$$\frac{d\delta}{dt}\sum_{g=1}^{N_g}\mathrm{X}_g = \sum_{g=1}^{N_g}\dot{w}_g \quad . \tag{2.1.4}$$

The final value of δ is computed by solving Eq. (2.1.2) together with Eq. (2.1.1) and Eq. (2.1.4). This solution of the finite-rate surface chemistry model should be equivalent to the thermodynamic equilibrium state obtained by minimizing the free energy of the system at constant temperature and pressure in most cases.

For all three of these cases, the system of equations may be integrated in time using a two-parameter implicit/explicit time integration formulation,[13]

$$\Delta^n[X] = \left(\frac{\theta_1 \Delta t}{1+\theta_2}\right)\left([\dot{w}]^{n+1} - [\dot{w}]^n\right) + \left(\frac{\Delta t}{1+\theta_2}\right)[\dot{w}]^n + \left(\frac{\theta_2}{1+\theta_2}\right)\Delta^{n-1}[X] \tag{2.1.5}$$

where $\Delta^n[X] \equiv [X]^{n+1} - [X]^n$ and the following choices of parameters provide first-order explicit, first-order implicit, or second-order implicit in time solutions:

Table 2.1.1 Parameters for Different Integration Schemes

	θ_1	θ_2
Euler explicit	0	0
Euler implicit	1	0
3-point backward	1	1/2

For the Euler explicit method, the equation reduces to the following form:

$$\Delta^n[X] = \Delta t[\dot{w}]^n \tag{2.1.6}$$

For the Euler implicit method, the equation reduces to the following form:

$$\left(\frac{[I]}{\Delta t} - \left.\frac{\partial[\dot{w}]}{\partial[X]}\right|_n\right)\Delta^n[X] = [\dot{w}]^n \tag{2.1.7}$$

For the three-point backward method, the equation reduces to the following form:

$$\left(\frac{3[I]}{2\Delta t} - \left.\frac{\partial[\dot{w}]}{\partial[X]}\right|_n\right)\Delta^n[X] = [\dot{w}]^n + \frac{[I]}{2\Delta t}\Delta^{n-1}[X] \tag{2.1.8}$$

which requires storage of two previous time levels of the concentration vector.

For the implicit methods, the Jacobian of the source term may be evaluated analytically for all forms of the finite-rate source term. The derivatives are taken with respect to the temperature at the surface and each concentration (regardless of phase). The general source term, Jacobian, is calculated for ease of coupling into CFD codes. For the stand-alone integration methods currently employed, the temperature degree of freedom is appended to the end of the state vector $[X]$, with a trivial equation for the update of this variable for a constant temperature solution. However, the code could be extended to handle gas-phase approximations involving changing temperature in the future.

2.2 Algebraic Solution for Steady-State Surface Coverage

The solution for quasi steady-state (QSS) surface coverage can be obtained for a set of fixed gas-phase concentrations, pressure, and temperature. The QSS solution is utilized in two ways in the finite-rate surface model implementation. First, the initial distribution of adsorbed surface species concentrations, which is assumed to consist entirely of empty sites by default, can alternately be set to the QSS distribution using the initial gas-phase concentrations. The system then changes in time as the gas-phase concentrations change as detailed in the previous section of this report. The alternate surface initialization using the QSS distribution can also be used when the algorithm is integrated with the DPLR CFD code. Second, the QSS distribution is computed as part of the post-processing in the stand-alone code using the final gas-phase species concentrations after the system has been integrated in time. This result can be used as an indicator of whether or not the time-accurate distribution has reached a steady state.

The solution of the QSS satisfies the set of requirements that the production source terms are identically zero for all adsorbed surface species and empty sites, as well as the constraints that the total density of active sites are conserved for all active site sets. All gas-phase species concentrations, surface temperature, and bulk-phase concentrations are considered constants. The system consists of one equation for each adsorbed species and one equation for each active site set.

Adsorbed surface species equations are formed by taking the previously derived expression for the molar production rate of that species and setting that rate to zero given by:

$$\dot{w}_s = \sum_{i=1}^{Nr} \left\{ \left(\nu''_{si} - \nu'_{si} \right) \left(k_{fi} \prod_{m=1}^{N} [X_m]^{\nu'_{mi}} - k_{bi} \prod_{m=1}^{N} [X_m]^{\nu''_{mi}} \right) \right\} = 0 . \tag{2.2.1}$$

Active site set conservation equations are given by:

$$\sum_{k=1}^{N_{ns,na}} X_k = \Phi_{ns,na} . \tag{2.2.2}$$

This set of equations may be solved for using a Newton-Raphson method by making the equations implicit as given by:

$$\left(\sum_{k=1}^{N_s} \frac{\partial \dot{w}_s}{\partial X_k} \Delta X_k \right) + \Lambda_{ns(s),na(s)} = -\dot{w}_s \tag{2.2.3}$$

where $\Lambda_{ns(s),na(s)}$ is the Lagrange multiplier associated with the particular surface phase and active site set of each species, and:

$$\left(\sum_{k=1}^{N_{ns,na}} \Delta X_k \right) = \Phi_{ns,na} - \sum_{k=1}^{N_{ns,na}} X_k \ . \tag{2.2.4}$$

This technique initially assumes that empty surface sites are equal to the active site set density and all other concentrations are zero. In the next section, a strategy of employing natural logs of the unknown concentrations for general free-energy minimization is discussed, but this was found not to be necessary since the QSS system of equations is numerically more benign. The only limit placed on the surface concentrations is to prevent them from becoming negative during solution updates.

The QSS distribution is numerically different from the general equilibrium distribution in several ways. Primarily, the general equilibrium calculation most often treats the gas-phase concentrations as variables also, whereas the QSS solution treats the gas-phase concentrations as fixed constants. Therefore, the two solutions will be different if the gas phase is not in equilibrium already. Additionally, the constraints on the system are implemented differently, and the equilibrium solver applies additional elemental constraints to the system that are not required for the QSS model. In many cases, the two solutions will be the same, but sometimes they will differ for valid reasons.

2.3 Equilibrium Composition Using Free-Energy Minimization

The calculation of the composition of the finite-rate surface system at equilibrium can be found by minimizing either the Gibbs or the Helmholtz free-energy of the system, including the presence of both gaseous, adsorbed surface, and bulk species. Both the stand-alone and the integrated DPLR algorithms already employ Gibbs free-energy values for each species to compute backward rates for each of the finite-rate reactions. In the case of adsorbed species, this Gibbs energy is most typically calculated from specified adsorption/desorption reaction pairs, but, in any case, the result is a Gibbs energy that is known as a function of temperature.

The algorithm for the calculation of the equilibrium composition is adapted from Gordon and McBride as implemented in the CEA code.[14] The algorithm solves for the composition of each species subject to an arbitrary number of elemental constraints at a given thermodynamic state. The elemental constraints are enforced in the system using a Lagrange multiplier degree of freedom for each element. The CEA code is much more generalized, as it operates on any combination of two thermodynamic variables specified by the user. CEA also solves using the mole-mass ratio of the species as the state variables, while the generalized concentrations are used directly for this application. With generalized concentrations, neither the mixture pressure nor the mixture density appear in the Gibbs energy equations as they do in the CEA's formulation; however, a volume parameter appears in the elemental mass conservation constraints for constant-pressure equilibrium.

The set of equations consists of a Gibbs energy equation for each gas, surface, and bulk species in the system, as well a number of elemental constraints that enforce element conservation in the equilibrium state based on the stoichiometry of the initial state.

The Gibbs energy equation for each gas species in the system is given by:

$$\frac{G_g^0}{RT} + \ln\left(X_g\right) + \ln\left(\frac{RT}{P_{ref}}\right) + \sum_{i=1}^{Ne} a_{i,g}\Lambda_i = 0 \ . \tag{2.3.1}$$

The Gibbs energy equation for each adsorbed surface species is given by:

$$\frac{G_s^0}{RT} + \ln\left(X_s\right) + \ln\left(\Phi_{ref}\right) + \sum_{i=1}^{Ne} a_{i,s}\Lambda_i = 0 \ . \tag{2.3.2}$$

The Gibbs energy equation for each bulk phase species is:

$$\frac{G_b^0}{RT} + \ln\left(\chi_b\right) + \sum_{i=1}^{Ne} a_{i,b}\Lambda_i = 0 \ . \tag{2.3.3}$$

The elemental constraints are given by:

$$\delta\sum_{j=1}^{Ng} a_{i,j}X_j + \sum_{j=Ng+1}^{Nq} a_{i,j}X_i - b_i^0 = 0 \quad \left(b_i^0 = \delta_0\sum_{j=1}^{Ng} a_{i,j}X_j^0 + \sum_{j=Ng+1}^{Nq} a_{i,j}X_j^0\right) . \tag{2.3.4}$$

Finally, if the system is computed for constant pressure, an additional volume equation is required to close the set, which is given by:

$$\sum_{i=1}^{Ng} X_g - \frac{P}{RT} = 0 \, . \tag{2.3.5}$$

In general, both the initial state of the system and the set of stoichiometric coefficients must be specified. The elemental stoichiometry of each species is determined using a parsing algorithm based on certain conventions in naming species used in the stand-alone code and in DPLR.

These conventions are:

(1) Each element begins with a capital (upper case) letter. One or more lower-case letters may follow the starting letter.

(2) After each complete element name, an optional number may be given to indicate stoichiometric multiplicity.

(3) Ionization may be specified using a "+" sign for each instance of ionization. Ions (positive or negative) are treated like any other elemental constraint with a special designation of "charge."

(4) A single formatting exception is made for free electrons that are represented by the lower case letter "e," which, if found by itself, is converted to a single negative-charge constraint.

(5) Species in a non-gas state are indicated with a set of parenthesis after the element names using the designation of the non-gas state contained within the parentheses. Different non-gas state names are treated as different elements, such as "(s1)" or "(s2)" or "(b1)."

(6) Surface sites are considered as a species in the system with the designation of "E," followed by the name of the active site set within parenthesis.

This set of naming conventions allows the elemental balance constraints to be automatically determined by any system of species in the finite-rate code algorithm.

The final set of equations consists of Gibbs energy equations for Ng gas species, Ns surface species, and Nb bulk species, together with Ne elemental constraint equations and a possible volume equation, for a total of $Nq + Ne$ or $Nq+Ne+1$ equations, where $Nq = Ng + Ns + Nb$.

The set of equations is solved numerically using Newton iteration with "under relaxation" and limiting to enforce stability of the inherently unstable system. The set of degrees of freedom is taken as the natural log of the generalized concentrations of each active species and the Lagrange multipliers. Using the natural log of the variables is a trick used by Gordon and McBride[14] to prevent errors occurring in the solution due to negative concentrations and to improve stability of the system for cases with many orders of magnitude between the most- and least-populated species.

Using this set of variables, the implicit form of the gas species energy equation is:

$$\Delta\left(\ln\left(X_g\right)\right)+\sum_{i=1}^{Ne} a_{i,g}\Delta\Lambda_i = -\left[\frac{G_g^0}{RT}+\ln\left(X_g\right)+\ln\left(\frac{RT}{P_{ref}}\right)+\sum_{i=1}^{Ne} a_{i,g}\Lambda_i\right] . \qquad (2.3.6)$$

The implicit form of the adsorbed surface species energy equation is:

$$\Delta\left(\ln\left(X_s\right)\right)+\sum_{i=1}^{Ne} a_{i,s}\Delta\Lambda_i = -\left[\frac{G_s^0}{RT}+\ln\left(X_s\right)+\ln\left(\Phi_{ref}\right)+\sum_{i=1}^{Ne} a_{i,s}\Lambda_i\right] . \qquad (2.3.7)$$

The implicit form of the bulk species energy equation is:

$$\sum_{i=1}^{Ne} a_{i,b}\Delta\Lambda_i = -\left[\frac{G_b^0}{RT} + \ln(\chi_b) + \sum_{i=1}^{Ne} a_{i,b}\Lambda_i\right]. \tag{2.3.8}$$

The implicit form of the elemental constraint equation is:

$$\sum_{j=1}^{Ng} \delta a_{i,j}\Delta\left(\ln\left(X_j\right)\right) + \sum_{j=Ng+1}^{Nq} a_{i,j}\Delta\left(\ln\left(X_j\right)\right) + \left(\sum_{j=1}^{Ng} a_{i,j}X_j\right)\Delta\delta = -\left[\sum_{j=1}^{Ng}\delta a_{i,j}X_j + \sum_{j=Ng+1}^{Nq} a_{i,j}X_j - b_i^0\right]. \tag{2.3.9}$$

The implicit form of the volume constraint is:

$$\sum_{g=1}^{Ng} X_g\Delta\left(\ln\left(X_g\right)\right) = -\left[\sum_{g=1}^{Ng} X_g - \frac{P}{RT}\right]. \tag{2.3.10}$$

It is possible to significantly reduce the number of equations by substituting in the relationship for each gaseous and adsorbed species and solving a reduced set of $Ne + Nb + 1$ equations. For arbitrarily large systems with many species, this substitution greatly reduces the required memory and solution time. However, in the current application, the full set of equations is solved because the number of species is typically on the order of 10, and the savings are not significant. Making this reduced matrix modification is straightforward and is described in detail by Gordon and McBride.[14]

The concentration (mole fraction) of a bulk species is assumed to be constant, which is why it does not appear on the left-hand side of Eq. (2.3.8). This equation, therefore, acts more as a constraint on the values of the Lagrange multipliers. For the case in which the gas-phase concentrations are held constant, the first term on the left-hand side of Eq. (2.3.6) is removed, and the gas-phase equations become constraints on the Lagrange multipliers as well.

The closed system of equations is solved iteratively by building a matrix and inverting the Jacobian of the system using L-U decomposition. The matrix form of the equation set is

$$
\begin{bmatrix}
1 & \cdots & 0 & 0 & \cdots & 0 & 0 & \cdots & 0 & a_{1,1} & \cdots & a_{Ne,1} & 0 \\
\vdots & \ddots & \vdots & \vdots & \ddots & \vdots & \vdots & \ddots & \vdots & \vdots & \ddots & \vdots & \vdots \\
0 & \cdots & 1 & 0 & \cdots & 0 & 0 & \cdots & 0 & a_{1,Ng} & \cdots & a_{Ne,Ng} & 0 \\
0 & \cdots & 0 & 1 & \cdots & 0 & 0 & \cdots & 0 & a_{1,Ng+1} & \cdots & a_{Ne,Ng+1} & 0 \\
\vdots & \ddots & \vdots & \vdots & \ddots & \vdots & \vdots & \ddots & \vdots & \vdots & \ddots & \vdots & \vdots \\
0 & \cdots & 0 & 0 & \cdots & 1 & 0 & \cdots & 0 & a_{1,Ng+Ns} & \cdots & a_{Ne,Ng+Ns} & 0 \\
0 & \cdots & 0 & 0 & \cdots & 0 & 0 & \cdots & 0 & a_{1,Ng+Ns+1} & \cdots & a_{Ne,Ng+Ns+1} & 0 \\
\vdots & \ddots & \vdots & \vdots & \ddots & \vdots & \vdots & \ddots & \vdots & \vdots & \ddots & \vdots & \vdots \\
0 & \cdots & 0 & 0 & \cdots & 0 & 0 & \cdots & 0 & a_{1,Ng+Ns+Nb} & \cdots & a_{Ne,Ng+Ns+Nb} & 0 \\
a_{1,1}X_1 & \cdots & a_{1,Ng}X_{Ng} & a_{1,Ng+1}X_{Ng+1} & \cdots & a_{1,Ng+Ns}X_{Ng+Ns} & a_{1,Ng+Ns+1}X_{Ng+Ns+1} & \cdots & a_{1,Ng+Ns+Nb}X_{Ng+Ns+Nb} & 0 & \cdots & 0 & \sum_{j=1}^{Ng} a_{1,j}X_j \\
\vdots & \ddots & \vdots & \vdots & \ddots & \vdots & \vdots & \ddots & \vdots & \vdots & \ddots & \vdots & \vdots \\
a_{Ne,1}X_1 & \cdots & a_{Ne,Ng}X_{Ng} & a_{Ne,Ng+1}X_{Ng+1} & \cdots & a_{Ne,Ng+Ns}X_{Ng+Ns} & a_{Ne,Ng+Ns+Nb}X_{Ng+Ns+Nb} & \cdots & a_{Ne,Ng+Ns+Nb}X_{Ng+Ns+Nb} & 0 & \cdots & 0 & \sum_{j=1}^{Ng} a_{Ne,j}X_j \\
X_1 & \cdots & X_{Ng} & 0 & \cdots & 0 & 0 & \cdots & 0 & 0 & \cdots & 0 & 0
\end{bmatrix}
$$

$$
\begin{Bmatrix}
\Delta \ln(X_1) \\
\vdots \\
\Delta \ln(X_{Ng}) \\
\Delta \ln(X_{Ng+1}) \\
\vdots \\
\Delta \ln(X_{Ng+Ns}) \\
\Delta \ln(X_{Ng+Ns+1}) \\
\vdots \\
\Delta \ln(X_{Ng+Ns+Nb}) \\
\Delta\Lambda_1 \\
\vdots \\
\Delta\Lambda_{Ne} \\
\Delta\delta
\end{Bmatrix}
=
\begin{Bmatrix}
-\dfrac{G_1^0}{RT} - \ln(X_1) - \ln\left(\dfrac{RT}{P_{ref}}\right) \\
\vdots \\
-\dfrac{G_{Ng}^0}{RT} - \ln(X_{Ng}) - \ln\left(\dfrac{RT}{P_{ref}}\right) \\
-\dfrac{G_{Ng+1}^0}{RT} - \ln(X_{Ng+1}) - \ln(\Phi_{ref}) \\
\vdots \\
-\dfrac{G_{Ng+Ns}^0}{RT} - \ln(X_{Ng+Ns}) - \ln(\Phi_{ref}) \\
-\dfrac{G_{Ng+Ns+1}^0}{RT} + \ln(\chi_{nb,1}) \\
\vdots \\
-\dfrac{G_{Ng+Ns+Nb}^0}{RT} + \ln(\chi_{nb,Nb}) \\
-\sum_{j=1}^{Nq} a_{1,j}X_j + b_1^0 \\
\vdots \\
-\sum_{j=1}^{Nq} a_{Ne,j}X_j + b_{Ne}^0 \\
-\sum_{j=1}^{Ng} X_j + \dfrac{P}{RT}
\end{Bmatrix}
\qquad (2.3.11)
$$

This system of equations is solved iteratively for the change in the variable set. Values of $\ln(X_i)$ for all unfrozen species are updated but limited to a change of ±1.0 on any iteration. The Lagrange multiplier variables are set to zero to initialize the system and are reset to zero for all subsequent iterations. Gordon and McBride point out that there is no reason to assume any non-zero value for the Lagrange multipliers at any iteration, and there is no performance penalty in doing so.[14] If it is used, the volume constraint is initialized to 1.0 and reset to 1.0 for all subsequent iterations by the same logic. The algorithm, as coded, converges quickly, typically in approximately 20-30 iterations.

Finally, we note one numerical issue that can arise in building the system as related to some situations. For species that are fixed in this system (bulk species and possibly gas species), it is possible to create systems with reduced rank of the Jacobian matrix, meaning the matrix will have zero determinant. This occurs when two species that are defined in the finite-rate surface system have identical elemental composition, or when one species has an elemental composition that is a linear sum of other species.

One case in which this has come up is in assigning bulk carbon to multiple bulk phases of the material. This causes carbon (with the same Gibbs energy and composition) to appear multiple times in the system as manifested by a redundant row of the form of Eq. (2.3.8) in the matrix.

A second case in which this can occur is if the gas phase concentrations are fixed and equilibrium surface coverage is computed. Redundant records occur, for example, with N_2 and N species, O_2 and O, while a linear sum redundancy occurs between NO species and N and O atoms. In any of these cases, it is necessary to parse the species list and remove the redundant equations.

An intelligent selection of basis species constraints has been employed by using the simplex method from linear programming to select the set of basis species that will result in the minimum Gibbs free energy of the system. However, we note again that, for frozen gas composition, the resulting system predicted will not necessarily coincide with a thermodynamic equilibrium state. In such cases, it is more appropriate to compare the QSS state with the result of the finite-rate integration.

2.4 Stand-Alone Code Utilities

The stand-alone code implementing the finite-rate surface chemistry algorithm was developed mostly as a tool to diagnose and test out the basic algorithm numerics, as well as to debug surface chemistry systems that are developed both under this effort and in the future. The advantage of this approach is that the input data and core algorithm can be debugged and decoupled from the interaction with the gas-phase CFD solver.

The current implementation of the stand-alone code (Version 3-08-10) consists of a build system and four executable programs. The standard UNIX *make* program can be used to automatically compile all of the executables. The *make* program can be run from a UNIX command line by simply issuing the command "make" in the build directory; it will automatically use the settings in the text file called "*Makefile*" that exist in the build directory. The only setting in *Makefile* that is likely to routinely change is the name of the compiler at the very top of the file defined by the variable *F90C*. The stand-alone code adheres to the Fortran 90 standard, so any Fortran 90 compiler should be able to compile all four utilities with no trouble. The GNU compiler, *gfortran* (version 4.4.0), was used to develop the code, but any other compiler should work fine.

After the four utilities are successfully compiled, they should perform as follows:

srmodel (the main stand-alone code utility)

The *srmodel* utility is the main Fortran 90 implementation of the stand-alone code. This code integrates the non-convecting system in time for a specified number of iterations using a set of specifications provided in the file called *input.inp*. This special filename is always read in when the code is run, and an error will be issued if it is not present. Details of the required file format for *input.inp* are provided in section 5.3.

The *input.inp* file feeds the desired surface reaction model file, *filename.surf*, to the stand-alone code, as well as, the file *filename.blw* in the case of a system with blowing. The format of these two files is given in sections 5.1 and 5.2, respectively.

Using *input.inp*, the pressure, temperature, and initial gas phase composition of the system is specified, and the system (with surface and bulk species) is iterated to the number of specified iterations with a specified time step. Switches for time integration and optional output of the concentration history are available. System convergence using L1 and L2 norms is written by default to standard output, STDOUT, (the screen) at a frequency that can be controlled with a flag. Additional diagnostic information, including the equilibrium composition by free-energy minimization, is also controllable by a flag.

In addition to the *input.inp*, *filename.surf*, and *filename.blw* files, the files *lewis.thermo* and *lewis.bulk* are required to run the stand-alone code. These files provide Gibbs energy data from the NASA Glenn/Lewis thermodynamic database.[14-15] They are the same files used within the DPLR code.

checkinputs

The *checkinputs* utility was simply used to verify the Fortran 90 code by hardwiring the parameters from the original *SRmodel3.f* Fortran 77 code and performing calculations and output in exactly the same way. This utility simply insures that the Fortran 77 and the Fortran 90 codes are consistent. There is very little practical use for this utility.

checkders

The *checkders* utility is used to numerically verify all derivative combinations of the forward rate and desorption rate/equilibrium constant forms. A set of hard-wired parameters was implemented for the reaction parameters for all forms (the values of these parameters are unimportant for verifying the correctness of the derivatives). For each rate combination, the derivatives with respect to gas and wall temperatures are obtained from the subroutine analytically, and the result is compared to the numerically computed derivative of that rate by successively calling the subroutine with perturbed values of the temperatures. The analytical and numerical derivatives should match for all forms. If additional forms are implemented into the finite rate algorithm in the future, the bounds on this utility should be updated, and it should be used to verify the new forms (in fact, a couple of bugs in the sublimation reaction derivatives were caught in this way when it was added).

checksystem

The checksystem utility checks the Jacbobian of the source term of a real system. It reads in the same *input.inp* file as *srmodel* does, and it performs one iteration of the system to generate the analytical Jacobian matrix. This analytical Jacobian is compared against the numerically computed Jacobian by perturbing the temperatures and each concentration (one at a time) and by making calls to build the explicit system. Additional diagnostics are performed individually for all forward rates, Gibbs energies, desorption rates, and equilibrium constants. The total diagnostic output of this utility is used to verify that the derivatives computed for the system are exact for every term in the practical case of interest.

Chapter 3: DPLR Code Implementation

The general mass and energy balance control volumes for the surface of an ablating and pyrolyzing material, along with the steady-state ablation approximation, are described in Section 3.1.

For integration of the finite-rate surface reaction algorithm into DPLR, a mass balance at the surface is used to set the boundary condition between the surface chemistry model and the gas phase. Convective and diffusive transport between the gas phase and surface are incorporated into this boundary condition. The boundary condition is derived in Section 3.2.

The core finite-rate system source term algorithm is consistent (identical) between DPLR and the stand-alone code. However, a large number of auxiliary changes were required to make the algorithm function within the DPLR framework. Section 3.3 gives a very brief overview of the major changes; comprehensive details are in the DPLR source CVS repository hosted on the NASA Columbia computer.

Although the present finite-rate algorithm has been developed to run within the NASA Ames Research Center DPLR CFD code,[16] an effort was made to make the core routines easily portable to any other chemically-reacting CFD code. Section 3.4 gives a brief overview of how the finite-rate algorithm could be ported into other CFD codes.

3.1 General Mass and Energy Balance Control Volumes for Ablating Surfaces

For an ablating thermal protection system in which the surface is recessing with time, mass may be lost either by finite-rate surface reactions converting a bulk-phase reactant into a gas-phase product or through the specification of pyrolysis blowing as detailed in Section 1.11.

A schematic of the fronts associated with a generic decomposing material is shown in Figure 3.1.1. The char front is the depth of complete pyrolysis, the pyrolysis front is the depth where pyrolysis is initiated, and the unaffected front is the depth where both the initial composition and temperature are unchanged. The char zone (the material between the recessing surface and the char front) is associated with the bulk phase of the finite-rate surface chemistry framework.

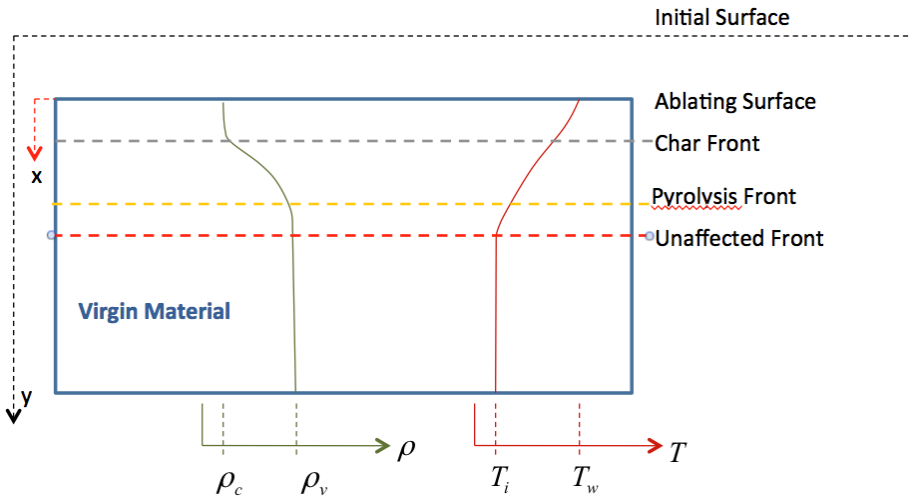

Figure 3.1.1 Schematic of Generic TPS Material Undergoing Pyrolysis and Char Mass Losses.

For a general case, in which both bulk mass loss and pyrolysis mass loss occur in unrelated proportions, the char front, the pyrolysis front, and the unaffected front all recede at different rates. Figure 3.1.2 shows the mass balance for a control volume at the ablating surface for this case.

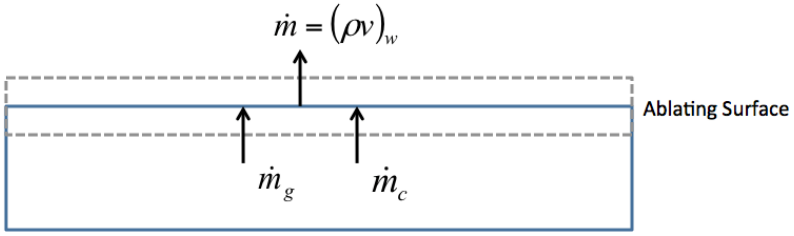

Figure 3.1.2 General Mass Control Volume at Ablating Surface.

The relationship for mass balance from this control volume is given in Eq. (3.1.1):

$$\dot{m}_c + \dot{m}_g = \dot{m} = (\rho v)_W \ . \tag{3.1.1}$$

The energy balance for the same control volume is shown in Fig. 3.1.3.

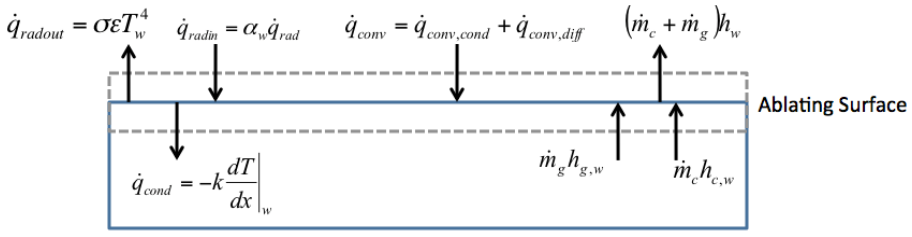

Figure 3.1.3 General Energy Control Volume at Ablating Surface.

The relationship for energy balance is given in Eq. (3.1.2):

$$\dot{q}_{conv} + \dot{m}_c h_{c,w} + \dot{m}_g h_{g,w} + \alpha_w \dot{q}_{rad} = \left(\dot{m}_c + \dot{m}_g\right) h_w + \sigma \varepsilon T_w^4 + \dot{q}_{cond} \ . \tag{3.1.2}$$

If the bulk phase in the finite-rate surface model framework is required to be at the same temperature as the gas at the surface and, if pyrolysis is modeled as inert to the surface reaction system, then no energy deposition to the surface is allowed, and the terms involving the enthalpy of the blown gases will cancel out:

$$\dot{q}_{conv} + \alpha_w \dot{q}_{rad} = \sigma \varepsilon T_w^4 + \dot{q}_{cond} \ . \tag{3.1.3}$$

Evaluation of the heat conduction term requires a model for conduction heat transfer into the ablating TPS. In the radiative equilibrium boundary condition approximation, heat conduction is simply neglected, resulting in Eq. (3.1.4):

$$\dot{q}_{conv} + \alpha_w \dot{q}_{rad} = \sigma \varepsilon T_w^4 \tag{3.1.4}$$

The required conduction model may also be eliminated by extending the control volume beyond the unaffected front to encompass the entire volume of material experiencing decomposition and heating. This extended control volume is defined in the coordinate system of the recessing surface; thus, reacting mass enters the gas phase by moving out of the top of the control volume as virgin mass enters from the bottom of the control volume. The control volume may be used to compute the balance of mass and energy in terms of the virgin material shown in Figures 3.1.4 and 3.1.5 and written in Eqs. (3.1.5) and (3.1.6).

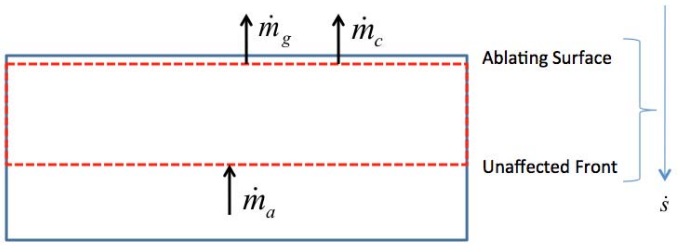

Figure 3.1.4 Mass Balance Control Volume for an Ablating Material Undergoing Steady-State Ablation.

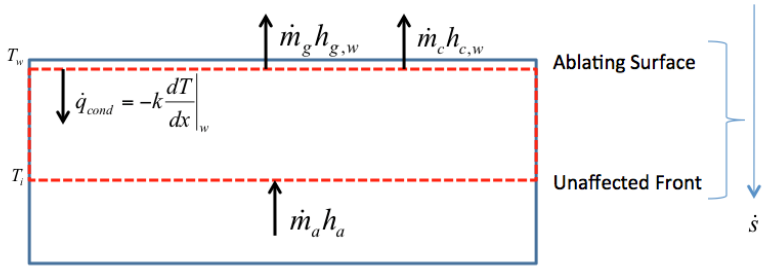

Figure 3.1.5 Energy Balance Control Volume for an Ablating Material Undergoing Steady-State Ablation.

$$\dot{m}_c + \dot{m}_g = \dot{m}_a \ . \tag{3.1.5}$$

$$\dot{q}_{cond} = \dot{m}_c \left(h_{c,w} - h_a \right) + \dot{m}_g \left(h_{g,w} - h_a \right) \ . \tag{3.1.6}$$

In general, the mass and energy relationships introduce additional unknowns, since the extension of the control volume to the unaffected front effectively replaces the unknown pyrolysis consumption rate with the unknown virgin material consumption rate. However, if the assumption of steady-state ablation is made,[17] meaning that the ablating surface, char front, pyrolysis front, and unaffected front all recede at the same rate such that the density and temperature profiles remain invariant within the control volume, the unknown virgin consumption rate may be replaced by the known ratio of char to virgin material density (the char yield C_y):

$$\dot{m}_g = \dot{m}_c \left[\frac{\dot{m}_a}{\dot{m}_c} - 1 \right] = \dot{m}_c \left[\frac{(\dot{s})\rho_a}{(\dot{s})\rho_c} - 1 \right] = \dot{m}_c \left[\frac{1}{C_y} - 1 \right] \ . \tag{3.1.7}$$

Using Eqs. (3.1.6) and (3.1.7), the heat conduction into the TPS may be written as:

$$\dot{q}_{cond} = \dot{m}_c h_{c,w} + \dot{m}_g h_{g,w} - \frac{\dot{m}_c}{C_y} h_a \ . \tag{3.1.8}$$

Substitution of the heat conduction from Eq. (3.1.8) into the surface energy balance, Eq. (3.1.2) gives the relationship for steady-state energy balance (SSEB) for CFD applications:

$$\dot{q}_{conv} + \alpha_w \dot{q}_{rad} = \frac{\dot{m}_c}{C_y} \left(h_w - h_a \right) + \sigma \varepsilon T_w^4 \ . \tag{3.1.9}$$

The enthalpy of the virgin (unaffected) material is treated as a constant associated with the particular material. Within the DPLR framework, this constant should be the absolute enthalpy of the material defined relative to 0 K to be consistent with the gas-phase convention.

3.2 Tightly Coupled Implicit Surface Boundary Condition for DPLR

For the integration of the finite-rate surface-chemistry model with DPLR, mass balance at the surface is utilized to set the boundary condition for each species in the gas-phase environment. For the infinitely thin control volume at the surface at any instant in time, the rate of diffusion of gaseous species away from the surface into the gas-phase interior and the rate that the entire mixture is convected away from the surface due to bulk production will exactly balance the rate of production from surface reactions of that species.

In this section, we use the subscripts *g* and *s* exclusively to indicate a vector length over all gas or surface species, respectively. A partial derivative of a vector of an indicated length implies that the resulting term is a matrix with a number of rows matching the indicated length, while a partial derivative with respect to an indicated length vector implies that the result has a number of columns matching the indicated length.

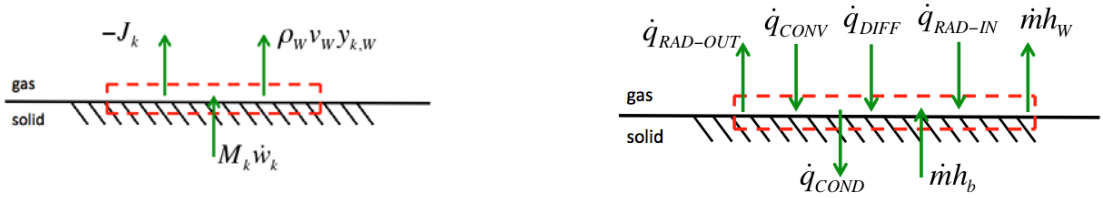

(a) Gas-species mass balance **(b) Energy balance**

Figure 3.2.1. Surface Control Volumes for DPLR Boundary Conditions.

Mass balance for each gaseous species, *k*, at the surface from Fig. 3.2.1a, is written in Eq. (3.2.1), which represents the rate at which mass of each gas phase species changes at the surface (e.g. in units of kg/m^2-s). The source term from the finite-rate surface chemistry model is computed on a molar basis (noting that a conversion factor of 0.001 is required to convert from gmol/m^2-s to kgmol/m^2-s for use in DPLR), and the finite-rate framework allows for production to come from either finite-rate reactions occurring at the surface and/or from simple approximations to pyrolysis flow as discussed in Section 1.11.

$$-\rho_w D_k \nabla y_k \Big|_w + \rho_w v_w y_{k,w} = M_k \dot{w}_k \tag{3.2.1}$$

Here, we note that the derivation of the implicit mass balance relationship is performed assuming Fickian diffusion with mass fractions as the unknowns for simplicity, but it is straightforward to extend these results to better diffusion models, such as self-consistent effective binary diffusion (SCEBD)[18-19] or iterative Stefan-Maxwell,[20] since those models amount to adding one or more correction terms to the flux appearing in the first term of Eq. (3.2.1). Gosse and Candler[21] discuss these improved flux schemes more thoroughly.

Energy balance at the surface shown in Fig. 3.2.1b is typically enforced using the radiative equilibrium boundary condition, with the model formulation constraint that material gained from the bulk phase has the same temperature as the gas at the surface, and by assuming that the conduction term into the TPS is negligible. However, as detailed in the previous section, by assuming steady-state ablation conditions, the control volume in Fig. 3.2.1b may be extended into the material to the unaffected front to eliminate the unknown conduction term. The solution of the steady-state energy balance (SSEB) equation is a straightforward extension of radiative equilibrium, since the only additional term imposed by the surface model is the enthalpy of the virgin material, which we consider to be a constant of the particular material. The SSEB equation is given in Eq. (3.2.2):

$$\dot{q}_{CONV} + \dot{q}_{DIFF} + \dot{q}_{RAD-IN} = \dot{m}h_W - \dot{m}h_a + \dot{q}_{RAD-OUT}$$
$$\sum_{m=1}^{N_T} k_m \nabla T_m \Big|_w + \sum_{k=1}^{N_g} h_k \rho D_k \nabla y_k \Big|_w + \alpha_w \dot{q}_{rad} = (\rho v)_W (h_w - h_a) + \sigma \varepsilon T_w^4 \qquad (3.2.2)$$

The discretized form of Eq. (3.2.1) is given in Eq. (3.2.3), where the function, F_k, is defined to be zero, a constraint that will be enforced using a Newton iteration scheme.

$$F_k = (y_{k,w} - y_{k,1}) + \frac{\Delta n}{D_k} v_w y_{k,w} - \frac{\Delta n M_k}{\rho_w D_k} \dot{w}_k = 0 \ . \qquad (3.2.3)$$

Purely for convenience, the set of (assumed constant) coefficients preceding the production source term and the convection term are grouped as:

$$\alpha_k \equiv \frac{\Delta n M_k}{\rho_w D_k} \qquad (3.2.4)$$

and,

$$\beta_k \equiv \frac{\Delta n}{D_k} \ . \qquad (3.2.5)$$

Implicit coupling is required for the production term that appears in the gas-phase boundary equations. The implicit form of the gas-phase boundary condition in Eq. (3.2.3) can be expressed as a series expansion about the n + 1 time level and enforcing $F_k^{n+1} = 0$ as shown in Eq. (3.2.6) for each gaseous species, where the bracket notation, [ ], is used to indicate a vector:

$$\frac{\partial F_k}{\partial [y]_{g,w}} \Delta^n [y]_{g,w} + \frac{\partial F_k}{\partial [y]_{g,1}} \Delta^n [y]_{g,1} + \frac{\partial F_k}{\partial [X]_s} \Delta^n [X]_s + \frac{\partial F_k}{\partial T} \Delta^n T + \frac{\partial F_k}{\partial v} \Delta^n v = -F_k \qquad (3.2.6)$$

Expressed in this form, the boundary condition is dependent on the state of the gas-phase interior composition away from the wall at the first cell center (subscript "*g*,1"), the gas-phase composition at the wall (subscript "*g*,*w*"), the gas-phase wall temperature, the wall-normal velocity, and the adsorbed surface composition (subscript "s"). The rate of change of the bulk phase is defined to be identically zero for all situations, so no term appears from bulk species dependencies.

The total production of each gaseous species is given in Eq. (3.2.7). The composite expression can include contributions from surface reactions (labeled with a "*c*") as well as additional contributions from pyrolysis. For explicit pyrolysis or transpiration (labeled with an "*e*"), additional mass production is added to the total production rate. For steady-state pyrolysis (last

term), the additional production of the gaseous species is proportional to the bulk-phase production rate, so the Jacobian of the source term must be modified:

$$\dot{w}_k = \dot{w}_{k,c} + \dot{w}_{k,e} + \frac{\chi_k}{\sum_{j=1}^{Ng} \chi_j M_j} \left(\frac{1}{C_y} - 1 \right) \left(- \sum_{b=1}^{Nb} M_b \dot{w}_b \right) \tag{3.2.7}$$

Here, the char yield parameter, C_y, accounts for any steady-state pyrolysis, and C_y is set equal to 1.0 if there is no pyrolysis present. The implicit Jacobian of this source term is given in Eq. (3.2.8), where *q* is used to represent a generic independent variable:

$$\frac{\partial \dot{w}_k}{\partial q} = \frac{\partial \dot{w}_{k,c}}{\partial q} + \frac{\chi_k}{\sum_{j=1}^{Ng} \chi_j M_j} \left(\frac{1}{C_y} - 1 \right) \left(- \sum_{b=1}^{Nb} M_b \frac{\partial \dot{w}_b}{\partial q} \right) . \tag{3.2.8}$$

For adsorbed surface species and bulk-phase species, there is no possibility of diffusion or convection, so the rate of change of the vector of those species is given in Eq. (3.2.9):

$$\frac{\partial [X]_s}{\partial t} = [\dot{w}]_s . \tag{3.2.9}$$

The implicit form of the adsorbed surface species concentration vector may be written by expanding Eqn.(3.2.9) at the *n+1* time level as given in Eq. (3.2.10):

$$\frac{\Delta^n [X]_s}{\Delta t} = [\dot{w}]_s + \frac{\partial [\dot{w}]_s}{\partial [X]_s} \Delta^n [X]_s + \frac{\partial [\dot{w}]_s}{\partial [X]_g} \Delta^n [X]_g + \frac{\partial [\dot{w}]_s}{\partial T} \Delta^n T \tag{3.2.10}$$

This set of equations is dependent on the gas-phase composition at the wall, the gas-phase wall temperature (assumed equal to the surface-phase wall temperature), and the surface-phase composition. The vector of non-gaseous concentrations may be solved for as shown in Eq. (3.2.11):

$$\begin{aligned} \Delta^n [X]_s = & \left(\frac{[I]_s}{\Delta t} - \left. \frac{\partial [\dot{w}]_s}{\partial [X]_s} \right|_n \right)^{-1} [\dot{w}]_s \big|_n + \left(\frac{[I]_s}{\Delta t} - \left. \frac{\partial [\dot{w}]_s}{\partial [X]_s} \right|_n \right)^{-1} \left. \frac{\partial [\dot{w}]_s}{\partial [X]_g} \right|_n \Delta^n [X]_g \\ & + \left(\frac{[I]_s}{\Delta t} - \left. \frac{\partial [\dot{w}]_s}{\partial [X]_s} \right|_n \right)^{-1} \left. \frac{\partial [\dot{w}]_s}{\partial T} \right|_n \Delta^n T \end{aligned} \tag{3.2.11}$$

The surface variable vector of unknowns in Eq. (3.2.11) may be substituted into Eq. (3.2.6).

Additionally, a relationship is required for the conversion of the gas-phase concentrations to the gas-phase mass fractions, or whatever variable is used consistent with the flux approximation (mass fractions, mole fractions, concentrations, etc.). This is given in Eq. (3.2.12) for this derivation in terms of mass fractions:

$$\frac{\partial X_{k,w}}{\partial y_{k,w}} = \frac{\rho_w}{M_k} \ . \tag{3.2.12}$$

After rearranging the remaining terms, the implicit form of the gas-phase boundary condition is given in Eq. (3.2.13), where all derivatives are evaluated at the *n* time level (the subscripts are dropped). All terms in the equation are known in the gas phase, but the implicit contribution of the surface reactions remain:

$$\begin{aligned}
&\left\{(1+\beta_k \nu_w)\delta_{g,k} - \alpha_k \left[\frac{\partial \dot{w}_k}{\partial [X]_{g,w}} + \frac{\partial \dot{w}_k}{\partial [X]_s} \left(\frac{[I]_s}{\Delta t} - \frac{\partial [\dot{w}]_s}{\partial [X]_s} \right)^{-1} \frac{\partial [\dot{w}]_s}{\partial [X]_{g,w}} \right] \frac{\partial [X]_{g,w}}{\partial [c]_{g,w}} \right\} \Delta^n [y]_{g,w} \\
&\quad - (1)\Delta^n [y]_{k,1} + (\beta_k y_{k,w}) \Delta^n \nu_w - \alpha_k \left[\frac{\partial \dot{w}_k}{\partial T} + \frac{\partial \dot{w}_k}{\partial [X]_s} \left(\frac{[I]_s}{\Delta t} - \frac{\partial [\dot{w}]_s}{\partial [X]_s} \right)^{-1} \frac{\partial [\dot{w}]_s}{\partial T} \right] \Delta^n T \\
&\quad = -\left[(y_{k,w} - y_{k,1}) + \beta_k \nu_w y_{k,w} - \alpha_k \dot{w}_k \right] + \alpha_k \frac{\partial \dot{w}_k}{\partial [X]_s} \left(\frac{[I]_s}{\Delta t} - \frac{\partial [\dot{w}]_s}{\partial [X]_s} \right)^{-1} [\dot{w}]_s
\end{aligned} \tag{3.2.13}$$

In addition to the equations for the gas-phase species masses, the rate of wall-normal velocity blowing also needs to be computed as a function of the non-gas-phase production terms. Specifically, the wall-normal mass blowing (the product of wall density and the velocity normal to the surface) is equal to the negative of the production of the bulk-phase species, or the rate at which solid-phase material is removed from the surface. This relationship is shown in Eq. (3.2.14):

$$\rho_w \nu_w = -\frac{1}{C_y} \sum_{b=1}^{NB} M_b \dot{w}_b + \dot{m}_{p,e} \ . \tag{3.2.14}$$

Explicit gaseous mass addition that is not proportional to bulk production is added to the explicit mass balance by the last term.

The implicit form of the wall blowing velocity is given in Eq. (3.2.15), which includes dependencies on the wall-normal velocity component, the gas-phase species mass fraction vector, and the surface-phase species concentrations:

$$\rho_w \Delta^n \nu_w + \left(\sum_{b=1}^{NB} \frac{M_b}{C_y} \frac{\partial \dot{w}_b}{\partial [X]_g} \frac{\partial [X]_{g,w}}{\partial [y]_{g,w}} \right) \Delta^n [y]_{g,w} + \left(\sum_{b=1}^{NB} \frac{M_b}{C_y} \frac{\partial \dot{w}_b}{\partial T} \right) \Delta^n T$$

$$+\left(\sum_{b=1}^{NB}\frac{M_b}{C_y}\frac{\partial \dot{w}_b}{\partial [X]_s}\right)\Delta^n[X]_s = -\left[\rho_w v_w + \sum_{b=1}^{NB}\frac{M_b}{C_y}\dot{w}_b - \dot{m}_{p,e}\right] \tag{3.2.15}$$

As before, the expression for the surface-phase concentration vector can be substituted in from Eq. (3.2.10), and the result is shown in Eq. (3.2.16):

$$\begin{aligned}
&\rho_w \Delta^n v_w + \left\{\left(\sum_{b=1}^{NB}\frac{M_b}{C_y}\frac{\partial \dot{w}_b}{\partial [X]_s}\right)\left(\frac{[I]_s}{\Delta t} - \frac{\partial [\dot{w}]_s}{\partial [X]_s}\right)^{-1}\frac{\partial [\dot{w}]_s}{\partial T}\right\}\Delta^n T \\
&+\left[\left(\sum_{b=1}^{NB}\frac{M_b}{C_y}\frac{\partial \dot{w}_b}{\partial [X]_g}\right)+\left(\sum_{b=1}^{NB}\frac{M_b}{C_y}\frac{\partial \dot{w}_b}{\partial [X]_s}\right)\left(\frac{[I]_s}{\Delta t} - \frac{\partial [\dot{w}]_s}{\partial [X]_s}\right)^{-1}\frac{\partial [\dot{w}]_s}{\partial [X]_{g,w}}\right]\frac{\partial [X]_{g,w}}{\partial [y]_{g,w}}\Delta^n [y]_{g,w} \\
&= -\left[\rho_w v_w + \sum_{b=1}^{NB}\frac{M_b}{C_y}\dot{w}_b - \dot{m}_{p,e}\right] - \left(\sum_{b=1}^{NB}\frac{M_b}{C_y}\frac{\partial \dot{w}_b}{\partial [X]_s}\right)^T\left(\frac{[I]_s}{\Delta t} - \frac{\partial [\dot{w}]_s}{\partial [X]_s}\right)^{-1}[\dot{w}]_s
\end{aligned} \tag{3.2.16}$$

For systems with no bulk-phase production (i.e., only gas- and surface-phase production rates), the blowing velocity is zero. The combined set of equations given in Eq. (3.2.13), and Eq. (3.2.16) represents the implicitly coupled implementation of the finite-rate surface system.

As a post-processing step to each solution iteration, the surface species concentrations are updated using Eq. (3.2.11) and the newly computed delta values of all gas phase quantities. It should also be noted that the time step appears in the surface system. This time step should be the physical time step of the gas flow for a globally time-accurate method but, for steady-state problems, the possibility exists of adjusting this time step to improve stability or maximize convergence rate. Strategies for doing this have not been studied, but the potential exists.

3.3 Changes Required to Implement the Finite-Rate Algorithm into DPLR

The core finite-rate system source term algorithm is consistent between DPLR and the stand-alone code. This means that the source code has been copied from the stand-alone code directly into DPLR. However, in addition to the core code, a large number of auxiliary additions were required to make the algorithm function within the DPLR framework. These changes amounted to several thousand lines of additional code spread in many places throughout the DPLR source tree. The details of the changes are in the DPLR source CVS repository hosted on the NASA Columbia computer, but a very brief list of major elements is given here for documentation purposes:

- Wrapping of the finite-rate source term into the gas-phase boundary condition (discussed in Section 3.2 above). This includes logic-to-handle cases in which some gas-phase species do not participate in the surface system or in which gas-phase species are stored in a different order than the gas-phase participant species in the finite-rate surface system.
- Update of surface concentrations as part of the post-iteration boundary update process.
- Use of boundary condition logic required to enable to the finite-rate surface model which is tied to the flag icatmd=990 in the DPLR input file.
- Logic to allocate storage for and pass all the surface model rate and species data to all processes via MPI.
- Flags and arrays to track multiple surface models and which boundary cells are using which model (or none at all).
- Allocation of surface data storage arrays to efficiently store surface cell objects on a face by face basic without wasting memory on unused cells.
- Logic to collect surface concentrations from all processes via message passing interface (MPI) and to write to the DPLR restart file for archival storage.
- Logic-to-read surface concentrations from the DPLR restart file; distribute to all processes via MPI for clean restart of a solution.
- Logic-to-write all finite-rate model data flags (for potentially multiple models) to the restart file for post-processing.
- Logic to have postflow extract restart model data flags from the restart file and rebuild the finite rate data file(s) used to run the problem.
- Extraction of surface data with postflow and calculation of global loss efficiencies and branching fractions defined in section 1.10.

3.4 Steps Required to Port the Finite-Rate Algorithm into a New CFD Code

The Finite-Rate Surface Reaction Model has been developed to run within the NASA Ames Research Center DPLR CFD code, but an effort has been made to make the core routines of the model easily portable to any other chemically reacting CFD code using the source in the stand-alone code package. In fact, there is no additional complexity associated with making the model work with an unstructured code, as long as the code enforces wall boundary conditions at cell faces. A brief discussion of the likely set of minimal steps necessary (in order) to port the model into a different CFD code is as follows:

- Copy the *surfacemod.F* and *FiniteRateSurface.F* files into the CFD code build environment. The first file contains a Fortran Module that defines several global parameters and two derived type definitions–one derived type that contains all data

associated with a single finite-rate surface model, and one derived type that contains all data associated with a single surface cell.

- Gas phase Gibbs energies in the Gordon/McBride format are expected from the solver. DPLR already uses this data so the existing stored arrays were used. For a solver that does not currently have this data, the *readlewis.F* file has a basic routine to read and parse the data from the *lewis.thermo* data file.
- Make one or more calls during code initialization to read_finite_rate_surf_file(). Required arguments are: (1) the finite-rate surface data file name, (2) an object of the derived type finiteRateSurfaceModelType, and (3) error flag. This routine will read model data and initialize the object data fields.
- Next, make a call during initialization to read_lewis_bulk_file() for each initialized model object. Required arguments to this routine are: (1) file name for the bulk phase data (*lewis.bulk*), (2) an initialized object of derived type finiteRateSurfaceModelType, (3) gas-phase Gibbs coefficient data array, (4) gas-phase Gibbs temperature range array, (5) number of temperature ranges, (6) error flag. This routine will copy the gas-phase Gibbs data for internal use, read in the bulk-phase Gibbs data, and generate surface-phase Gibbs data as needed.
- Next, for each model object, make a call to finite_rate_surf_sanity_check(). Required arguments are: (1) an initialized model object. This routine will verify the object data that was read in and issue warnings or errors if the data is inappropriate.
- Next, one object of derived type finiteRateSurfaceCell should be declared or allocated for each surface cell face that the solver wishes to use the finite-rate surface model on. This can either be static arrays of objects or allocated arrays depending on the solver implementation. In DPLR, for example, this is dynamically allocated as efficiently as possible by allocating ranged arrays for only the cell ranges that have the finite-rate surface boundary condition applied.
- Next, for each finiteRateSurfaceCell object, make one call to finite_rate_surf_initialize(). Required arguments are: (1) the finiteRateSurfaceCell object, and (2) a finiteRateSurfaceModelType object to associate to. There can be more than one finiteRateSurfaceModelType, since each cell will permanently store a local pointer to the correct model object and allocate memory appropriately.
- For each iteration of the flow solver, the following steps are necessary for each active cell:
    - Manually set the local wall temperature in degrees Kelvin and pressure in Pascals into the cell fields gas_tmpr, wall_tmpr, and wall_pres. Separate gas and wall temperatures fields were initially employed in building the model with the intention of allowing for thermal slip at the surface, but this capability has never been finished, so both fields should be set to the same value. Then, manually set all the current gas-phase concentrations in mol/m^3-s into the concentration(1-NG) array.
    - Call finite_rate_compute_system() with the only required argument as the cell object.

- At this state, the *cell%srhs* array is populated with the molar production rates and the *cell%sjacobian* array is populated with all the derivatives of the finite-rate surface system. The species and derivatives are stored, in order, as gas-phase species (1:cell%num_gas), surface-phase species (cell%num_gas+1:cell%num_nonbulk), bulk-phase species (cell%num_nonbulk:cell%num_species), and temperature derivatives (cell%num_species:cell%num_eqns). The Jacobian array is a square matrix that stores these derivatives for each species in the system.
- The way the solver chooses to use this information is code dependent. As detailed in section 3.2, the implementation in DPLR wraps the non-gas phase dependencies implicitly into the boundary condition. It is important to note that the Jacobian array stores two temperature derivatives–one for the derivative with respect to T_s, and one with respect to T_w. For a fully accommodated surface, these two derivatives should be added together. The surface blowing rate is computed from the inverse of the mass-weighted sum of all the bulk production rates.
- Finally, as a post-processing step to each iteration, the surface-phase species concentrations need to be updated manually using the *cell%sjacobian* and *cell%srhs* arrays in each cell and the computed local values for changes in each gas phase concentration and temperatures obtained in the solver.

There are several additional implementation issues that need to be considered (as noted in the previous section) such as reading/writing restart data, dynamic array allocation, boundary condition wrapping, and post-processing. However, these steps allow the core routines to be used directly in nearly any CFD code.

Chapter 4: Analytic Derivatives for the Jacobian

The derivatives required for the Jacobian for implicit solutions of the equation set can all be evaluated analytically and are derived below.

4.1 Species and Temperature Derivatives of the Source Term

The source term of any species (gas, surface, or bulk) is the sum of the production of all reactions in which that species participates:

$$\dot{w}_k = \sum_{i=1}^{I} \nu_{ki} \left\{ k_{fi} \left[\prod_{k=1}^{K} X_k^{\nu'_{ki}} - \frac{1}{K_{ci}} \prod_{k=1}^{K} X_k^{\nu''_{ki}} \right] \right\} , \tag{4.1.1}$$

where the backward rate coefficient k_{bi} has been substituted using the equilibrium constant relationship $k_{bi} = k_{fi} / K_{ci}$.

The derivative of the source term with respect to each species concentration is given in Eq. (4.1.2), where the concentration must be limited to some very small value greater than zero:

$$\frac{\partial \dot{w}_k}{\partial [X_k]} = \sum_{i=1}^{I} \nu_{ki} \left\{ k_{fi} \left[\frac{\nu'_{ki}}{[X_k]} \prod_{k=1}^{K} X_k^{\nu'_{ki}} - \frac{1}{K_{ci}} \frac{\nu''_{ki}}{[X_k]} \prod_{k=1}^{K} X_k^{\nu''_{ki}} \right] \right\} . \tag{4.1.2}$$

The derivative of the source term with respect to the temperature is given in Eq. (4.1.3):

$$\frac{\partial \dot{w}_k}{\partial T} = \sum_{i=1}^{I} \nu_{ki} \left\{ \frac{\partial k_{fi}}{\partial T} \prod_{k=1}^{K} X_k^{\nu'_{ki}} - \frac{1}{K_{ci}} \left(\frac{\partial k_{fi}}{\partial T} - \frac{k_{fi}}{K_{ci}} \frac{\partial K_{ci}}{\partial T} \right) \prod_{k=1}^{K} X_k^{\nu''_{ki}} \right\} . \tag{4.1.3}$$

Further analytic evaluation of Eq. (4.1.3) requires explicit expressions for the temperature derivatives of the forward reaction rate coefficients, k_{fi}, and the concentration-based equilibrium constants, K_{ci}. These are presented in the following two sections.

4.2 Temperature Derivatives of the Forward Rate Coefficients

The forward rate coefficient for each surface reaction is specified in a form that depends on the type of reaction being modeled.

Type 0: Arrhenius

For an Arrhenius rate expression with constant values of A, β, and E_a:

$$k_f^{(0)} = AT'^{\beta} \exp\left[-\frac{E_a}{RT}\right] \tag{4.2.1}$$

and the derivative with respect to temperature is:

$$\frac{\partial k_f^{(0)}}{\partial T} = \frac{k_f^{(0)}}{T}\left(\beta + \frac{E_a}{RT}\right) . \tag{4.2.2}$$

Type 1: Adsorption

For an adsorption reaction, the explicit expressions for the sticking coefficient and the thermal velocity are substituted to obtain the expression in Eq. (4.2.3):

$$k_f^{(1)} = \left(\frac{1}{4\Phi_s^{\nu_s}}\right)\left(\sqrt{\frac{8RT}{\pi M_k}}\right)\min\left[1.0, S_0 T'^{\beta}\right]\exp\left(-\frac{E_{ad}}{RT}\right) . \tag{4.2.3}$$

The derivative with respect to the wall temperature is given by either Eq. (4.2.4) or Eq. (4.2.5), depending on which branch of the min function is active:

$$\frac{\partial k_f^{(1)}}{\partial T} = \frac{k_f^{(1)}}{T}\left(\beta + \frac{1}{2} + \frac{E_{ad}}{RT}\right) \tag{4.2.4}$$

$$\frac{\partial k_f^{(1)}}{\partial T} = \frac{k_f^{(1)}}{T}\left(\frac{1}{2} + \frac{E_{ad}}{RT}\right) \tag{4.2.5}$$

Type 2: Eley-Rideal Recombination

The form of the Eley-Rideal recombination reaction is functionally identical to that of the adsorption reaction and contains the same dependencies on temperature:

$$k_f^{(2)} = \left(\frac{1}{4\Phi_s^{\nu_s}}\right)\left(\sqrt{\frac{8RT}{\pi M_k}}\right)\min\left[1.0, \gamma_{er} T'^{\beta}\right]\exp\left(-\frac{E_{er}}{RT}\right) . \tag{4.2.6}$$

The derivatives of this form are given by either Eq. (4.2.7) or Eq. (4.2.8):

$$\frac{\partial k_f^{(2)}}{\partial T} = \frac{k_f^{(2)}}{T}\left(\beta + \frac{1}{2} + \frac{E_{er}}{RT}\right) \tag{4.2.7}$$

$$\frac{\partial k_f^{(2)}}{\partial T} = \frac{k_f^{(2)}}{T}\left(\frac{1}{2} + \frac{E_{er}}{RT}\right) . \tag{4.2.8}$$

Type 3: Langmuir-Hinshelwood Recombination

Langmuir-Hinshelwood recombination is given in Eq. (4.2.9):

$$k_f^{(3)} = \left(\sqrt{\frac{\pi RT}{2M_k}}\right)\sqrt{A_v}\,\Phi_s^{(1.5-\nu_s)} C_{lh} T'^{\beta} \exp\left(-\frac{E_{lh}}{RT}\right) . \tag{4.2.9}$$

The temperature derivative of Eq. (4.2.9) is given in Eq. (4.2.10):

$$\frac{\partial k_f^{(3)}}{\partial T} = \frac{k_f^{(3)}}{T}\left(\beta + \frac{1}{2} + \frac{E_{lh}}{RT}\right) . \tag{4.2.10}$$

Type 4: Sublimation

The sublimation reaction rate coefficient is given by Eq. (4.2.11):

$$k_f^{(4)} = \left(\sqrt{\frac{8RT}{\pi M_k}}\right)\left(\frac{1}{4\Phi_s^{\nu_s}}\right)\left(\frac{\gamma_{sub} T'^{\beta}}{RT}\right)\exp\left(-\frac{E_{sub}}{RT}\right) . \tag{4.2.11}$$

The temperature derivative of Eq. (4.2.11) is given in Eq. (4.2.12):

$$\frac{\partial k_f^{(4)}}{\partial T} = \frac{k_f^{(4)}}{T}\left(\beta - \frac{1}{2} + \frac{E_{sub}}{RT}\right) . \tag{4.2.12}$$

4.3 Temperature Derivatives of the Equilibrium Constants

The *activity-based* equilibrium constant for a surface reaction is a function of the Gibbs energies:

$$K_{ai} = \exp\left(\frac{-\sum_{k=1}^{K} \nu_{ki} G_k^0(T)}{RT}\right) . \tag{4.3.1}$$

The *concentration-based* equilibrium constant is related to the activity-based equilibrium constant by:

$$K_{ci} = \left(\frac{P_{ref}}{RT}\right)^{\nu_{gi}} K_{ai} = \left(\frac{P_{ref}}{RT}\right)^{\nu_{gi}} \exp\left(\frac{-\sum_{k=1}^{K} \nu_{ki} G_k^0(T)}{RT}\right) . \tag{4.3.2}$$

The temperature derivatives of Eq. (4.3.1) and Eq. (4.3.2) are, respectively:

$$\frac{\partial K_{ai}}{\partial T} = \frac{K_{ai}}{RT}\left(\frac{\sum_{k=1}^{K} \nu_{ki} G_k^0(T)}{T} - \sum_{k=1}^{K} \nu_{ki} \frac{\partial G_k^0(T)}{\partial T}\right) \tag{4.3.3}$$

and,

$$\frac{\partial K_{ci}}{\partial T} = \frac{K_{ci}}{RT}\left(\frac{\sum_{k=1}^{K} \nu_{ki} G_k^0(T)}{T} - \sum_{k=1}^{K} \nu_{ki} \frac{\partial G_k^0(T)}{\partial T} - \nu_{gi} R\right) . \tag{4.3.4}$$

Further evaluation requires analytic expressions for the temperature derivatives of the Gibbs energies.

4.4 Temperature Derivatives of the Gibbs Energy

Gas and Bulk Species

For gas-phase or bulk-phase species, these Gibbs energy values are provided in non-dimensional forms as a function of temperature from the database provided by NASA Lewis (Glenn) from the work of Gordon and McBride[14] on the CEA code. This database is also used by DPLR, so the calculation of Gibbs energy between the CFD solver and the surface algorithm is consistent:

$$\frac{G_k^0}{RT} = \frac{H_k^0}{RT} - \frac{S_k^0}{R} \tag{4.4.1}$$

The dimensionless enthalpy and entropy terms on the right-hand side of Eq. (4.4.1) are provided by the Lewis database for several ranges of temperatures (usually 200K-1,000K, 1,000K-6,000K, and 6,000K-20,000K). The latest release of the database enforces continuity of the values and the first derivatives of the enthalpy and entropy functions between curve fits for adjacent temperature ranges. This ensures continuity of the Jacobian of the system for integration into the CFD and stand-alone solvers.

The dimensionless enthalpy and entropy functions are given by

$$\frac{H_k^0}{RT} = -a_1 T^{-2} + a_2 \frac{\ln T}{T} + a_3 + \frac{1}{2}a_4 T + \frac{1}{3}a_5 T^2 + \frac{1}{4}a_6 T^3 + \frac{1}{5}a_7 T^4 + \frac{b_1}{T} \tag{4.4.2}$$

and

$$\frac{S_k^0}{R} = -\frac{1}{2}a_1 T^{-2} - a_2 T^{-1} + a_3 \ln T + a_4 T + \frac{1}{2}a_5 T^2 + \frac{1}{3}a_6 T^3 + \frac{1}{4}a_7 T^4 + b_2 \ . \tag{4.4.3}$$

The temperature derivatives of these two functions are given in Eq. (4.4.4) and Eq. (4.4.5):

$$\frac{\partial\left(H_k^0 / RT\right)}{\partial T} = 2a_1 T^{-3} + a_2 T^{-2}\left(1 - \ln T\right) + \frac{1}{2}a_4 + \frac{2}{3}a_5 T + \frac{3}{4}a_6 T^2 + \frac{4}{5}a_7 T^3 - b_1 T^{-2} \tag{4.4.4}$$

and,

$$\frac{\partial\left(S_k^0 / R\right)}{\partial T} = a_1 T^{-3} + a_2 T^{-2} + a_3 T^{-1} + a_4 + a_5 T + a_6 T^2 + a_7 T^3 \ . \tag{4.4.5}$$

The temperature derivative of the dimensional Gibbs energy is given by:

$$\frac{\partial G_k^0}{\partial T} = \left[\frac{\partial\left(H_k^0 \middle/ RT \right)}{\partial T} - \frac{\partial\left(S_k^0 \middle/ R \right)}{\partial T} \right] RT + \left(\frac{H_k^0}{RT} - \frac{S_k^0}{R} \right) R \ . \tag{4.4.6}$$

Surface Species

Experimental Gibbs data are typically not available for adsorbed surface species, and the Gibbs energy is computed from the unitary adsorption/desorption reaction $A + [s] \leftrightarrow [A]_s$, using the definition:

$$G_{As}^0 = G_A^0 - RT \ln\left(K_a\right) \ , \tag{4.4.7}$$

where the Gibbs energy of the empty site, G_s^0, has been set to zero. Eq. (4.4.7) can be expressed in terms of the *concentration-based* equilibrium constant by inverting Eq. (4.3.2) as:

$$G_{As}^0 = G_A^0 - RT \ln\left(\frac{K_c P_{ref}}{RT} \right) \ , \tag{4.4.8}$$

where the substitution $v_{gi} = -1$ has been made in the exponent of the $\left(P_{ref} \ / \ RT\right)$ term. The relation $v_{gi} = -1$ holds for all adsorption reactions.

The temperature derivative of the Gibbs energy for an adsorbed species is then:

$$\frac{\partial G_{As}^0}{\partial T} = \frac{\partial G_A^0}{\partial T} - R\left(\ln\left(\frac{K_c P_{ref}}{RT} \right) + \frac{T}{K_c} \frac{\partial K_c}{\partial T} - 1 \right) \ . \tag{4.4.9}$$

The temperature derivative of the Gibbs energy for the gas-phase species (the first term on the right-hand side) can be obtained from Eq. (4.4.6) and the Lewis database curve fits.

As discussed earlier in Section 1.6, either k_b or K_c must be specified for each adsorption/desorption reaction for which no experimental adsorbed-species Gibbs energy exists.

If k_b is specified then the values of K_c and $\partial K_c / \partial T$ required by Eq. (4.4.9) can obtained from the definition of the concentration-based equilibrium constant, $K_c = k_f / k_b$, and the expression:

$$\frac{\partial K_c}{\partial T} = \frac{1}{k_b}\left[\frac{\partial k_f}{\partial T} - K_c \frac{\partial k_b}{\partial T}\right] \quad . \tag{4.4.10}$$

The analytic derivatives for the forward rate coefficient have already been given in Section 4.2 above as Eq. (4.2.4) and Eq. (4.2.5). The analytic derivatives of the backward (desorption) rate coefficient are given below in Section 4.5.

If instead K_c is specified, only the analytic derivative $\partial K_c / \partial T$ is additionally required to evaluate Eq. (4.4.9); these derivatives are given in Section 4.6.

4.5 Temperature Derivatives of the Desorption Rate Coefficients

Desorption reactions may be specified in several of the following forms:

Form 0: Arrhenius Desorption

For an Arrhenius expression with given constant values of A_{des}, β, and E_{des},

$$k_b^{(0)} = A_{des} T'^{\beta} \exp\left(-\frac{E_{des}}{RT}\right) \tag{4.5.1}$$

and the temperature derivative is given by,

$$\frac{\partial k_b^{(0)}}{\partial T} = \frac{k_b^{(0)}}{T}\left(\beta + \frac{E_{des}}{RT}\right) \quad . \tag{4.5.2}$$

Form 1: Constant Attempt Frequency Desorption

The constant attempt frequency form is functionally identical to the pure Arrhenius form with a specified constant value of ν:

$$k_b^{(1)} = A_{des} T'^{\beta} \nu \exp\left(-\frac{E_{des}}{RT}\right) \tag{4.5.3}$$

and the derivative with respect to wall temperature is the same as for the Arrhenius case:

$$\frac{\partial k_b^{(1)}}{\partial T} = \frac{k_b^{(1)}}{T}\left(\beta + \frac{E_{des}}{RT}\right) . \tag{4.5.4}$$

Form 2: Simple Transition State Theory Desorption

The simple TST desorption form is given by:

$$k_b^{(2)} = A_{des} T'^{\beta}\left(\frac{RT}{A_v h}\right)\exp\left(-\frac{E_{des}}{RT}\right) \tag{4.5.5}$$

and its derivative with respect to temperature by,

$$\frac{\partial k_b^{(2)}}{\partial T} = \frac{k_b^{(2)}}{T}\left(\beta + 1 + \frac{E_{des}}{RT}\right) . \tag{4.5.6}$$

Form 3: Complex Transition State Theory Desorption

The complex TST desorption form is given by:

$$k_b^{(3)} = A_{des} T'^{\beta}\left(\frac{RT}{A_v h}\right)\left(\frac{1-\exp\left(\frac{RT}{A_v h\nu}\right)}{\exp\left(\frac{RT}{2A_v h\nu}\right)}\right)\exp\left(-\frac{E_{des}}{RT}\right) \tag{4.5.7}$$

and its derivative with respect to wall temperature is,

$$\frac{\partial k_b^{(3)}}{\partial T} = \frac{k_b^{(3)}}{T}\left[\left(\beta + 1 + \frac{E_{des}}{RT}\right) - \frac{RT}{2A_v h\nu}\left(\frac{1+\exp\left(\frac{RT}{A_v h\nu}\right)}{1-\exp\left(\frac{RT}{A_v h\nu}\right)}\right)\right] . \tag{4.5.8}$$

4.6 Temperature Derivatives of the Concentration-Based Adsorption/Desorption Equilibrium Constants

The concentration-based equilibrium constant for an adsorption/desorption reaction may be specified in several forms:

Form 0: Arrhenius

The Arrhenius form of the concentration-based equilibrium constant is:

$$K_c^{(0)} = A_{eq} T'^{\beta} \exp\left(\frac{E_{des} - E_{ad}}{RT} \right) \tag{4.6.1}$$

and its temperature derivative is,

$$\frac{\partial K_c^{(0)}}{\partial T} = \frac{K_c^{(0)}}{T} \left(\beta - \frac{E_{des} - E_{ad}}{RT} \right) . \tag{4.6.2}$$

Form 1: Immobile Simple Transition State Theory

The simple TST form of the concentration-based equilibrium constant for immobile adsorption is given by:

$$K_c^{(1)} = A_{eq} T'^{\beta} \left(\frac{2\pi M_k RT}{(A_v h)^2} \right)^{-3/2} \exp\left(- \frac{E_{des} - E_{ad}}{RT} \right) \tag{4.6.3}$$

and its derivative with respect to temperature is,

$$\frac{\partial K_c^{(1)}}{\partial T} = \frac{K_c^{(1)}}{T} \left(\beta - \frac{3}{2} - \frac{E_{des} - E_{ad}}{RT} \right) . \tag{4.6.4}$$

Form 2: Immobile Complex Transition State Theory

The complex TST form of the concentration-based equilibrium constant for immobile adsorption is given by:

$$K_c^{(2)} = A_{eq} T'^{\beta} \left(\frac{2\pi M_A RT}{(A_v h)^2} \right)^{-3/2} \left(\frac{\exp\left(\frac{RT}{2A_v h\nu} \right)}{1 - \exp\left(\frac{RT}{A_v h\nu} \right)} \right)^3 \exp\left(\frac{E_{des} - E_{ad}}{RT} \right) \tag{4.6.5}$$

and the derivative with respect to temperature is,

$$\frac{\partial K_c^{(2)}}{\partial T} = \frac{K_c^{(2)}}{T} \left[\beta - \frac{3}{2} - \frac{E_{des} - E_{ad}}{RT} + 1.5 \left(\frac{A_v h\nu}{RT} \right) \left(\frac{1 + \exp\left(\frac{RT}{A_v h\nu} \right)}{1 - \exp\left(\frac{RT}{A_v h\nu} \right)} \right) \right] . \tag{4.6.6}$$

Form 3: Mobile Simple Transition State Theory

The simple TST form of the concentration-based equilibrium constant for mobile adsorption is given by:

$$K_c^{(2)} = A_{eq} T'^{\beta} \left(\frac{2\pi M_A RT}{(A_v h)^2} \right)^{-1/2} \exp\left(\frac{E_{des} - E_{ad}}{RT} \right) \tag{4.6.7}$$

and the derivative with respect to temperature is,

$$\frac{\partial K_c^{(3)}}{\partial T} = \frac{K_c^{(3)}}{T} \left(\beta - \frac{1}{2} - \frac{E_{des} - E_{ad}}{RT} \right) . \tag{4.6.8}$$

Form 4: Mobile Complex Transition State Theory

The complex TST form of the concentration-based equilibrium constant for mobile adsorption is given by:

$$K_c^{(4)} = A_{eq} T'^{\beta} \left(\frac{2\pi M_A RT}{(A_v h)^2} \right)^{-1/2} \left(\frac{\exp\left(\frac{RT}{2A_v h\nu} \right)}{1 - \exp\left(\frac{RT}{A_v h\nu} \right)} \right) \exp\left(\frac{E_{des} - E_{ad}}{RT} \right) \tag{4.6.9}$$

and its derivative with respect to temperature is,

$$\frac{\partial K_c^{(4)}}{\partial T} = \frac{K_c^{(4)}}{T} \left[\beta - \frac{1}{2} - \frac{E_{des} - E_{ad}}{RT} + \frac{1}{2} \left(\frac{A_v h\nu}{RT} \right) \left(\frac{1 + \exp\left(\frac{RT}{A_v h\nu} \right)}{1 - \exp\left(\frac{RT}{A_v h\nu} \right)} \right) \right] . \tag{4.6.10}$$

Chapter 5: Input Files for the Stand-Alone Code and DPLR

The stand-alone code and DPLR read information from various input files that define the surface reaction model, provide thermodynamic data, and set parameters for the desired numerical computation.

Both codes read thermodynamic property data for gas-phase and condensed species from two files, *lewis.thermo* and *lewis.bulk*. Data for relevant species has been extracted from compiled data by Gordon and McBride and is in the form of nine coefficients used to compute C_P/R, S_0/R, and $H_0/(RT)$ as a function of temperature.[14-15]

Both codes also read the surface reaction model input file, *filename.surf*, and in the case of blowing, the blowing species input file *filename.blw*. The format of these two files is identical for both codes, so that it is possible (and recommended) to use the stand-alone code to develop and test specific surface reaction models, and then use the vetted input files directly for DPLR simulations.

The stand-alone code additionally reads in the file *input.inp*, which defines the environmental and computational parameters for a desired calculation.

DPLR computations require a number of database files that are normally used to run the code. A main input file contains a list of flags for controlling all the physical models and conditions of the code. These files are all discussed in the User's Manual that gets distributed with each version of DPLR.

The only settings that must be specified to run the finite-rate surface reaction model are in the surface record for the wall that is to be modeled in this manner. Within this record, the surface reaction input file name given by the ***scname*** field (the *filename.surf* file) must be specified and the flag ***icatmd*** must be set to 990.

5.1 Surface Reaction Input File Structure

The generic file structure for the surface reaction input file is given below. Input file text is indicated in black and maroon. Maroon text is program input read by either the stand-alone code or DPLR; black text is not read in by either program, but it is included in the input file for clarity.

Comments indicating the number of lines that need to be entered in each section of the input file are included here, but not in the actual input file. Comments are preceded by an exclamation point, are positioned at the right hand margin, and are in blue text.

Blank lines in the file are indicated explicitly in blue text by BLANK LINE.

The surface reaction input file is divided into three different sections: the phase and active site section, the species section, and the surface reaction section. These are indicated in the file format below but can be replaced by blank lines in actual input files.

```
Input File Name                                                                    !1 line
-------------------- PHASE AND ACTIVE SITE SECTION ----------------------          !1 line
Number of surface and bulk phases (gas phase=1 by definition)                      !1 line
nsp, nbp                                                                           !1 line
#,    #                                                                            !1 line
BLANK LINE                                                                         !1 line
Blowing/pyrolyzing gas flows?(0=NO, 1=Yes); Surface Initial.(0=empty,1=QSS)        !1 line
nblwflag     initsurf                                                              !1 line
#,            #                                                                    !1 line
BLANK LINE                                                                         !1 line
Number of gas phase species in surface reaction and blowing model                  !1 line
Name      ngps  #Phase                                                             !1 line
NAME,       #      #                                                               !1 line
BLANK LINE                                                                         !1 line
For each surface phase: list  name, surface fraction,                              !1 line
number of active site sets, thermo availablity (0=No, 1=Yes)                       !1 line
Name      sfrc       nspas     iThermo    #Phase                                  !1 line
NAME,       #,          #,         #         #                                !nsp lines
BLANK LINE                                                                         !1 line
For each surface phase with 1 or more sets of active sites, list                   !1 line
the site density and number of species for each active site set                    !1 line
sdenas (mol/m2)       nspass          phase#/site#                                 !1 line
#,                       #                #/#                           !Sum(nspas) lines
BLANK LINE                                                                 !1 line, if nbp>0
For each bulk phase: list  name, mass density, porosity,                   !1 line, if nbp>0
phase volume fraction and number of bulk species                           !1 line, if nbp>0
Name     density (kg/m3)  porosity   vol. frac.    nbps      #Phase      !1 line, if nbp>0
NAME,       #,             #,             #,          #         #    !nbp lines, if nbp>0
------------------------- SPECIES SECTION -------------------------                !1 line
Order of gas species                                                               !1 line
Name   Molar mass(kg/mol)  Ediss (J/mole)     #Species  Dissociation Reaction     !1 line
NAME,       #,               #,               #        Name <=>Name+Name    !ngps lines
BLANK LINE                                                                         !1 line
Order of surface species (number each consecutively)                               !1 line
Name      Molar mass(kg/mole) Ed (J/mole)        #Species                          !1 line
NAME,          #,                 #,              #                   !Sum(nspass) lines
BLANK LINE                                                                 !1 line, if nbp>0
Order of bulk species (number each consecutively)                          !1 line, if nbp>0
Name      Molar mass(kg/mole)  Mole fraction     #Species               !1 line, if nbp>0
NAME,           #,                  #,            #           !Sum(nbps) lines, if nbp>0
--------------------- SURFACE REACTION SECTION ------------------------          !1 line
Total number of surface reactions                                                  !1 line
nsrt                                                                               !1 line
#                                                                                  !1 line
BLANK LINE                                                                         !1 line
Reactant/product species for each forward surface reaction                         !1 line
#, #, #, #, #, #             #   Name + Name <---> Name + Name                !nsrt lines
BLANK LINE                                                                         !1 line
```

```
Stoichiometric coefficients for each surface reaction                          !1 line
#, #, #, #, #, #             #   Name + Name <---> Name + Name              !nsrt lines
BLANK LINE                                                                     !1 line
Reaction parameters for each type of reaction:                                 !1 line
Type 0: Arrhenius:              0, Cf,         beta, Ea,   isrfon, isrbon      !1 line
Type 1: Adsorption:             1, S0(0 to 1), beta, Eads, isrfon, isrbon      !1 line
Type 2: Eley-Rideal:            2, Ger(0 to 1),beta, Eer,  isrfon, isrbon      !1 line
Type 3: Langmuir-Hinschelwood:  3, Clh(0 to 1),beta, Em,   isrfon, isrbon      !1 line
Type 4: Sublimation   a0Pv(T)   4, a0Pv0,     beta, Esub, isrfon, isrbon      !1 line
Type 5: Arrhenius Adsorption:   5, Cf,        beta, Ea,   isrfon, isrbon      !1 line
Type, A, beta, E (J/mole), isrfon, isrbon (isr(f,b)on: 1=ON,0=OFF)             !1 line
#,    #, #,     #,          #,      #     #  Name+Name<--->Name+Name        !nsrt lines
BLANK LINE                                                                     !1 line
Desorption reaction or equilibrium constant parameters:                        !1 line
Type 1: Desorption:                                                            !1 line
     Form 0:  Arrhenius                                                        !1 line
     Form 1:  Constant attempt frequency                                       !1 line
     Form 2:  Simple transition state theory                                   !1 line
     Form 3:  Complex transition state theory                                  !1 line
Type 2: Equilibrium:                                                           !1 line
     Form 0:  Arrhenius                                                        !1 line
     Form 1:  Immobile adsorption - simple transition state theory             !1 line
     Form 2:  Immobile adsorption - complex transition state theory            !1 line
     Form 3:  Mobile adsorption - simple transition state theory               !1 line
     Form 4:  Mobile adsorption - complex transition state theory              !1 line
Type, Form, Cf, eta, vdes (Hz), Edes (J/mole)                                  !1 line
#,     #,    #,    #,    #,     #                    !Sum(Type 1 and 5 reactions) lines
```

Note that many surface models will not require a bulk phase. In this case, nbp=0 and the various sections of the file with the comment "`...if nbp>0`" are omitted.

It is important to keep the order of listed reactions the same in each part of the SURFACE REACTION SECTION with the comment "`!nsrt lines`". If this is not done, the stoichiometry, species, and reaction types will get mixed up.

5.2 Blowing Species Input File Structure

The blowing species input file is only read by the stand-alone code or DPLR if the ***nblwflag*** is set to 1 in the surface reaction input file. If required, it must have the same *filename* as the surface reaction file *filename.surf*, and reside in the same directory.

Input file text is indicated in black and maroon. Maroon text is program input read by either the stand-alone code or DPLR; black text is not read in by either program, but it is included in the input file for clarity.

Comments indicating the number of lines that need to be entered in each section of the file are included here, but not in the actual input file. Comments are preceded by an exclamation point, are positioned at the right hand margin and are in blue text.

There are three main input types for this file:

0) The mass flux and the composition of one or more blowing flows are specified.

1) The blowing mass flux is computed from the steady-state ablation approximation and its composition is specified.

2) The blowing mass flux is computed from the steady-state ablation approximation, and its composition is specified. In addition, the enthalpy of the ablator in its unheated state is used in the surface energy balance.

The distinction between type 1 and 2 inputs are only important to DPLR computations and are irrelevant for the stand-alone code, which does not perform a steady-state energy balance. The stand-alone code will read in the ablator enthalpy, but it is not used for anything.

The generic file structure for the blowing species input files of type 0 and type (1, 2) are given below.

Type EBC=0 blowing file:

```
Name                                                                    !1 line
-------------------------------------------------------                 !1 line
0       EBC type (0: mdotg (kg/s)) (1: cyield) (2: cyield, ha (J/kg))   !1 line
#       nblw, Number of blowing/pyrolyzing flows                        !1 line
#       mdotg, mass flux (kg/s)                          !1 line, nblw columns
#       NAME      species mole fractions in blowing gas   !ngps lines, nblw columns
```

Type EBC=1,2 blowing file:

```
Name                                                                    !1 line
-------------------------------------------------------                 !1 line
2       EBC type (0: mdotg (kg/s)) (1: cyield) (2: cyield, ha (J/kg))   !1 line
#, #    cyield, ha (J/kg)                                               !1 line
#       NAME      species mole fractions in blowing gas               !ngps lines
```

5.3 Stand-Alone Code Input File Structure

The stand-alone code requires an input file named *input.inp*, which provides the environmental and computational parameters for a desired calculation. In practice, different input files can be constructed for specific computations and saved as individual *filename.inp* files. These files must be copied to or symbolically linked as the *input.inp* file when a stand-alone code computation is made. An error will result if this file is not present.

The *input.inp* file takes on the format given below, where lines in black that define the variables are ignored and the lines in maroon text are read by the utility.

Comments indicating the number of lines that need to be entered in various places are included here, but not in the actual input files. Comments are preceded by an exclamation point, are positioned at the right hand margin and are in blue text.

We indicate blank lines explicitly in blue text by "BLANK LINE".

```
[surface file name]                                              !1 line
'NAME'                                                           !1 line
BLANK LINE                                                       !1 line
output conv freq,  file save freq,  [output file name]           !1 line
               #,              #,    'NAME'                      !1 line
BLANK LINE                                                       !1 line
Tw (K),  Ptotal (Pa),  gas phase model,  scan mode               !1 line
   #,         #,                  #,           #                !1 line
BLANK LINE                                                       !1 line
 dt(s),  num steps,  time order,  diagnostic,  equilibrium       !1 line
   #,         #,            #,        #,          #             !1 line
BLANK LINE                                                       !1 line
[num gas phase species, ngps]                                    !1 line
  #                                                              !1 line
BLANK LINE                                                       !1 line
[name and mole fraction of each species]                         !1 line
'NAME',   #                                                  !ngps lines
=================================================                !1 line
BLANK LINE                                                       !1 line
Pressure & Temperature Scan (-1.0 to end)                        !1 line
Ptotal(Pa)  Tw (K)                                               !1 line
    #,       #.                                        !Arb. # of lines
BLANK LINE                                                       !1 line
Mole Fraction Scan (-1.0 to end)                                 !1 line
  Species names                                  !1 line w/ngps entries
  #, ……                                !Arb. # of lines w/ngps entries
BLANK LINE                                                       !1 line
=================================================                !1 line

surface file name | surface chemistry file name

output conv freq  | number of iterations between convergence
                    write to STDOUT (<=0 for no output)
```

```
file save freq    | number of iterations between concentration
                    write to "output file name" (<=0 for no output)

output file name  | file to write concentration data to

Tw                | surface wall temperature (deg K)

Ptotal            | gas phase pressure (Pascals)

gas phase model   | 0 = constant volume gas phase
                    1 = frozen gas phase concentrations
                        (+constant volume and pressure)
                    2 = constant pressure gas phase

scan mode         | 0 = scan mode off
                    1 = scan mode on: read additional data below mole
                        fraction record to run parametrics scans of
                        P,T and mole fractions
                        (turns off most diagnostics outputs)

dt                | time step/constant (seconds)

num steps         | number of iterations

time order        | 0 = explicit
                    1 = Euler implicit
                    2 = 3-pt backwards implicit

diagnostic        | 1 = compute Gibbs free energy minimization
                    2 = output finite rate diagnostics
                    3 = output finite rate diagnostics plus
                        write FRM system file back out

equilibrium       | -1 = compute Gibbs free-energy minimization
                         consistent with finite rate solution
                      0 = compute T,V Gibbs free-energy minimization
                      1 = compute T,V Gibbs free-energy minimization
                          with frozen gas phase species
                      2 = compute P,T Gibbs free-energy minimization

number of gas phase species | number of species to follow
                              (must match requirement in chemistry file)

name and mole fraction of each species | gas phase mole fractions

Pressure & Temperature Scan | scan records for pressure and temperature
                              (only if "scan mode" is 1)
                              (read until <0.0 is found)

Mole Fraction Scan | scan records for pressure and temperature
                     (only if "scan mode" is 1)
                     (read until <0.0 is found)
```

The number and order of the species specified in the *input.inp* file should agree exactly with that in the surface reaction file, *filename.surf*.

When running a mole fraction scan, the number and order of the specified species mole fractions must agree with those specified earlier in the *input.inp* file.

If a set of mole fractions is specified that does not sum to 1 (as it should), the stand-alone code will automatically normalize them to meet this constraint.

5.4 DPLR Surface Record Structure

An example of a surface record file with the key flags indicated in maroon:

```
================================================================
 Surface Record #2: Carbon Wall
================================================================
scname
'Park_Carbon_Model3_v1.surf'

  icatmd    ireqmd     iblow     islip     ixxxx
     990         1         0         0         0

   twall      epsr    gamcat     vwall    irough   rheight
   2000.    0.90d0     1.0d0     0.0d0         0     1.d-3
```

The path for the finite-rate surface reaction file, ***scname***, should either be absolute or relative to the current working directory. Unlike other database files used by the DPLR code, the path of the gas-phase chemistry file is not automatically prepended to the surface reaction input file. Copies of common surface reaction input and blowing species input files are included in the *cfdinput/* directory of the DPLR distribution that may either be used in place or copied into the current working directory and modified.

Within DPLR, a check is performed on solver start-up to ensure that each gas phase species requested in the surface reaction input file is included in the gas-phase chemistry file; however, the order of gas-phase species can be different in the gas-phase chemistry model and the surface reaction model (an internal index reordering is automatically performed), and additional gas-phase chemistry species can be included in DPLR that are not considered in the surface reaction model.

There is no limit to the number of independent finite-rate surface chemistry models that can be incorporated using separate surface records.

5.5 DPLR Post-Processing Structure

In addition to input files controlling the solver behavior, additional capabilities have been included in the DPLR post-processor, ***postflow***. No additional input fields have been included, but several possible additional variables have been added to the ***ivarp*** array for extraction from the restart file. Surface reaction data can be extracted using variables numbers 20001 to 21999 with the following list conventions:

```
20001       ==>   Finite Rate Model index number (sFRM#)
20002       ==>   Bulk phase recession rate (srecess)
20500       ==>   all gas, surface & bulk species generalized
                  concentrations for all FRM models
20500+n     ==>   generalized concentration for species n (sx_n)

21000       ==>   all gas, surface & bulk species production rates for
                  all FRM models
21000+n     ==>   production rate for species n (sw_n)

21500       ==>   all gas recombination efficiency ["gamma"] for all
                  models
21500+n     ==>   recombination efficiency ["gamma"] for species n
                  (sg_n)
```

Finite-rate surface chemistry variables are defined only at solid surfaces, so they will only be non-zero for surface zones where ***ifac*** is greater than 0 and for cells that were associated to a finite-rate surface chemistry model during the solution. Variables 20500, 21000, 21500 are convenience indices to extract all respective species variables from all finite-rate models used in the simulation. Species from multiple finite-rate surface models are indexed in series in order of the surface records that they are called from.

Bulk-phase recession rate is defined as the bulk-phase loss rate from Eq. (1.10.3) divided by the averaged bulk phase density from Eq. (1.2.6). The recession rate is given in Eq. (5.5.1):

$$\dot{s} = \frac{\dot{m}_c}{\rho_b} = \frac{-\sum_{nb=1}^{N_b}\sum_{k=1}^{K_{nb}} M_k \dot{w}_k}{\sum_{nb=1}^{N_b} \nu_{nb}\rho_{nb}} \quad . \tag{5.5.1}$$

Species generalized concentrations are defined in Eqs. (1.3.1), (1.3.2), and (1.3.3). It should be noted these concentrations are extracted in units of mol/m^3 or mol/m^2, in which dimensions of gram-mole are used instead of the standard SI unit convention of kgmol used by DPLR.

Species production rates are defined by Eq. (1.4.6) using the converged solution state. For a well-converged solution, the production rate of surface species should be approximately machine zero. . Again, the production rates are output in mol/m^2-s instead of kgmol, so a conversion factor of 1000 is necessary to compute the terms of the surface mass balance.

Gas phase recombination efficiency is defined by Eq. (1.10.1).

Chapter 6: Stand-Alone Code Examples

6.1 Catalytic Recombination in Dissociated Oxygen

Consider a simple finite-rate surface chemistry model for partially-dissociated oxygen in contact with a catalytic surface. The model has a gas phase containing O and O_2 and a surface phase with a single set of active sites containing empty and filled sites, E(s) and O(s).

Specified surface chemistry is limited to three forward reactions: O-atom adsorption (Type 1); Eley-Rideal (ER) recombination of a gas-phase O-atom with an adsorbed O-atom (Type 2); and Langmuir-Hinshelwood (LH) recombination of two adsorbed O-atoms with each other (Type 3):

$$\mathrm{O} + [s] \rightarrow [\mathrm{O}]_s \tag{6.1.1}$$

$$\mathrm{O} + [\mathrm{O}]_s \rightarrow \mathrm{O}_2 + [s] \tag{6.1.2}$$

$$2[\mathrm{O}]_s \rightarrow \mathrm{O}_2 + 2[s] \tag{6.1.3}$$

We set the following model parameters. For O-atom adsorption: $S_0 = 0.05$, $\beta = 0$, and $E_{ad} = 0$; for ER recombination: $\gamma_{er} = 0.001$, $\beta = 0$, and $E_{er} = 9000\,\mathrm{J\ mol^{-1}}$; for LH recombination: $C_{lh} = 0.1$, $\beta = 0$, and $E_m = 300000\,\mathrm{J\ mol^{-1}}$. The active site density is set to $\Phi_s = 7.5 \times 10^{-6}\,\mathrm{mol\ m^{-2}}$.

The corresponding backward reactions are computed by the stand-alone code from the reaction equilibrium constants. Thermodynamic data are provided for gas phase oxygen species by the Glenn/Lewis thermodynamic data base. Because no thermodynamic data are available for adsorbed O-atoms, we specify a thermal desorption reaction of Form 1 with $A_{des} = 1$, $\beta = 0$, $\nu = 1.0 \times 10^{12}\ \mathrm{s^{-1}}$ and $E_{des} = 350000\,\mathrm{J\ mol^{-1}}$.

In this particular model, O-atoms are pictured to adsorb strongly to the surface, with large barriers for thermal desorption and surface diffusion. A lower energy barrier for ER recombination is set because the exothermic recombination of two O-atoms releases more energy than the energy barrier for thermal desorption of a single O-atom.

The surface reaction input file for this model is given below:

File *O2Recomb.surf*:

```
Oxygen-Silica Catalysis: 2 gas species, 3 surface reactions
-----------------------------------------------------------------------
Number of surface and bulk phases (gas phase=1 by definition)
nsp, nbp
1    0

Blowing/pyrolyzing gas flows? (0=NO, 1=Yes) and Surface Init. (0=empty, 1=QSS)
nblwflag     initsurf
0            0

Number of gas phase species participating in surface reactions
Name      ngps  #Phase
Air5s     2      1

For each surface phase: list  name, surface fraction,
number of active site sets, thermo availability (0=NO, 1=Yes)
Name      sfrc         nspas      iThermo    #Phase
Silica    1.0          1          0          2

For each surface phase with 1 or more sets of active sites, list
the site density and number of species for each active site set
sdenas (mol/m2)     nspass
7.5d-06             2

Order of gas species
Name      Molar mass  Ediss     #Species
O2        0.03200000  498000.0   1
O         0.01600000  0.0        2

Order of surface species (number each consecutively)
Name      Molar mass  Edes      #Species
E(s1)     0.00000000  0.0       3
O(s1)     0.01600000  350000.0  4

Total number of surface reactions
nsrt
3

Reactant/product species for each forward surface reaction
2, 3, 0, 4, 0, 0                 #1   O + (s1) <---> O(s1)
2, 4, 0, 1, 3, 0                 #2   O + O(s1) <---> O2 + (s1)
4, 0, 0, 1, 3, 0                 #3   2O(s1) <---> O2 + 2(s1)

Stoichiometric coefficients for each surface reaction
1, 1, 0, 1, 0, 0                 #1   O + (s1) <---> O(s1)
1, 1, 0, 1, 1, 0                 #2   O + O(s1) <---> O2 + (s1)
2, 0, 0, 1, 2, 0                 #3   2O(s1) <---> O2 + 2(s1)

Reaction parameters for each type of reaction:
Type 0: Arrhenius:         0, Cf,         beta, Ea,   isrfon, isrbon
Type 1: Adsorption:        1, S0(0 to 1), beta, Eads, isrfon, isrbon
Type 2: Eley-Rideal:       2, Ger(0 to 1),beta, Eer,  isrfon, isrbon
Type 3: Langmuir-H:        3, Clh(0 to 1),beta, Em,   isrfon, isrbon
Type 4: Sublimation:       4, a0Pv,       beta, Esub, isrfon, isrbon
Type 5: Arrhenius Ad:      5, Cf,         beta, Ea,   isrfon, isrbon

1, 5.0d-02, 0.0d+00, 0.0000d+00, 1, 1   #1 O + (s1) <---> O(s1)
2, 1.0d-03, 0.0d+00, 9.0000d+03, 1, 1   #2 O + O(s1) <---> O2 + (s1)
3, 1.0d-01, 0.0d+00, 3.0000d+05, 1, 1   #3 2O(s1) <---> O2 + 2(s1)
```

```
Desorption reaction or equilibrium constant parameters:
Type 1: Desorption:
       Form 0:       Arrhenius
       Form 1:       Constant attempt frequency
       Form 2:       Simple transition state theory
       Form 3:       Complex transition state theory
Type 2: Equilibrium:
       Form 0:       Arrhenius
       Form 1:       Immobile adsorption - simple tran. state theory
       Form 2:       Immobile adsorption - complex tran. state theory
       Form 3:       Mobile adsorption - simple transition state theory
       Form 4:       Mobile adsorption - complex transition state theory
Type, Form, Cf, eta, vdes, Edes
1, 1, 1.0, 0.0, 1.e12, 350000.0
```

As an example, we set up a fixed gas-phase finite-rate computation with a bounding molar gas composition of 90% O_2-10% O, a total pressure of 2000 Pa, and a wall temperature of 2000 K.

File *input.inp*:

```
[surface file name]
'O2Recomb.surf'

output conv freq,  file save freq,   [output file name]
           500,             -1,    'long-output.dat'

Tw (K),     Ptotal (Pa),    gas phase model,      scan mode
 2000.,          2000.,                  1,             0

 dt(s),     num steps,   time order,    diagnostic,      equilibrium
1.0d-3,       5000,         1,              2,               -1

[num gas phase species]
2

[name and mole fraction of each species]
'O2',   0.90
 'O',   0.10
=====================================================================

Pressure & Temperature Scan (-1.0 to end)
Ptotal(Pa)  Tw (K)
    -1.,     -1.

Mole Fraction Scan (-1.0 to end)
  yO2    yO
  -1.,   -1.

=====================================================================
```

Here, we have eliminated the comment section shown in Section 5. 3, typically appended to the end of the *input.inp* file.

The standard output resulting from this input file is given below:

```
SRModel
   version:     3.07.9
   written by:  Joe Marschall   (jochen.marschall@sri.com)
                Matthew MacLean (maclean@cubrc.org)


---Initial Conditions-----------------------------
      Wall Tmpr   =    2.0000E+03 K
      Pressure    =    2.0000E+03 Pa
      xO2         =    1.0824E-01 mol/m^3
      xO          =    1.2027E-02 mol/m^3
      xE(s1)      =    7.5000E-06 mol/m^2
      xO(s1)      =    1.0000E-15 mol/m^2

------------------------------------------------
iteration         time       L1-norm       L2-norm
     500    5.0000E-01    1.1782E-22    1.6662E-22
    1000    1.0000E+00    1.1782E-22    1.6662E-22
    1500    1.5000E+00    1.1782E-22    1.6662E-22
    2000    2.0000E+00    1.1782E-22    1.6662E-22
    2500    2.5000E+00    1.1782E-22    1.6662E-22
    3000    3.0000E+00    1.1782E-22    1.6662E-22
    3500    3.5000E+00    1.1782E-22    1.6662E-22
    4000    4.0000E+00    1.1782E-22    1.6662E-22
    4500    4.5000E+00    1.1782E-22    1.6662E-22
    5000    5.0000E+00    1.1782E-22    1.6662E-22

---Final Conditions-------------------------------
      Wall Tmpr   =    2.0000E+03 K
      Pressure    =    2.0000E+03 Pa
      Rel Volume  =    1.0000E+00
      xO2         =    1.0824E-01 mol/m^3
      xO          =    1.2027E-02 mol/m^3
      xE(s1)      =    1.2616E-06 mol/m^2
      xO(s1)      =    6.2384E-06 mol/m^2

---Loss Efficiencies ------------------------------
      gO2         =   -6.2571E-04
      gO          =    7.9639E-03

---Blowing & Recession Rate-----------------------
      blowing rate    =    0.0000E+00  kg/m^2-s
      recession rate  =    0.0000E+00  m/s

---QSS Surface Coverage Distribution--------------
      Residual =    7.6275E-22
      Concentrations
         xE(s1)      =    1.2616E-06 mol/m^2
         xO(s1)      =    6.2384E-06 mol/m^2

---Gibbs Free-energy Minimization-----------------
      Element List
         O  s1
      Stoichiometry
         O2        :   2.   0.
         O         :   1.   0.
         E(s1)     :   0.   1.
         O(s1)     :   1.   1.
      Species Considered for System:
         O2  E(s1)  O(s1)
```

```
      Concentrations
         xO2         =    1.0824E-01 mol/m^3
         xO          =    1.2027E-02 mol/m^3
         xE(s1)      =    2.4808E-06 mol/m^2
         xO(s1)      =    5.0192E-06 mol/m^2

---Additional Diagnostics-----------------------------------------
      <<Reaction Constants>>
react    kf       kb          KeqC       KeqC-actual    wf-actual    wb-actual
1    2.7114E+06  7.2305E+02  3.7499E+03  4.1113E+02   4.1142E-02   4.5107E-03
2    3.1563E+04  3.1830E+02  9.9159E+01  1.8201E+00   2.3681E-03   4.3469E-05
3    5.2940E+08  2.0020E+10  2.6443E-02  4.4271E-03   2.0603E-02   3.4493E-03
      <<Species Production>>
      species      concentration     molar prod.      mass prod.
      O2              1.0824E-01      1.9478E-02      6.2330E-04
      O               1.2027E-02     -3.8956E-02     -6.2330E-04
      E(s1)           1.2616E-06     -6.9389E-18      0.0000E+00
      O(s1)           6.2384E-06      6.9389E-18      1.1102E-19
      <<Species Production Per Reaction>>
      species          w-dot             w1             w2             w3
      O2          1.9478E-02     0.0000E+00     2.3247E-03     1.7153E-02
      O          -3.8956E-02    -3.6631E-02    -2.3247E-03     0.0000E+00
      E(s1)      -6.9389E-18    -3.6631E-02     2.3247E-03     3.4307E-02
      O(s1)       6.9389E-18     3.6631E-02    -2.3247E-03    -3.4307E-02
```

The time integration converges very rapidly, since only the surface concentrations of species E(s) and O(s) need to come to steady state, and the pressure, volume, and gas-phase concentrations remain fixed. The initial and final conditions and the integration convergence are shown in the first three sections of the standard output.

The fourth section of the output shows the effective loss efficiencies of the gas-phase reactants for this surface reaction model and set of environmental conditions. Approximately 7.96 out of every 1,000 O-atom collisions with the surface result in loss of an O-atom from the gas phase and approximately 6.26 oxygen molecules are added to the gas phase by surface recombination for every 10,000 O_2 collisions with the surface.

The fifth section of the output file indicates that no mass is exchanged between the surface and the gas phase for a purely catalytic system.

The sixth section of the output gives the quasi-steady-state surface coverage for the set of initial conditions, by way of the algebraic solution described in Section 2.2. In this case, because the gas phase is fixed, the QSS surface coverage should agree with the converged time-integrated solution, and this is shown to be true.

The seventh section gives the results of a Gibbs energy minimization computation for the fixed gas-phase condition. The meaning of the Gibbs minimization solution under this constraint is unclear. The fixed gas-phase condition leads to a steady-state surface distribution that is not a thermodynamic equilibrium state, and the Gibbs minimization procedure produces different values for the E(s1) and O(s1) surface coverage than the integrated finite-rate and QSS solutions, which are in agreement with each other.

Finally, additional diagnostic output is given that allows evaluation and comparison of various reaction and species production rates. These outputs can be used as further checks on the solution–for example, if the final system state is in thermodynamic equilibrium (not in this case) or if there is net production of species in the final state (yes for O and O2, no for E(s1) and O(s1)).

It is also possible to check reaction pathways for different species. For example, here most O-atoms are lost from the gas phase by adsorption to empty sites, and most O_2 is produced by the recombination of adsorbed O-atoms by the LH mechanism.

By running the stand-alone code in scan mode, it is possible to perform parameter space studies by systematically varying the temperature and initial pressure, or the initial mole fractions. These solutions use the same surface reaction input file, *O2Recomb.surf*, together with an *input.inp* file modified to run the desired scan mode.

A modified *input.inp* file for the case of fixed gas-phase finite-rate computations with a bounding molar gas composition of 90% O_2-10% O, a total pressure of 200 Pa, and a range of wall temperatures from 300 K to 3500 K is shown below:

```
[surface file name]
'O2test/O2Recomb.surf'

output conv freq,  file save freq,   [output file name]
           500,             -1,    'long-output.dat'

Tw (K),     Ptotal (Pa),    gas phase model,      scan mode
 300.,     200.,                  1,             1

 dt(s),     num steps,    time order,     diagnostic,      equilibrium
1.0d-3,       5000,             1,              2,               -1

[num gas phase species]
2

[name and mole fraction of each species]
'O2',   0.90
 'O',   0.10
=====================================================================

Pressure & Temperature Scan (-1.0 to end)
Ptotal(Pa)  Tw (K)
   200.,   300.
   200.,   400.
   200.,   500.
   200.,   600.
   200.,   700.
   200.,   800.
   200.,   900.
   200.,   1000.
   200.,   1100.
   200.,   1200.
   200.,   1300.
   200.,   1400.
   200.,   1500.
   200.,   1600.
   200.,   1700.
```

```
   200.,   1800.
   200.,   1900.
   200.,   2000.
   200.,   2100.
   200.,   2200.
   200.,   2240.
   200.,   2250.
   200.,   2260.
   200.,   2270.
   200.,   2280.
   200.,   2290.
   200.,   2291.5
   200.,   2300.
   200.,   2310.
   200.,   2320.
   200.,   2330.
   200.,   2340.
   200.,   2400.
   200.,   2500.
   200.,   2600.
   200.,   2700.
   200.,   2800.
   200.,   2810.
   200.,   2900.
   200.,   3000.
   200.,   3100.
   200.,   3200.
   200.,   3300.
   200.,   3400.
   200.,   3500.
    -1.,     -1.

Mole Fraction Scan (-1.0 to end)
  yO2    yO
  -1.,   -1.

=====================================================================
```

In scan mode, most of the detailed output from the stand-alone code is suppressed and is replaced by tabulated output that can be read into a spreadsheet for plotting. The tabulated output includes the final species concentrations, the loss efficiencies for gas-phase species, and the reaction-specific productions rates of each species.

The tabulated output for the *input.inp* file above is shown below:

```
SRModel
   version:     3.07.9
   written by:  Joe Marschall   (jochen.marschall@sri.com)
                Matthew MacLean (maclean@cubrc.org)


---Initial Conditions-----------------------------
      Wall Tmpr   =    3.0000E+02 K
      Pressure    =    2.0000E+03 Pa
      xO2         =    7.2163E-01 mol/m^3
      xO          =    8.0181E-02 mol/m^3
      xE(s1)      =    7.5000E-06 mol/m^2
      xO(s1)      =    1.0000E-15 mol/m^2

---Pressure/Temperature Scan----------------------
```

```
             Pi             Tw         Volume             Pf            xO2
xO         xE(s1)         xO(s1)            gO2             gO          wO2_1
wO2_2          wO2_3           wO_1           wO_2           wO_3       wE(s1)_1
wE(s1)_2       wE(s1)_3       wO(s1)_1       wO(s1)_2       wO(s1)_3
   2.000000E+02   3.000000E+02   1.000000E+00   2.000000E+02   7.216300E-02
8.018111E-03   4.063089E-09   7.495937E-06  -4.256352E-06   5.417452E-05
0.000000E+00   3.421103E-05  -7.150922E-24  -3.421103E-05  -3.421103E-05
0.000000E+00  -3.421103E-05   3.421103E-05  -1.430184E-23   3.421103E-05  -3.421103E-
05   1.430184E-23
   2.000000E+02   4.000000E+02   1.000000E+00   2.000000E+02   5.412225E-02
6.013583E-03   1.000603E-08   7.489994E-06  -1.048197E-05   1.334137E-04
0.000000E+00   7.296292E-05  -7.659377E-19  -7.296292E-05  -7.296292E-05
0.000000E+00  -7.296292E-05   7.296292E-05  -1.531875E-18   7.296292E-05  -7.296292E-
05   1.531875E-18
   2.000000E+02   5.000000E+02   1.000000E+00   2.000000E+02   4.329780E-02
4.810867E-03   1.717496E-08   7.482825E-06  -1.799190E-05   2.289995E-04
0.000000E+00   1.120163E-04  -8.410407E-16  -1.120163E-04  -1.120163E-04
0.000000E+00  -1.120163E-04   1.120163E-04  -1.682081E-15   1.120163E-04  -1.120163E-
04   1.682081E-15
   2.000000E+02   6.000000E+02   1.000000E+00   2.000000E+02   3.608150E-02
4.009055E-03   2.461296E-08   7.475387E-06  -2.578369E-05   3.281728E-04
0.000000E+00   1.465409E-04  -9.213610E-14  -1.465409E-04  -1.465409E-04
0.000000E+00  -1.465409E-04   1.465409E-04  -1.842722E-13   1.465409E-04  -1.465409E-
04   1.842722E-13
   2.000000E+02   7.000000E+02   1.000000E+00   2.000000E+02   3.092700E-02
3.436333E-03   3.181805E-08   7.468182E-06  -3.333150E-05   4.242407E-04
0.000000E+00   1.753861E-04  -2.683047E-12  -1.753861E-04  -1.753861E-04
0.000000E+00  -1.753861E-04   1.753861E-04  -5.366093E-12   1.753861E-04  -1.753861E-
04   5.366093E-12
   2.000000E+02   8.000000E+02   1.000000E+00   2.000000E+02   2.706112E-02
3.006792E-03   3.856801E-08   7.461432E-06  -4.040252E-05   5.142402E-04
0.000000E+00   1.988625E-04  -3.395213E-11  -1.988624E-04  -1.988625E-04
0.000000E+00  -1.988624E-04   1.988625E-04  -6.790427E-11   1.988624E-04  -1.988625E-
04   6.790427E-11
   2.000000E+02   9.000000E+02   1.000000E+00   2.000000E+02   2.405433E-02
2.672704E-03   4.478740E-08   7.455213E-06  -4.691779E-05   5.971660E-04
0.000000E+00   2.177239E-04  -2.412358E-10  -2.177234E-04  -2.177239E-04
0.000000E+00  -2.177234E-04   2.177239E-04  -4.824715E-10   2.177234E-04  -2.177239E-
04   4.824715E-10
   2.000000E+02   1.000000E+03   1.000000E+00   2.000000E+02   2.164890E-02
2.405433E-03   5.047257E-08   7.449527E-06  -5.287354E-05   6.729702E-04
0.000000E+00   2.327712E-04  -9.041785E-10  -2.327694E-04  -2.327712E-04
0.000000E+00  -2.327694E-04   2.327712E-04  -1.808357E-09   2.327694E-04  -2.327712E-
04   1.808357E-09
   2.000000E+02   1.100000E+03   1.000000E+00   2.000000E+02   1.968082E-02
2.186758E-03   5.565540E-08   7.444345E-06  -5.830169E-05   7.420593E-04
0.000000E+00   2.447186E-04   4.008370E-09  -2.447266E-04  -2.447186E-04
0.000000E+00  -2.447266E-04   2.447186E-04   8.016740E-09   2.447266E-04  -2.447186E-
04  -8.016740E-09
   2.000000E+02   1.200000E+03   1.000000E+00   2.000000E+02   1.804075E-02
2.004528E-03   6.043005E-08   7.439570E-06  -6.327289E-05   8.053324E-04
0.000000E+00   2.541599E-04   1.224840E-07  -2.544049E-04  -2.541599E-04
0.000000E+00  -2.544049E-04   2.541599E-04   2.449680E-07   2.544049E-04  -2.541599E-
04  -2.449680E-07
   2.000000E+02   1.300000E+03   1.000000E+00   2.000000E+02   1.665300E-02
1.850333E-03   6.536924E-08   7.434631E-06  -6.810155E-05   8.667912E-04
0.000000E+00   2.615594E-04   1.391394E-06  -2.643422E-04  -2.615594E-04
0.000000E+00  -2.643422E-04   2.615594E-04   2.782788E-06   2.643422E-04  -2.615594E-
04  -2.782788E-06
   2.000000E+02   1.400000E+03   1.000000E+00   2.000000E+02   1.546350E-02
1.718167E-03   7.416636E-08   7.425834E-06  -7.466300E-05   9.503049E-04
0.000000E+00   2.671703E-04   1.062866E-05  -2.884277E-04  -2.671703E-04
```

0.000000E+00 -2.884277E-04   2.671703E-04   2.125732E-05   2.884277E-04 -2.671703E-
04 -2.125732E-05
   2.000000E+02   1.500000E+03   1.000000E+00   2.000000E+02   1.443260E-02
1.603622E-03   1.055315E-07   7.394468E-06 -9.224912E-05   1.174140E-03
0.000000E+00   2.706047E-04   6.098873E-05 -3.925821E-04 -2.706047E-04
0.000000E+00 -3.925821E-04   2.706047E-04   1.219775E-04   3.925821E-04 -2.706047E-
04 -1.219775E-04
   2.000000E+02   1.600000E+03   1.000000E+00   2.000000E+02   1.353056E-02
1.503396E-03   2.309222E-07   7.269078E-06 -1.557386E-04   1.982228E-03
0.000000E+00   2.693893E-04   2.726432E-04 -8.146758E-04 -2.693893E-04
0.000000E+00 -8.146758E-04   2.693893E-04   5.452865E-04   8.146758E-04 -2.693893E-
04 -5.452865E-04
   2.000000E+02   1.700000E+03   1.000000E+00   2.000000E+02   1.273465E-02
1.414961E-03   6.300420E-07   6.869958E-06 -3.500859E-04   4.455865E-03
0.000000E+00   2.566739E-04   9.253856E-04 -2.107445E-03 -2.566739E-04
0.000000E+00 -2.107445E-03   2.566739E-04   1.850771E-03   2.107445E-03 -2.566739E-
04 -1.850771E-03
   2.000000E+02   1.800000E+03   1.000000E+00   2.000000E+02   1.202717E-02
1.336352E-03   1.476966E-06   6.023034E-06 -7.439007E-04   9.468310E-03
0.000000E+00   2.251150E-04   2.215886E-03 -4.656887E-03 -2.251150E-04
0.000000E+00 -4.656887E-03   2.251150E-04   4.431772E-03   4.656887E-03 -2.251150E-
04 -4.431772E-03
   2.000000E+02   1.900000E+03   1.000000E+00   2.000000E+02   1.139416E-02
1.266018E-03   2.612961E-06   4.887039E-06 -1.214001E-03   1.545171E-02
0.000000E+00   1.794459E-04   3.697872E-03 -7.575190E-03 -1.794459E-04
0.000000E+00 -7.575190E-03   1.794459E-04   7.395744E-03   7.575190E-03 -1.794459E-
04 -7.395744E-03
   2.000000E+02   2.000000E+03   1.000000E+00   2.000000E+02   1.082445E-02
1.202717E-03   3.711047E-06   3.788953E-06 -1.524799E-03   1.940752E-02
0.000000E+00   1.310455E-04   4.615600E-03 -9.362246E-03 -1.310455E-04
0.000000E+00 -9.362246E-03   1.310455E-04   9.231201E-03   9.362246E-03 -1.310455E-
04 -9.231201E-03
   2.000000E+02   2.100000E+03   1.000000E+00   2.000000E+02   1.030900E-02
1.145444E-03   4.616203E-06   2.883797E-06 -1.496897E-03   1.905239E-02
0.000000E+00   8.499211E-05   4.462496E-03 -9.009985E-03 -8.499211E-05
0.000000E+00 -9.009985E-03   8.499211E-05   8.924992E-03   9.009985E-03 -8.499211E-
05 -8.924992E-03
   2.000000E+02   2.200000E+03   1.000000E+00   2.000000E+02   9.840409E-03
1.093379E-03   5.318500E-06   2.181500E-06 -9.920727E-04   1.262702E-02
0.000000E+00   4.075951E-05   2.903807E-03 -5.848374E-03 -4.075951E-05
0.000000E+00 -5.848374E-03   4.075951E-05   5.807614E-03   5.848374E-03 -4.075951E-
05 -5.807614E-03
   2.000000E+02   2.240000E+03   1.000000E+00   2.000000E+02   9.664687E-03
1.073854E-03   5.550318E-06   1.949682E-06 -6.259429E-04   7.966953E-03
0.000000E+00   2.305390E-05   1.818142E-03 -3.659338E-03 -2.305390E-05
0.000000E+00 -3.659338E-03   2.305390E-05   3.636284E-03   3.659338E-03 -2.305390E-
05 -3.636284E-03
   2.000000E+02   2.250000E+03   1.000000E+00   2.000000E+02   9.621733E-03
1.069081E-03   5.604406E-06   1.895594E-06 -5.179959E-04   6.593012E-03
0.000000E+00   1.859315E-05   1.501689E-03 -3.021972E-03 -1.859315E-05
0.000000E+00 -3.021972E-03   1.859315E-05   3.003379E-03   3.021972E-03 -1.859315E-
05 -3.003379E-03
   2.000000E+02   2.260000E+03   1.000000E+00   2.000000E+02   9.579159E-03
1.064351E-03   5.657027E-06   1.842973E-06 -4.032044E-04   5.131954E-03
0.000000E+00   1.411339E-05   1.166643E-03 -2.347399E-03 -1.411339E-05
0.000000E+00 -2.347399E-03   1.411339E-05   2.333286E-03   2.347399E-03 -1.411339E-
05 -2.333286E-03
   2.000000E+02   2.270000E+03   1.000000E+00   2.000000E+02   9.536960E-03
1.059662E-03   5.708221E-06   1.791779E-06 -2.814309E-04   3.582030E-03
0.000000E+00   9.612002E-06   8.127216E-04 -1.635055E-03 -9.612002E-06
0.000000E+00 -1.635055E-03   9.612002E-06   1.625443E-03   1.635055E-03 -9.612002E-
06 -1.625443E-03

```
   2.000000E+02   2.280000E+03   1.000000E+00   2.000000E+02   9.495131E-03
1.055015E-03   5.758027E-06   1.741973E-06  -1.525398E-04   1.941515E-03
0.000000E+00   5.086429E-06   4.396524E-04  -8.843912E-04  -5.086429E-06
0.000000E+00  -8.843912E-04   5.086429E-06   8.793048E-04   8.843912E-04  -5.086429E-
06  -8.793048E-04
   2.000000E+02   2.290000E+03   1.000000E+00   2.000000E+02   9.453668E-03
1.050408E-03   5.806482E-06   1.693518E-06  -1.639760E-05   2.087074E-04
0.000000E+00   5.341266E-07   4.716955E-05  -9.487323E-05  -5.341266E-07
0.000000E+00  -9.487323E-05   5.341266E-07   9.433910E-05   9.487323E-05  -5.341266E-
07  -9.433910E-05
   2.000000E+02   2.291500E+03   1.000000E+00   2.000000E+02   9.447480E-03
1.049720E-03   5.813636E-06   1.686364E-06   4.657287E-06  -5.927759E-05
0.000000E+00  -1.511795E-07  -1.339330E-05   2.693778E-05   1.511795E-07
0.000000E+00   2.693778E-05  -1.511795E-07  -2.678660E-05  -2.693778E-05   1.511795E-
07   2.678660E-05
   2.000000E+02   2.300000E+03   1.000000E+00   2.000000E+02   9.412565E-03
1.045841E-03   5.853624E-06   1.646376E-06   1.271270E-04  -1.618062E-03
0.000000E+00  -4.047412E-06  -3.649838E-04   7.340150E-04   4.047412E-06
0.000000E+00   7.340150E-04  -4.047412E-06  -7.299676E-04  -7.340150E-04   4.047412E-
06   7.299676E-04
   2.000000E+02   2.310000E+03   1.000000E+00   2.000000E+02   9.371818E-03
1.041313E-03   5.899487E-06   1.600513E-06   2.781624E-04  -3.540429E-03
0.000000E+00  -8.660657E-06  -7.970547E-04   1.602770E-03   8.660657E-06
0.000000E+00   1.602770E-03  -8.660657E-06  -1.594109E-03  -1.602770E-03   8.660657E-
06   1.594109E-03
   2.000000E+02   2.320000E+03   1.000000E+00   2.000000E+02   9.331422E-03
1.036825E-03   5.944107E-06   1.555893E-06   4.368339E-04  -5.559988E-03
0.000000E+00  -1.330804E-05  -1.249280E-03   2.511868E-03   1.330804E-05
0.000000E+00   2.511868E-03  -1.330804E-05  -2.498560E-03  -2.511868E-03   1.330804E-
05   2.498560E-03
   2.000000E+02   2.330000E+03   1.000000E+00   2.000000E+02   9.291373E-03
1.032375E-03   5.987518E-06   1.512482E-06   6.032634E-04  -7.678290E-03
0.000000E+00  -1.799197E-05  -1.721884E-03   3.461760E-03   1.799197E-05
0.000000E+00   3.461760E-03  -1.799197E-05  -3.443768E-03  -3.461760E-03   1.799197E-
05   3.443768E-03
   2.000000E+02   2.340000E+03   1.000000E+00   2.000000E+02   9.251667E-03
1.027963E-03   6.029753E-06   1.470247E-06   7.775688E-04  -9.896835E-03
0.000000E+00  -2.271480E-05  -2.215079E-03   4.452873E-03   2.271480E-05
0.000000E+00   4.452873E-03  -2.271480E-05  -4.430159E-03  -4.452873E-03   2.271480E-
05   4.430159E-03
   2.000000E+02   2.400000E+03   1.000000E+00   2.000000E+02   9.020375E-03
1.002264E-03   6.260222E-06   1.239778E-06   1.994822E-03  -2.538995E-02
0.000000E+00  -5.199562E-05  -5.616762E-03   1.128552E-02   5.199562E-05
0.000000E+00   1.128552E-02  -5.199562E-05  -1.123352E-02  -1.128552E-02   5.199562E-
05   1.123352E-02
   2.000000E+02   2.500000E+03   1.000000E+00   2.000000E+02   8.659560E-03
9.621733E-04   6.569324E-06   9.306758E-07   4.713520E-03  -5.999331E-02
0.000000E+00  -1.053388E-04  -1.301861E-02   2.614256E-02   1.053388E-04
0.000000E+00   2.614256E-02  -1.053388E-04  -2.603722E-02  -2.614256E-02   1.053388E-
04   2.603722E-02
   2.000000E+02   2.600000E+03   1.000000E+00   2.000000E+02   8.326500E-03
9.251667E-04   6.803997E-06   6.960032E-07   8.323446E-03  -1.059402E-01
0.000000E+00  -1.659408E-04  -2.255915E-02   4.528425E-02   1.659408E-04
0.000000E+00   4.528425E-02  -1.659408E-04  -4.511831E-02  -4.528425E-02   1.659408E-
04   4.511831E-02
   2.000000E+02   2.700000E+03   1.000000E+00   2.000000E+02   8.018111E-03
8.909012E-04   6.981295E-06   5.187054E-07   1.278926E-02  -1.627807E-01
0.000000E+00  -2.353118E-04  -3.402984E-02   6.829500E-02   2.353118E-04
0.000000E+00   6.829500E-02  -2.353118E-04  -6.805969E-02  -6.829500E-02   2.353118E-
04   6.805969E-02
   2.000000E+02   2.800000E+03   1.000000E+00   2.000000E+02   7.731750E-03
8.590833E-04   7.114186E-06   3.858139E-07   1.801418E-02  -2.292831E-01
0.000000E+00  -3.146697E-04  -4.707947E-02   9.447362E-02   3.146697E-04
```

```
0.000000E+00   9.447362E-02  -3.146697E-04  -9.415895E-02  -9.447362E-02   3.146697E-
04   9.415895E-02
   2.000000E+02   2.810000E+03   1.000000E+00   2.000000E+02   7.704235E-03
8.560261E-04   7.125445E-06   3.745547E-07   1.857369E-02  -2.364045E-01
0.000000E+00  -3.231944E-04  -4.845596E-02   9.723511E-02   3.231944E-04
0.000000E+00   9.723511E-02  -3.231944E-04  -9.691192E-02  -9.723511E-02   3.231944E-
04   9.691192E-02
   2.000000E+02   2.900000E+03   1.000000E+00   2.000000E+02   7.465138E-03
8.294598E-04   7.212889E-06   2.871111E-07   2.387489E-02  -3.038777E-01
0.000000E+00  -4.049994E-04  -6.131581E-02   1.230366E-01   4.049994E-04
0.000000E+00   1.230366E-01  -4.049994E-04  -1.226316E-01  -1.230366E-01   4.049994E-
04   1.226316E-01
   2.000000E+02   3.000000E+03   1.000000E+00   2.000000E+02   7.216300E-03
8.018111E-04   7.285614E-06   2.143859E-07   3.025795E-02  -3.851208E-01
0.000000E+00  -5.070976E-04  -7.640030E-02   1.533077E-01   5.070976E-04
0.000000E+00   1.533077E-01  -5.070976E-04  -1.528006E-01  -1.533077E-01   5.070976E-
04   1.528006E-01
   2.000000E+02   3.100000E+03   1.000000E+00   2.000000E+02   6.983516E-03
7.759462E-04   7.338929E-06   1.610713E-07   3.708117E-02  -4.719663E-01
0.000000E+00  -6.215998E-04  -9.209593E-02   1.848135E-01   6.215998E-04
0.000000E+00   1.848135E-01  -6.215998E-04  -1.841919E-01  -1.848135E-01   6.215998E-
04   1.841919E-01
   2.000000E+02   3.200000E+03   1.000000E+00   2.000000E+02   6.765281E-03
7.516979E-04   7.377965E-06   1.220355E-07   4.429669E-02  -5.638048E-01
0.000000E+00  -7.489923E-04  -1.082658E-01   2.172806E-01   7.489923E-04
0.000000E+00   2.172806E-01  -7.489923E-04  -2.165317E-01  -2.172806E-01   7.489923E-
04   2.165317E-01
   2.000000E+02   3.300000E+03   1.000000E+00   2.000000E+02   6.560273E-03
7.289192E-04   7.406617E-06   9.338326E-08   5.188289E-02  -6.603614E-01
0.000000E+00  -8.896179E-04  -1.248454E-01   2.505805E-01   8.896179E-04
0.000000E+00   2.505805E-01  -8.896179E-04  -2.496909E-01  -2.505805E-01   8.896179E-
04   2.496909E-01
   2.000000E+02   3.400000E+03   1.000000E+00   2.000000E+02   6.367323E-03
7.074804E-04   7.427764E-06   7.223561E-08   5.983365E-02  -7.615581E-01
0.000000E+00  -1.043681E-03  -1.418113E-01   2.846662E-01   1.043681E-03
0.000000E+00   2.846662E-01  -1.043681E-03  -2.836225E-01  -2.846662E-01   1.043681E-
03   2.836225E-01
   2.000000E+02   3.500000E+03   1.000000E+00   2.000000E+02   6.185400E-03
6.872667E-04   7.443495E-06   5.650513E-08   6.814970E-02  -8.674041E-01
0.000000E+00  -1.211257E-03  -1.591573E-01   3.195258E-01   1.211257E-03
0.000000E+00   3.195258E-01  -1.211257E-03  -3.183146E-01  -3.195258E-01   1.211257E-
03   3.183146E-01
---Mole Fraction Scan----------------------
         mfi_O2          mfi_O         Volume             Pf            xO2
xO         xE(s1)         xO(s1)            gO2             gO          wO2_1
wO2_2          wO2_3           wO_1           wO_2           wO_3       wE(s1)_1
wE(s1)_2       wE(s1)_3       wO(s1)_1       wO(s1)_2       wO(s1)_3
```

These and similar computations at 2000 Pa and 20000 Pa were used to create Figure 6.1.1.

Figure 6.1.1 shows the variation of O-atom surface coverage and the O or O_2 loss efficiency with temperature, for three different pressures of 20,000, 2000, and 200 Pa.

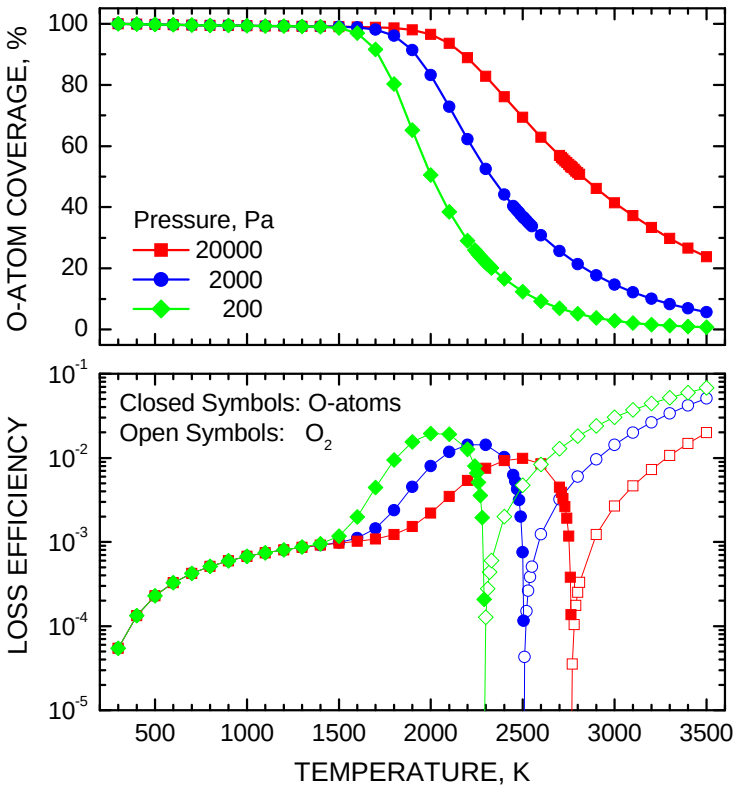

Figure 6.1.1 O-atom Surface Coverage (top panel) and O-atom or O_2 Loss Efficiency (bottom panel) as a Function of Temperature for ER + LH Surface Catalytic Recombination in a 90% O_2-10% O Mixture at 20,000 , 2000, and 200 Pa.

Since the adsorbed O-atom is bound tightly to the surface, surface coverage is high at low temperatures. As the temperature increases, the rates of thermal desorption and ER and LH recombination overwhelm the rate of adsorption, and the surface coverage rapidly decreases. This drop in coverage happens at lower temperatures at which the gas pressure is low because the rate of adsorption depends on the gas-phase O-atom concentration, while the O-atom desorption and LH recombination mechanisms only depend on temperature.

The O-atom loss efficiency shows three characteristic regimes with increasing temperature. At low temperatures, the O-atom loss efficiency increases as the ER recombination rate increases and the O-atom surface coverage remains high. The LH mechanism is not effective in the low-temperature regime. At moderate temperatures, LH recombination accelerates with increasing temperature as the available thermal energy becomes sufficient for effective surface diffusion. At even higher temperatures, O-atom loss rate drops sharply with increasing temperature, as the O-atom surface coverage falls and the ER and LH recombination reactions are effectively countered by their corresponding backward dissociative adsorption reactions. Above a certain temperature, the dissociation reactions dominate and the net effect is a loss of O_2 from the gas phase that increases with temperature.

The *activity-based* equilibrium constant for the gas phase of this simple system can be written in terms of the system pressure and oxygen species mole fractions as:

$$K_a(T) = \frac{P_{ref}}{P}\frac{\chi_{O_2}}{\chi_O^2} \quad . \tag{6.1.4}$$

This equilibrium constant equals 456, 4560, and 45,600, for a 90% O_2-10% O mixture at the pressures 20000 Pa, 2000 Pa, and 200 Pa, respectively. The corresponding equilibrium temperatures can be found as 2765 K, 2506 K, and 2291 K.[14]

Since a catalytic surface should not alter the thermochemical equilibrium state of the gas phase, the net production of both O-atoms and O_2 molecules should equal zero under these conditions. From Fig. 6.1.1, it is seen that the loss efficiencies for O and O_2 tend to zero at exactly these three temperatures (as they should).

6.2 Specified Loss Efficiencies

In the finite-rate surface reaction formulation, the effective reaction efficiency for a gas-phase reactant consumed in a surface reaction process is *a result* of competing finite-rate processes under a given set of experimental conditions. Traditionally, surface reactions in CFD simulations have been implemented by *specifying* these reaction rate efficiencies, either as constants or as functions of temperature. Although the general finite-rate reaction approach is a more physically justified model for surface reactions, we note that it is still possible to implement the specified-reaction-efficiency (SRE) approach within its framework through the judicious choice of reaction types and parameters.

For the simple example given in Section 6.1, it is possible to derive analytic expressions for the O-atom surface coverage and the O-atom loss efficiency in terms of the reaction rate coefficients and the fixed gas-phase concentrations. The surface concentration of adsorbed O atoms is obtained from the quadratic equation,

$$a\Phi_{s,O}^2 + b\Phi_{s,O} + c = 0\,, \tag{6.2.1}$$

with

$$a = 2k_{b3}C_{O_2} - 2k_{f3} \tag{6.2.2}$$

$$b = -k_{f1}C_O - k_{b1} - k_{b2}C_{O_2} - k_{f2}C_O - 4k_{b3}C_{O_2}\Phi_s \tag{6.2.3}$$

$$c = \left(k_{f1}C_O + k_{b2}C_{O_2} + 2k_{b3}C_{O_2}\Phi_s\right)\Phi_s \tag{6.2.4}$$

Once the surface coverage is known, the O-atom and O_2 loss efficiencies can be computed from:

$$\gamma_O = \frac{\Phi_s\left(k_{f1}C_O - k_{b2}C_{O_2}\right) - \Phi_{s,O}\left(k_{f1}C_O + k_{b1} - k_{f2}C_O - k_{b2}C_{O_2}\right)}{\Gamma_O} \quad . \tag{6.2.5}$$

$$\gamma_{O_2} = \frac{\Phi_s\left(k_{b2}C_{O_2}\right) + \Phi_s^2\left(k_{b3}C_{O_2}\right) - \Phi_{s,O}\left(k_{f2}C_O + k_{b2}C_{O_2} + k_{b3}C_{O_2}2\Phi_s\right) - \Phi_{s,O}^2\left(k_{f3} - k_{b3}C_{O_2}\right)}{\Gamma_{O_2}} \tag{6.2.6}$$

Excellent numerical agreement between these analytic solutions and the integrated finite rate solutions was confirmed for all cases presented in Section 6.1.

As an example of the implementation of an SRE model into the finite-rate framework, consider catalytic oxygen recombination with a specified temperature-dependent surface recombination efficiency of $\gamma_O = \gamma \exp(-E/RT)$. Curve fits of this type are given, for example by Stewart[22-23] for a wide range of thermal protection system materials.

This simple SRE model can be recreated by neglecting the LH process and setting the backward rate coefficients for the adsorption and ER reactions to zero. After substituting the appropriate kinetic rate formula from Section 1.9 for the adsorption and ER forward rate coefficients (with $\beta = 0$), the expressions for O-atom surface coverage and the O-atom loss efficiency become:

$$\Phi_{s,O} = \frac{\Phi_s k_{f1}}{k_{f1} + k_{f2}} = \frac{\Phi_s S_0 \exp\left(-\frac{E_{ad}}{RT}\right)}{S_0 \exp\left(-\frac{E_{ad}}{RT}\right) + \gamma_0 \exp\left(-\frac{E_{er}}{RT}\right)} \tag{6.2.7}$$

$$\gamma_O = \frac{\Phi_s\left(k_{f1}C_O\right) - \Phi_{s,O}\left(k_{f1}C_O - k_{f2}C_O\right)}{\Gamma_O} = \frac{2S_0\gamma_0 \exp\left(-\frac{E_{ad}}{RT} - \frac{E_{er}}{RT}\right)}{S_0 \exp\left(-\frac{E_{ad}}{RT}\right) + \gamma_0 \exp\left(-\frac{E_{er}}{RT}\right)} \; . \tag{6.2.8}$$

It is easy to show that the choices $S_0 = \gamma_0 = \gamma$ and $E_{ad} = E_{er} = E$ lead directly to $\Phi_{s,O} = \Phi_s/2$ and $\gamma_O = \gamma \exp(-E/RT)$. One can also show that any combination of S_0 and γ_0 that satisfies $2S_0\gamma_0/(S_0 + \gamma_0) = \gamma$ will reproduce the even simpler $\gamma_O = \gamma$ (or $E = 0$) SRE model.

Often two (or more) independent surface reactions are modeled using the SRE approach (for example O + O and N + N recombination in dissociated air). These models can also be reproduced by the approach described above, with each process restricted to its own set of active sites on a single surface phase. However, with multiple active site sets in a single surface phase, the site density fraction of a particular active site set also scales these simple relationships.

Consider the example of parallel SRE models for O-atom and N-atom recombination, where we want to reproduce $\gamma_O = 0.01\exp(-5000/RT)$ and $\gamma_N = 0.003$.

This can be accomplished by limiting O-atom recombination to an active site set with $\Phi_{s1,O} = \Phi_s/4$ and N-atom recombination to an active site set with $\Phi_{s1,N} = 3\Phi_s/4$ (the value of Φ_s is arbitrary in this simple model and cancels from the final expression), and setting the following model parameters: $S_0 = \gamma_0 = 0.04$, $E_{ad,O} = E_{er,O} = 5000$ J mol^{-1}, $S_N = 0.006$, $\gamma_N = 0.003$, and $E_{ad,N} = E_{er,N} = 0$.

With these parameters:

$$\gamma_O = \frac{1}{4}\left[0.04\exp\left(-5000/RT\right)\right] = 0.01\exp\left(-5000/RT\right) \tag{6.2.9}$$

$$\gamma_N = \frac{3}{4}\left[\frac{2\cdot 0.006\cdot 0.003}{0.006+0.003}\right] = 0.003 \tag{6.2.10}$$

The surface reaction input file *O2N2SRE.surf* is given below:

```
Oxygen-Nitrogen SRE catalysis: 4 gas species, 4 surf. reactions
------------------------------------------------------------------------
Number of surface and bulk phases (gas phase=1 by definition)
nsp, nbp
1    0

Blowing/pyrolyzing gas flows? (0=NO, 1=Yes) and Surface Init. (0=empty, 1=QSS)
nblwflag     initsurf
0            0

Number of gas phase species participating in surface reactions
Name      ngps  #Phase
Air4s     4      1

For each surface phase: list  name, surface fraction,
number of active site sets, thermo avilability (0=NO, 1=Yes)
Name      sfrc         nspas      iThermo    #Phase
Silica    1.0          2          0          2

For each surface phase with 1 or more sets of active sites, list
the site density and number of species for each active site set
sdenas (mol/m2)     nspass
1.0d-06             2
3.0d-06             2

Order of gas species
Name      Molar mass  Ediss     #Species
O2        0.03200000  498000.0   1
O         0.01600000  0.0        2
N2        0.02801600  945000.0   3
N         0.01400800  0.0        4

Order of surface species (number each consecutively)
Name      Molar mass  Edes      #Species
E(s1)     0.00000000  0.0       5
O(s1)     0.01600000  350000.0  6
```

```
E(s2)     0.00000000  0.0       7
N(s2)     0.01400800  350000.0  8

Total number of surface reactions
nsrt
4

Reactant/product species for each forward surface reaction
2, 5, 0, 6, 0, 0                 #1   O + (s1) <---> O(s1)
4, 7, 0, 8, 0, 0                 #2   N + (s1) <---> N(s1)
2, 6, 0, 1, 5, 0                 #3   O + O(s1) <---> O2 + (s1)
4, 8, 0, 3, 7, 0                 #4   N + N(s1) <---> N2 + (s1)

Stoichiometric coefficients for each surface reaction
1, 1, 0, 1, 0, 0                 #1   O + (s1) <---> O(s1)
1, 1, 0, 1, 0, 0                 #2   N + (s1) <---> N(s1)
1, 1, 0, 1, 1, 0                 #3   O + O(s1) <---> O2 + (s1)
1, 1, 0, 1, 1, 0                 #4   N + N(s1) <---> N2 + (s1)

Reaction parameters for each type of reaction:
Type 0: Arrhenius:               0, Cf,         beta, Ea,   isrfon, isrbon
Type 1: Adsorption:              1, S0(0 to 1), beta, Eads, isrfon, isrbon
Type 2: Eley-Rideal:             2, Ger(0 to 1),beta, Eer,  isrfon, isrbon
Type 3: Langmuir-Hinschelwood:   3, Clh(0 to 1),beta, Em,   isrfon, isrbon
Type 4: Sublimation              4, a0Pv,       beta, Esub, isrfon, isrbon
Type 5: Arrhenius Adsorption:    5, Cf,         beta, Ea,   isrfon, isrbon

1, 4.0d-02, 0.0d+00, 5.0000d+03, 1, 0          #1   O + (s1) <---> O(s1)
1, 6.0d-03, 0.0d+00, 0.0000d+00, 1, 0          #2   N + (s1) <---> N(s1)
2, 4.0d-02, 0.0d+00, 5.0000d+03, 1, 0          #3   O + O(s1) <---> O2 + (s1)
2, 3.0d-03, 0.0d+00, 0.0000d+00, 1, 0          #4   N + N(s1) <---> N2 + (s1)

Desorption reaction or equilibrium constant parameters:
Type 1: Desorption:
      Form 0:      Arrehenius
      Form 1:      Constant attempt frequency
      Form 2:      Simple transition state theory
      Form 3:      Complex transition state theory
Type 2: Equilibrium:
      Form 0:      Arrehenius
      Form 1:      Immobile adsorption - simple transition state theory
      Form 2:      Immobile adsorption - complex transition state theory
      Form 3:      Mobile adsorption - simple transition state theory
      Form 4:      Mobile adsorption - complex transition state theory
Type, Form, Cf, eta, vdes, Edes
1, 1, 1.0, 0.0, 1.e12, 350000.0
1, 1, 1.0, 0.0, 1.e12, 350000.0
```

As a specific example, we run a fixed gas phase computation for a 10%O_2-20%O-60%N_2-10%N molar mixture at 20000 Pa and 2000 K.

The *input.inp* file for this computation is:

```
[surface file name]
'O2test/O2N2SRE.surf'

output conv freq,  file save freq,   [output file name]
          500,             -1,    'long-output.dat'

Tw (K),     Ptotal (Pa),    gas phase model,      scan mode
```

```
 2000.,          20000.,                  1,              0

 dt(s),     num steps,    time order,     diagnostic,      equilibrium
1.0d-3,       5000,             1,              2,               -1

[num gas phase species]
4

[name and mole fraction of each species]
'O2',   0.10
 'O',   0.20
'N2',   0.60
 'N',   0.10
======================================================================

Pressure & Temperature Scan (-1.0 to end)
Ptotal(Pa)  Tw (K)
    -1.,     -1.

Mole Fraction Scan (-1.0 to end)
  yO2    yO     yN2    yN
  -1.,   -1.,   -1.,   -1.

======================================================================
```

The standard output for this computation is:

```
SRModel
   version:     3.07.9
   written by:  Joe Marschall   (jochen.marschall@sri.com)
                Matthew MacLean (maclean@cubrc.org)


---Initial Conditions-----------------------------
      Wall Tmpr   =    2.0000E+03 K
      Pressure    =    2.0000E+04 Pa
      xO2         =    1.2027E-01 mol/m^3
      xO          =    2.4054E-01 mol/m^3
      xN2         =    7.2163E-01 mol/m^3
      xN          =    1.2027E-01 mol/m^3
      xE(s1)      =    1.0000E-06 mol/m^2
      xO(s1)      =    1.0000E-15 mol/m^2
      xE(s2)      =    3.0000E-06 mol/m^2
      xN(s2)      =    1.0000E-15 mol/m^2

------------------------------------------------
iteration         time       L1-norm       L2-norm
     500    5.0000E-01    0.0000E+00    0.0000E+00
    1000    1.0000E+00    0.0000E+00    0.0000E+00
    1500    1.5000E+00    0.0000E+00    0.0000E+00
    2000    2.0000E+00    0.0000E+00    0.0000E+00
    2500    2.5000E+00    0.0000E+00    0.0000E+00
    3000    3.0000E+00    0.0000E+00    0.0000E+00
    3500    3.5000E+00    0.0000E+00    0.0000E+00
    4000    4.0000E+00    0.0000E+00    0.0000E+00
    4500    4.5000E+00    0.0000E+00    0.0000E+00
    5000    5.0000E+00    0.0000E+00    0.0000E+00

---Final Conditions-------------------------------
      Wall Tmpr   =    2.0000E+03 K
      Pressure    =    2.0000E+04 Pa
      Rel Volume  =    1.0000E+00
```

```
      xO2         =    1.2027E-01 mol/m^3
      xO          =    2.4054E-01 mol/m^3
      xN2         =    7.2163E-01 mol/m^3
      xN          =    1.2027E-01 mol/m^3
      xE(s1)      =    5.0000E-07 mol/m^2
      xO(s1)      =    5.0000E-07 mol/m^2
      xE(s2)      =    1.0000E-06 mol/m^2
      xN(s2)      =    2.0000E-06 mol/m^2

---Loss Efficiencies-----------------------------
      gO2         =   -1.0470E-02
      gO          =    7.4032E-03
      gN2         =   -3.5355E-04
      gN          =    3.0000E-03

---Blowing & Recession Rate----------------------
      blowing rate    =    0.0000E+00  kg/m^2-s
      recession rate  =    0.0000E+00  m/s

---QSS Surface Coverage Distribution--------------
      Residual =    3.9119E-22
      Concentrations
         xE(s1)      =    5.0000E-07 mol/m^2
         xO(s1)      =    5.0000E-07 mol/m^2
         xE(s2)      =    1.0000E-06 mol/m^2
         xN(s2)      =    2.0000E-06 mol/m^2

---Gibbs Free-energy Minimization-----------------
      Element List
         O  N  s1  s2
      Stoichiometry
         O2        :   2.   0.   0.   0.
         O         :   1.   0.   0.   0.
         N2        :   0.   2.   0.   0.
         N         :   0.   1.   0.   0.
         E(s1)     :   0.   0.   1.   0.
         O(s1)     :   1.   0.   1.   0.
         E(s2)     :   0.   0.   0.   1.
         N(s2)     :   0.   1.   0.   1.
      Species Considered for System:
         O2  N2  E(s1)  O(s1)  E(s2)  N(s2)
      Concentrations
         xO2         =    1.2027E-01 mol/m^3
         xO          =    2.4054E-01 mol/m^3
         xN2         =    7.2163E-01 mol/m^3
         xN          =    1.2027E-01 mol/m^3
         xE(s1)      =    2.9689E-07 mol/m^2
         xO(s1)      =    7.0311E-07 mol/m^2
         xE(s2)      =    3.0000E-06 mol/m^2
         xN(s2)      =    5.0798E-12 mol/m^2

---Additional Diagnostics------------------------------------------
      <<Reaction Constants>>
   react    kf        kb       KeqC     KeqC-actual   wf-actual   wb-actual
    1    3.0109E+06  7.2305E+02  4.1642E+03  4.1573E+00  3.6213E-01  0.0000E+00
    2    6.5200E+05  7.2305E+02  9.0173E+02  1.6629E+01  7.8417E-02  0.0000E+00
    3    3.0109E+06  3.3719E+04  8.9294E+01  5.0000E-01  3.6213E-01  0.0000E+00
    4    3.2600E+05  1.4365E-09  2.2694E+14  3.0000E+00  7.8417E-02  0.0000E+00
      <<Species Production>>
      species      concentration     molar prod.      mass prod.
      O2              1.2027E-01      3.6213E-01      1.1588E-02
      O               2.4054E-01     -7.2426E-01     -1.1588E-02
      N2              7.2163E-01      7.8417E-02      2.1969E-03
```

```
   N              1.2027E-01     -1.5683E-01     -2.1969E-03
   E(s1)          5.0000E-07      0.0000E+00      0.0000E+00
   O(s1)          5.0000E-07      0.0000E+00      0.0000E+00
   E(s2)          1.0000E-06      0.0000E+00      0.0000E+00
   N(s2)          2.0000E-06      0.0000E+00      0.0000E+00
   <<Species Production Per Reaction>>
species        w-dot           w1           w2           w3           w4
O2         3.6213E-01    0.0000E+00    0.0000E+00    3.6213E-01    0.0000E+00
O         -7.2426E-01   -3.6213E-01    0.0000E+00   -3.6213E-01    0.0000E+00
N2         7.8417E-02    0.0000E+00    0.0000E+00    0.0000E+00    7.8417E-02
N         -1.5683E-01    0.0000E+00   -7.8417E-02    0.0000E+00   -7.8417E-02
E(s1)      0.0000E+00   -3.6213E-01    0.0000E+00    3.6213E-01    0.0000E+00
O(s1)      0.0000E+00    3.6213E-01    0.0000E+00   -3.6213E-01    0.0000E+00
E(s2)      0.0000E+00    0.0000E+00   -7.8417E-02    0.0000E+00    7.8417E-02
N(s2)      0.0000E+00    0.0000E+00    7.8417E-02    0.0000E+00   -7.8417E-02
```

The fourth section of this output file gives the results $\gamma_O = 0.0074032$ and $\gamma_N = 0.003$, which agree exactly with the desired SRE values at 2000 K.

6.3 Silica Sublimation

Many thermal protection systems contain silica or silica formers. At sufficiently high temperatures, silica melts and its vapor pressure increases dramatically, leading to volatilization of silicon containing compounds.

Here, we use the case of silica vaporization into argon at 2500 K to illustrate the relationship between the steady-state solution of various steady-state finite-rate models and the Gibbs minimization equilibrium solutions.

We take the initial argon pressure to be 10,000 Pa. We model the system using a gas phase, a bulk silica phase (b1), and a surface phase containing two sets of active sites, one of which mediates SiO_2 vaporization (s1) and the other surface catalytic reactions (s2).

Six gas species are considered—O_2, O, Ar, SiO_2, SiO, and Si—and three surface species are considered: E(s1), E(s2), and O(s2).

Combinations of the following five surface reactions are used in the finite-rate surface model to illustrate different behaviors:

$$[s1] + [\mathrm{SiO_2}]_{b1} \rightarrow \mathrm{SiO_2} + [s1] \quad . \tag{6.3.1}$$

$$\mathrm{O} + [s2] \rightarrow [\mathrm{O}]_{s2} \tag{6.3.2}$$

$$\mathrm{O} + [\mathrm{O}]_{s2} \rightarrow \mathrm{O_2} + [s2] \quad . \tag{6.3.3}$$

$$\mathrm{SiO} + [\mathrm{O}]_{s2} \rightarrow \mathrm{SiO_2} + [s2] \quad . \tag{6.3.4}$$

$$\mathrm{Si} + [\mathrm{O}]_{s2} \rightarrow \mathrm{SiO} + [s2] \quad . \tag{6.3.5}$$

The same input parameters as in Section 6.1 above are used for the adsorption, desorption, and all Eley-Rideal reactions. For the vaporization (sublimation) reaction (6.3.1), we set $E_\alpha = 0$ and $\alpha_0 = 1$, leading to $E_{sub} = E_{vap}$ and $\gamma_{sub} = P_0$, where the vapor pressure of SiO_2 over silica can be represented by the function $P_{SiO2} = 3.5 \times 10^{13} \exp(-565352/RT)$ in Pa (David M. Driver, NASA Ames Research Center, private communication, 2011.) The active site densities are set to $\Phi_{s1} = \Phi_{s2} = 3.75 \times 10^{-6}$ mol m^{-2}.

The surface reaction file for this model, *SiO2Ar6.surf* is:

```
  SiO2 Sublimation v1: 6 gas species, 5 surf. reac.
-------------------------------------------------------------------------
Number of surface and bulk phases (gas phase=1 by definition)
nsp, nbp
1    1

Blowing/pyrolyzing gas flows? (0=No, 1=Yes)
nblwflag     initsurf
0            0

Number of gas phase species in surface reaction and blowing model
Name      ngps  #Phase
Ar6s      6      1

For each surface phase: list  name, surface fraction,
number of active site sets, thermo availability (0=No, 1=Yes)
Name      sfrc       nspas     iThermo    #Phase
SiO2(s1)   1.0        2         0          2

For each surface phase with 1 or more sets of active sites, list
the site density and number of species for each active site set
sdenas (mol/m2)      nspass       #phase#sites
3.75d-06              1            2/1
3.75d-06              2            2/2

For each bulk phase: list  name, mass density, porosity,
phase volume fraction and number of bulk species
Name      density      porosity     vol. frac.    nbps      #Phase
SiO2       2200.0       0.0          1.0           1         3

Order of gas species
Name      Molar mass  Ediss     #Species  Dissociation Reaction
O2        0.03200000  493440.0   1              O2=>O+O
O         0.01600000  0.0        2
Ar        0.03994800  0.0        3
SiO2      0.06008550  1797157.   4              SiO2=>Si+O+O
SiO       0.04408550  792388.0   5              SiO=>Si+O
Si        0.02808550  0.0        6

Order of surface species (number each consecutively)
Name      Molar mass  Ed              #Species
E(s1)     0.00000000  0.0                7
E(s2)     0.00000000  0.0                8
O(s2)     0.01600000  350000.0           9

Order of bulk species (number each consecutively)
Name      Molar mass  Mole fraction     #Species
SiO2(b1)  0.06008550  1.0                10
```

```
Total number of surface reactions
nsrt
5

Reactant/product species for each forward surface reaction
  7, 10, 0, 4, 7, 0        #1  (s1) + SiO2(b1) <---> SiO2 + (s1)
  2, 8, 0, 9, 0, 0         #2   O + (s2) <---> O(s2)
  2, 9, 0, 1, 8, 0         #3   O + O(s2) <---> O2 + (s2)
  5, 9, 0, 4, 8, 0         #4   SiO + O(s2) <---> SiO2 +(s2)
  6, 9, 0, 5, 8, 0         #5   Si + O(s2) <---> SiO +(s2)

Stoichiometric coefficients for each surface reaction
 1, 1, 0, 1, 1, 0          #1  (s1) + SiO2(b1) <---> SiO2 + (s1)
 1, 1, 0, 1, 0, 0          #2   O + (s2) <---> O(s2)
 1, 1, 0, 1, 1, 0          #3   O + O(s2) <---> O2 + (s2)
 1, 1, 0, 1, 1, 0          #4   SiO + O(s2) <---> SiO2 +(s2)
 1, 1, 0, 1, 1, 0          #5   Si + O(s2) <---> SiO +(s2)

 Reaction parameters for each type of reaction:
 Arrhenius:              0,   Cf, beta,   Ea, isrfon, isrbon
 Adsorption:             1,   S0, beta, Eads, isrfon, isrbon
 Eley-Rideal:            2,  Ger, beta,  Eer, isrfon, isrbon
 Langmuir-Hinschelwood: 3,  Clh, beta,   Em, isrfon, isrbon
 Sublimation:            4, a0Pv, beta, Esub, isrfon, isrbon
 Arrhenius Adsorption:  5,   Cf, beta,   Ea, isrfon, isrbon
 Type, (Param), beta,   Ea, isrfon, isrbon
4, 3.50d+13, 0.0d+00,  565350.0, 1, 1   #1  (s1) + SiO2(b1) <---> SiO2 + (s1)
1, 5.0d-02, 0.0d+00, 0.0000d+00, 1, 1   #2   O + (s2) <---> O(s2)
2, 1.0d-03, 0.0d+00, 9.0000d+03, 1, 1   #3   O + O(s2) <---> O2 + (s2)
2, 1.0d-03, 0.0d+00, 9.0000d+03, 1, 1   #4   SiO + O(s2) <---> SiO2 +(s2)
2, 1.0d-03, 0.0d+00, 9.0000d+03, 1, 1   #5   Si + O(s2) <---> SiO +(s2)

Desorption reaction or equilibrium constant parameters:
Type 1: Desorption:
       Form 0:      Arrhenius
       Form 1:      Constant attempt frequency
       Form 2:      Simple transition state theory
       Form 3:      Complex transition state theory
Type 2: Equilibrium:
       Form 0:      Arrhenius
       Form 1:      Immobile adsorption - simple transition state theory
       Form 2:      Immobile adsorption - complex transition state theory
       Form 3:      Mobile adsorption - simple transition state theory
       Form 4:      Mobile adsorption - complex transition state theory
Type, Form, Cf, eta, vdes, Edes
1, 1, 1.0, 0.0, 1.e12, 350000.0
```

The *input .inp* file to run a constant volume finite-rate solution for this model is:

```
[surface file name]
'SiO2Ar6.surf'

output conv freq,  file save freq,   [output file name]
          10000,             -1,    'long-output.dat'

Tw (K),   Ptotal (Pa),    gas phase model,      scan mode
 2500.,        10000.0,                  0,              0
```

```
 dt(s),     num steps,    time order,     diagnostic,      equilibrium
5.0d-2         100000,             1,              3,               -1

[num gas phase species]
 6

[name and mole fraction of each species]
'O2',   0.0
'O',    0.0
'Ar',   1.0
'SiO2', 0.0
'SiO',  0.0
'Si',   0.0
=====================================================================

Pressure & Temperature Scan (-1.0 to end)
Ptotal(Pa)  Tw (K)
    -1.,       -1.

Mole Fraction Scan (-1.0 to end)
  yO2    yO    yAr   ySiO2   ySiO     ySi
  -1.,   -1.,   -1.,   -1.,   -1.,    -1.

=====================================================================
```

The computed species concentrations for the constant pressure and constant volume solutions are listed in Tables 6.3.1 and 6.3.2, respectively. These tables give the initial condition, followed by time-integrated finite-rate solutions for models that include some or all of the surface reactions (e.g., R124 includes reactions 6.3.1, 6.3.2, and 6.3.4), as well as the Gibbs minimization solution. The bottom row in each table shows the final system volume (Table 6.3.1) or the final system pressure (Table 6.3.2) computed by each model.

The computations for different sets of reactions were specified by modifying the **isrfon** and **isrbon** flags in *SiO2Ar6.surf* file appropriately (1 = on and 0 = off).

Constant volume and constant pressure solutions were specified by setting the **gas-phase model** flag in the *input.inp* file (0 for constant volume, 2 for constant pressure.)

The RC1 model incorporates only the vaporization reaction. In this model, SiO_2 vaporizes into the gas phase until the partial pressure of SiO_2 equals its vapor pressure at 2500 K. If the system pressure is held constant, the volume expands slightly to accommodate the additional SiO_2 molecules; if the system volume is held constant, the total pressure rises as the SiO_2 partial pressure is added to the existing Ar partial pressure. Both RC1 solutions come to steady state, but they do not agree with the corresponding Gibbs minimization solutions because other Si and O containing species exist at equilibrium at 2500 K, and there is no reaction mechanism that can form them.

Table 6.3.1: Constant Pressure Solutions:
Gas (mole m^{-3}) and Surface (mole m^{-2}) Species Concentrations at 2500 K and 10,000 Pa

Species	Initial	RC1	RC124	RC1234	RC12345	Gibbs
O_2	0	0	0	1.0066E-02	1.0066E-02	1.0066E-02
O	0	0	8.6199E-03	3.1868E-03	3.1868E-03	3.1870E-03
Ar	4.8109E-01	4.7809E-01	4.6085E-01	4.4152E-01	4.4152E-01	4.4155E-01
SiO_2	0	2.9970E-03	2.9970E-03	2.9970E-03	2.9970E-03	2.9972E-03
SiO	0	0	8.6212E-03	2.3319E-02	2.3319E-02	2.3320E-02
Si	0	0	0	0	3.8644E-09	3.8647E-09
E(s1)	3.7500E-6	3.7500E-06	3.7500E-06	3.7500E-06	3.7500E-06	3.7500E-06
E(s2)	3.7500E-6	3.7500E-06	2.4401E-06	3.1290E-06	3.1290E-06	3.1290E-06
O(s2)	0	0	1.3099E-06	6.2098E-07	6.2098E-07	6.2098E-07
Rel. Volume	1	1.0063	1.0439	1.0896	1.0896	1.0896

Table 6.3.2: Constant Volume Solutions:
Gas (mole m^{-3}) and Surface (mole m^{-2}) Species Concentrations at 2500 K and 1 m^3.

Species	Initial	RC1	RC124	RC1234	RC12345	Gibbs
O_2	0	0	0	1.0066E-02	1.0066E-02	1.0066E-02
O	0	0	8.6199E-03	3.1868E-03	3.1868E-03	3.1870E-03
Ar	4.8109E-01	4.8109E-01	4.8109E-01	4.8109E-01	4.8109E-01	4.8109E-01
SiO_2	0	2.9970E-03	2.9970E-03	2.9970E-03	2.9970E-03	2.9972E-03
SiO	0	0	8.6212E-03	2.3319E-02	2.3319E-02	2.3320E-02
Si	0	0	0	0	3.8645E-09	3.8647E-09
E(s1)	3.7500E-6	3.7500E-06	3.7500E-06	3.7500E-06	3.7500E-06	3.7500E-06
E(s2)	3.7500E-6	3.7500E-06	2.4401E-06	3.1290E-06	3.1290E-06	3.1290E-06
O(s2)	0	0	1.3099E-06	6.2098E-07	6.2098E-07	6.2098E-07
Pressure, Pa	10000	10062	10421	10822	10822	10822

If reactions RC2 and RC4 are added to the set, it is now possible to form gas phase O and SiO species. Note that these species, generated as reactions RC2 and RC4, are driven in the backward direction under the initial conditions of the system. SiO_2 is added to the gas phase by vaporization, converted to SiO and O(s2) by RC4, and O(s2) is converted to O by RC2. These processes continue until species production in the forward and backward directions cancel. However, the O and SiO concentrations are still not equivalent to the Gibbs solutions. This is because there is no way for the surface reaction system to form O_2, which is in significant excess of O under equilibrium conditions. Thus, there are fewer gas-phase SiO molecules and more gas-phase and adsorbed O atoms in the final state reached by the finite-rate system than there should be in equilibrium.

By adding RC3 to the reaction set, O_2 can be efficiently formed by surface catalytic recombination, and the final gas and surface species concentrations are now essentially identical to the Gibbs minimization solutions. The only exception is the minor gas species Si. This situation is remedied by adding RC5 to set to enable surface formation of Si by the decomposition of SiO.

This example makes clear that finite-rate surface reaction model solutions for species concentrations can only be expected to agree with the Gibbs energy minimization equilibrium solutions if reaction mechanisms for the production of all species important at equilibrium are included in the surface model. This is no different than for purely gas-phase chemistry mechanisms, in which chemical equilibrium cannot be expected if key gas-phase formation reactions are omitted.

We note two further points:

First, agreement between time-integrated finite-rate solutions and Gibbs minimization solutions does not imply that the chosen set of surface reactions is either unique or even physically accurate—only that the constructed finite-rate surface reaction system is capable of reaching equilibrium.

Second, for applications where both surface and chemical reactions influence the species concentrations of the gas phase in contact with the surface (for example, in the surface volume of a CFD grid), it is not a requirement that the surface reactions alone equilibrate the system, so long as sufficient gas-phase reactions are included in the chemistry set to reach equilibrium.

Finally, we can consider the case in which the bounding gas phase is fixed at its initial state—for example, if silica vaporizes into a fast flow of argon that removes the gas-phase SiO_2 before it can build up or participate in further surface reactions. This case is run by setting the gas-phase model flag to 1 in the *input.inp* file. In this case, silica sublimates continuously at the rapid rate of 0.0183 kg m^{-2} s^{-1} without any re-condensation. Such rapid mass loss corresponds to a recession rate of about 8.32 μm s^{-1} assuming a silica density of 2200 kg m^{-3}.

6.4 Catalytic Recombination in the Martian Atmosphere

The Martian atmosphere is predominately carbon dioxide with approximately 3% nitrogen. Dissociation of these molecules during atmospheric entry gives rise to the possibility of various surface recombination reactions involving CO, C, O, and N. Under moderate entry conditions, the predicted C-atom and N-atom concentrations near the surface are much smaller than those of O atoms and CO molecules, and the main surface reactions contributing to catalytic heating are recombination to molecular oxygen and carbon dioxide.

A simple finite-rate surface reaction model can be constructed within the present framework based on two adsorption reactions and three Eley-Rideal recombination reactions:

$$\mathrm{O} + [s] \rightarrow [\mathrm{O}]_s \tag{6.4.1}$$

$$\mathrm{CO} + [s] \rightarrow [\mathrm{CO}]_s \tag{6.4.2}$$

$$\mathrm{O} + [\mathrm{O}]_s \rightarrow \mathrm{O}_2 + [s] \tag{6.4.3}$$

$$\mathrm{O} + [\mathrm{CO}]_s \rightarrow \mathrm{CO}_2 + [s] \tag{6.4.4}$$

$$\mathrm{CO} + [\mathrm{O}]_s \rightarrow \mathrm{CO}_2 + [s] \quad . \tag{6.4.5}$$

This is the same reaction set presented by Gupta et al.[24] and similar to that of Micheltree and Gnoffo,[25] who omitted the oxygen recombination reaction (6.4.3). This reaction set was also used by Afonina et al.,[26] although in most of their work CO adsorption (6.4.2) was neglected.

Many different surface reaction models can be constructed from this set of reactions, depending on the values assigned to the parameters in the forward reaction rate coefficient expressions and the desorption reactions. Here, we use this reaction set to illustrate how species production rates, and the loss efficiencies and branching fractions for O and CO, vary at a fixed temperature with the bounding gas composition.

We construct a simple surface reaction model, where the gas phase contains only O_2, O, CO, and CO_2, and the surface phase has one set of active sites with three surface species, E(s), O(s), and CO(s). We set $\Phi_s = 7.5\times10^{-6}$ mol m^{-2}, all $\beta = 0$, and the adsorption and Eley-Rideal energy barriers to zero ($E_{ad} = E_{er} = 0$. We specify both O-atom and CO thermal desorption by Form 1 (Eq. (1.7.11)) with $A_{des} = 1$, $\beta = 0$, $\nu = 1.0\times10^{12}$ s^{-1} and E_{des} = 300000 J mol^{-1}.
There is some evidence that O-atom recombination to O_2 is a more likely outcome than O + CO recombination to CO_2, at least under some conditions.[27-28] A rationalization for this behavior is that O atoms may adsorb more efficiently to a surface because they do not suffer from steric hindrances associated with the orientation of the impinging CO on the surface. A similar argument can be made for ER reactions involving O and CO partners.

We consider two cases: Case a) all surface reactions have identical rate coefficients of $S_{0,1} = S_{0,2} = \gamma_{er,3} = \gamma_{er,4} = \gamma_{er,5} = 0.01$; and Case b) we keep $S_{0,1} = \gamma_{er,3} = 0.01$ and reset set $S_{0,2} = \gamma_{er,4} = \gamma_{er,5} = 0.001$ to make reactions with CO more inefficient.

The surface reaction file for Case b, *CO2Mars.surf*, is:

```
CO2 Mars V1: 4 gas species, 2 surf. species, 5 surf. reac.
-----------------------------------------------------------------
Number of surface and bulk phases (gas phase=1 by definition)
nsp, nbp
1    0

Blowing/pyrolyzing gas flows?(0=NO, 1=Yes) Surf. Init. (0=empty, 1=QSS)
nblwflag     initsurf
0            0

Number of gas phase species in surface reaction and blowing model
Name      ngps  #Phase
Mars4s     4      1

For each surface phase: list  name, surface fraction,
number of active site sets, thermo availability (0=No, 1=Yes)
Name      sfrc       nspas     iThermo    #Phase
Surface    1.0        1         0          2

For each surface phase with 1 or more sets of active sites, list
the site density and number of species for each active site set
sdenas (mol/m2)      nspass       #phase#sites
7.5d-06              3             2/1

Order of gas species
Name      Molar mass  Ediss     #Species  Dissociation Reaction
O2        0.03200000  493440.0   1        O2=>O+O
O         0.01600000  0.0        2
CO        0.02801100  1071726.0  3        CO=>C+O
CO2       0.04401100  526054.0   4        CO2=>CO+O

Order of surface species (number each consecutively)
Name      Molar mass  Ed              #Species
E(s)     0.00000000  0.0             5
O(s)     0.01600000  300000.0        6
CO(s)    0.02801100  300000.0        7

Total number of surface reactions
nsrt
5

Reactant/product species for each forward surface reaction
2, 5, 0, 6, 0, 0        #1   O + (s)  <---> O(s)
3, 5, 0, 7, 0, 0        #2   CO + (s) <---> CO(s)
2, 6, 0, 1, 5, 0        #3   O + O(s) <---> O2 + (s)
2, 7, 0, 4, 5, 0        #4   O + CO(s) <---> CO2 + (s)
3, 6, 0, 4, 5, 0        #5   CO + O(s) <---> CO2 + (s)
```

```
Stoichiometric coefficients for each surface reaction
1, 1, 0, 1, 0, 0        #1   O + (s)  <---> O(s)
1, 1, 0, 1, 0, 0        #2   CO + (s) <---> CO(s)
1, 1, 0, 1, 1, 0        #3   O + O(s) <---> O2 + (s)
1, 1, 0, 1, 1, 0        #4   O + CO(s) <---> CO2 + (s)
1, 1, 0, 1, 1, 0        #5   CO + O(s) <---> CO2 + (s)

Reaction parameters for each type of reaction:
Type 0: Arrhenius:            0, Cf,         beta, Ea,   isrfon, isrbon
Type 1: Adsorption:           1, S0(0 to 1), beta, Eads, isrfon, isrbon
Type 2: Eley-Rideal:          2, Ger(0 to 1),beta, Eer,  isrfon, isrbon
Type 3: Langmuir-H.:          3, Clh(0 to 1),beta, Em,   isrfon, isrbon
Type 4: Sublimation   a0Pv(T) 4, a0Pv0,      beta, Esub, isrfon, isrbon
Type 5: Arrhenius Adsorption: 5, Cf,         beta, Ea,   isrfon, isrbon

1, 0.010d+00,  0.0d+00, 0.000d+00,  1, 1   #1 O + (s)  <---> O(s)
1, 0.001d+00,  0.0d+00, 0.000d+00,  1, 1   #2 CO + (s) <---> CO(s)
2, 0.010d+00,  0.0d+00, 0.000d+00,  1, 1   #3 O + O(s) <---> O2 + (s)
2, 0.001d+00,  0.0d+00, 0.000d+00,  1, 1   #4 O + CO(s) <---> CO2 + (s)
2, 0.001d+00,  0.0d+00, 0.000d+00,  1, 1   #5 CO + O(s) <---> CO2 + (s)

Desorption reaction or equilibrium constant parameters:
Type 1: Desorption:
      Form 0:     Arrhenius
      Form 1:     Constant attempt frequency
        Form 2:   Simple transition state theory
        Form 3:   Complex transition state theory
Type 2: Equilibrium:
      Form 0:     Arrhenius
        Form 1:   Immobile adsorption - simple transition state theory
        Form 2:   Immobile adsorption - complex transition state theory
        Form 3:   Mobile adsorption - simple transition state theory
        Form 4:   Mobile adsorption - complex transition state theory
Type, Form, Cf, eta, vdes, Edes
1, 1, 1.0, 0.0, 1.e12, 300000.0
1, 1, 1.0, 0.0, 1.e12, 300000.0
```

We fix the surface temperature and pressure as 2500 K and 10,000 Pa, respectively, and compute the species production rates, the reactant loss efficiencies, and the reactant branching ratios as the surface is exposed to a series of fixed gas compositions ranging from CO to O rich, as listed in Table 6.4.1

Table 6.4.1: Bounding Gas Compositions (mole fractions)

	1	2	3	4	5	6	7	8	9
O_2	0.01	0.01	0.01	0.01	0.01	0.01	0.01	0.01	0.01
O	0.09	0.19	0.29	0.39	0.49	0.59	0.69	0.79	0.89
CO	0.89	0.79	0.69	0.59	0.49	0.39	0.29	0.19	0.09
CO_2	0.01	0.01	0.01	0.01	0.01	0.01	0.01	0.01	0.01

The corresponding *input.inp* file is:

```
[surface file name]
'CO2Mars.surf'

output conv freq,  file save freq,   [output file name]
          1000,             1000,    'long-output.dat'

Tw (K),   Ptotal (Pa),    gas phase model,      scan mode
 2500.,        10000.,               1,              1

 dt(s),     num steps,    time order,    diagnostic,     equilibrium
5.0d-2         10000,          1,           3,              -1

[num gas phase species]
 4

[name and mole fraction of each species]
'O2',    0.01
'O',     0.09
'CO',    0.89
'CO2',   0.01
=====================================================================

Pressure & Temperature Scan (-1.0 to end)
Ptotal(Pa)  Tw (K)
    -1.,       -1.

Mole Fraction Scan (-1.0 to end)
  y02    yO     yCO    yCO2
  0.01  0.09    0.89   0.01
  0.01  0.19    0.79   0.01
  0.01  0.29    0.69   0.01
  0.01  0.39    0.59   0.01
  0.01  0.49    0.49   0.01
  0.01  0.59    0.39   0.01
  0.01  0.69    0.29   0.01
  0.01  0.79    0.19   0.01
  0.01  0.89    0.09   0.01
  -1.,   -1.,   -1.,   -1.

=====================================================================
```

The output file is in a tabular format and is not reproduced here because of it size (given the seven different species and 5 different reactions). The net global species production rates and the species loss efficiencies are available directly from the program output; the branching fractions were post-processed from the reaction-specific global species production rates, according to Eq. (1.10.3).

The results for Case a and Case b are plotted in Fig. 6.4.1.

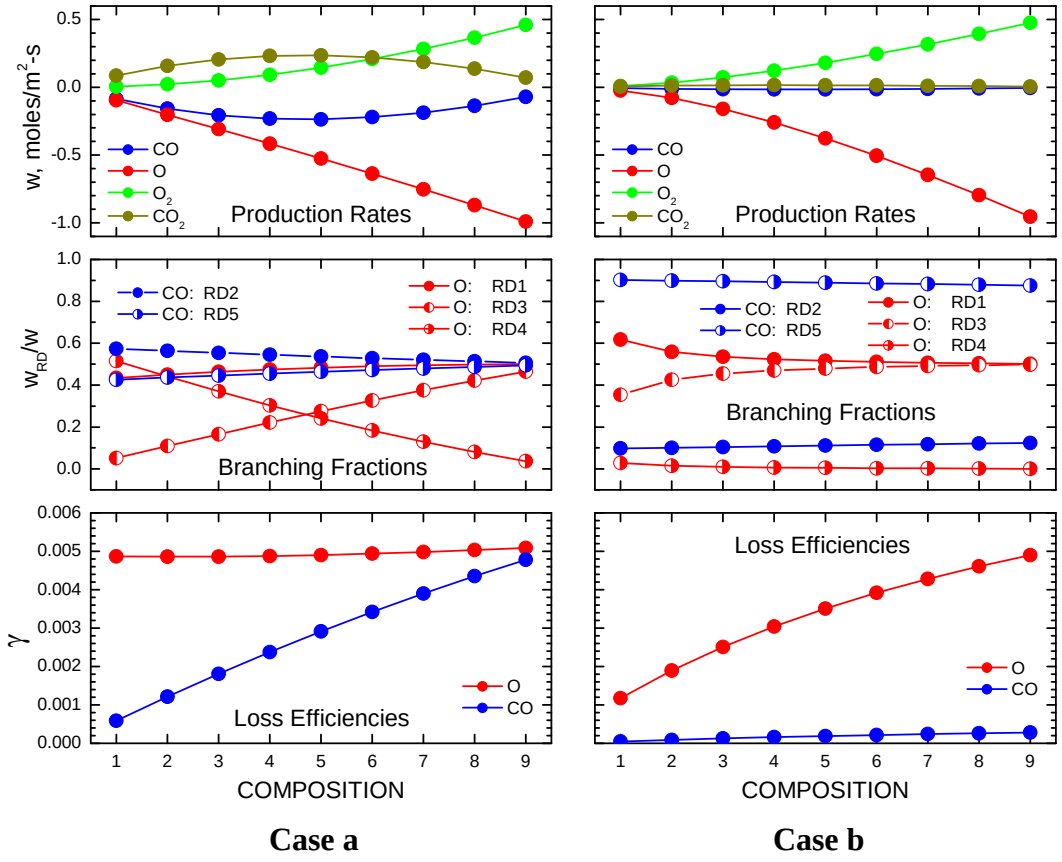

Figure 6.4.1 Species Production Rates at the Surface (top panels), O and CO Branching Fractions (middle panels), and O and CO Loss Efficiencies (bottom panels), at 2500 K and 10,000 Pa for the Compositions Listed in Table 6.4.1; Case a) on the Left, and Case b on the Right.

For Case a, the production rates of O and CO are negative because they are consumed, while those of O_2 and CO_2 are positive, which indicates species generation. As expected, CO loss and CO_2 generation are maximized when the gas-phase O and CO concentrations are similar, while O-atom loss and O_2 generation increase monotonically with increasing gas-phase O concentration.

Note that the O and CO loss efficiencies (the fraction of collisions with the surface that remove the gas species from the gas phase), as well as their branching fractions (the relative amounts of each species lost via different surface reactions), vary smoothly with changes in the bounding gas composition. In the finite-rate formulation, loss efficiencies and branching fractions are a result of finite-rate reactions competing for active surface sites in response to the imposed boundary conditions. This is a fundamental difference from SRE models, and we argue it is a more physically justified representation of surface chemistry in systems with multiple reactants participating in multiple reactions.

The O-atom loss efficiency is relatively constant, but the dominant loss pathway changes from adsorption and ER CO_2 formation to adsorption and ER O_2 formation as the gas-phase O-atom mole fraction increases. The CO branching fractions are about evenly split between adsorption and ER CO_2 formation, but the CO loss efficiency increases as with decreasing gas-phase CO.

For Case b), the production rates of CO and CO_2 are much smaller than those of O and O_2. The branching fractions show that almost all O-atom loss is due to adsorption and ER O_2 generation. Both the O-atom and CO loss efficiencies increase with increasing gas-phase O-atom mole fraction, but the former is much larger than the latter. The small CO loss is predominately due to ER formation of CO_2 by reaction with an adsorbed O atom.

Of course, many other reaction mechanisms and possible parameter choices exist, but these examples show the flexibility of the finite-rate formulation for modeling surface catalysis in the dissociated CO_2 system.

Chapter 7: DPLR Code Examples with Finite-Rate Surface Boundary Condition

7.1 Catalytic Recombination in Dissociated Oxygen

The first example case considers the 1.0 m cylinder studied by Sorensen and Schwartzentruber[29] using catalytic rate data for a silica surface in reacting air as part of an uncertainty sensitivity analysis at temperatures both at and above the nominal operability range of silica. The objective of their study was to assess sensitivity of the physical mechanisms of surface catalysis and not to validate a model of silica, per se.

The freestream conditions for the problem are $\rho = 0.001$ kg/m^3, U = 6.0 km/s, T = 200 K. A range of fixed wall temperatures were considered by Sorensen and Schwartzentruber, in which four cases at wall temperatures of 1750 K, 2000 K, 2250 K, and 2750 K have been used here to make direct comparisons to their results obtained using an independently developed finite-rate catalysis model installed in the US3D code.[30-31] Diffusion has been modeled for this problem in the same way as the US3D results by using Fickian diffusion and computing the diffusion coefficient using a common definition of constant Lewis number of 1.4.

Flags used for the DPLR input file are not shown here due to the long length of the file. Only a few are relevant to the surface reaction model boundary condition. Most important is the setting of ***icatmd****=990* in the surface record. The ***twall*** flag was set to the temperatures given above for each case. The diffusion model was set to match the diffusion model of US3D by setting ***idmod****=1*, ***ils****=3*, and ***Le/Sc****=1.40*. A single grid block was used with 128 x 96 cells with the surface face of the block set with a boundary condition ***ibc****=90* to represent a generic viscous wall with surface record settings.

The surface reaction input file for this case is given below:

File *Air_Silica_Model3_v1.surf*:

```
Air-Silica Catalysis: 5 gas species, 10 surf. reactions (Marschall 2009)
------------------------------------------------------------------------
Number of surface and bulk phases (gas phase=1 by definition)
nsp, nbp
1    0

Blowing/pyrolyzing gas flows?(0=NO, 1=Yes) Initialization(0=empty sites, 1=QSS)
nblwflag     initsurf
0            0

Number of gas phase species participating in surface reactions
Name      ngps  #Phase
Air5s     5      1

For each surface phase: list  name, surface fraction,
```

```
number of active site sets, thermo avilability (0=NO, 1=Yes)
Name      sfrc         nspas      iThermo    #Phase
Silica    1.0          1          0          2

For each surface phase with 1 or more sets of active sites, list
the site density and number of species for each active site set
sdenas (mol/m2)     nspass
7.5d-06             3

Order of gas species
Name      Molar mass  Ediss     #Species
N2        0.02801600  945000.0 1
O2        0.03200000  498000.0 2
NO        0.03000800  631000.0 3
N         0.01400800  0.0            4
O         0.01600000  0.0            5

Order of surface species (number each consecutively)
Name      Molar mass  Edes      #Species
E(s1)     0.00000000  0.0            6
N(s1)     0.01400800  350000.0 7
O(s1)     0.01600000  350000.0       8

Total number of surface reactions
nsrt
10

Reactant/product species for each forward surface reaction
5, 6, 0, 8, 0, 0               #1   O + (s1) <---> O(s1)
4, 6, 0, 7, 0, 0               #2   N + (s1) <---> N(s1)
5, 8, 0, 2, 6, 0               #3   O + O(s1) <---> O2 + (s1)
4, 7, 0, 1, 6, 0               #4   N + N(s1) <---> N2 + (s1)
5, 7, 0, 3, 6, 0               #5   O + N(s1) <---> NO + (s1)
4, 8, 0, 3, 6, 0               #6   N + O(s1) <---> NO + (s1)
8, 0, 0, 2, 6, 0               #7   2O(s1) <---> O2 + 2(s1)
7, 0, 0, 1, 6, 0               #8   2N(s1) <---> N2 + 2(s1)
8, 7, 0, 3, 6, 0               #9   O(s1) + N(s1) <---> NO + 2(s1)
7, 8, 0, 3, 6, 0               #10  N(s1) + O(s1) <---> NO + 2(s1)

Stoichiometric coefficients for each surface reaction
1, 1, 0, 1, 0, 0               #1   O + (s1) <---> O(s1)
1, 1, 0, 1, 0, 0               #2   N + (s1) <---> N(s1)
1, 1, 0, 1, 1, 0               #3   O + O(s1) <---> O2 + (s1)
1, 1, 0, 1, 1, 0               #4   N + N(s1) <---> N2 + (s1)
1, 1, 0, 1, 1, 0               #5   O + N(s1) <---> NO + (s1)
1, 1, 0, 1, 1, 0               #6   N + O(s1) <---> NO + (s1)
2, 0, 0, 1, 2, 0               #7   2O(s1) <---> O2 + 2(s1)
2, 0, 0, 1, 2, 0               #8   2N(s1) <---> N2 +2(s1)
1, 1, 0, 1, 2, 0               #9   O(s1) + N(s1) <---> NO + 2(s1)
1, 1, 0, 1, 2, 0               #10  N(s1) + O(s1) <---> NO + 2(s1)

Reaction parameters for each type of reaction:
```

```
Type 0: Arrhenius:              0, Cf,         beta, Ea,   isrfon, isrbon
Type 1: Adsorption:                   1, S0(0 to 1), beta, Eads, isrfon, isrbon
Type 2: Eley-Rideal:            2, Ger(0 to 1),beta, Eer,  isrfon, isrbon
Type 3: Langmuir-Hinschelwood: 3, Clh(0 to 1),beta, Em,   isrfon, isrbon
Type 4: Sublimation             4, a0Pv,       beta, Esub, isrfon, isrbon
Type 5: Arrhenius Adsorption:  5, Cf,         beta, Ea,   isrfon, isrbon
Type, param, beta, Ea, isrfon, isrbon
1, 5.0d-02, 0.0d+00, 0.0000d+00, 1, 1            #1
1, 5.0d-02, 0.0d+00, 0.0000d+00, 1, 1            #2
2, 1.0d-03, 0.0d+00, 9.0000d+03, 1, 1            #3
2, 1.0d-03, 0.0d+00, 9.0000d+03, 1, 1            #4
2, 1.0d-03, 0.0d+00, 9.0000d+03, 1, 1            #5
2, 1.0d-03, 0.0d+00, 9.0000d+03, 1, 1            #6
3, 1.0d-01, 0.0d+00, 3.0000d+05, 1, 1            #7
3, 1.0d-01, 0.0d+00, 3.0000d+05, 1, 1            #8
3, 1.0d-01, 0.0d+00, 3.0000d+05, 1, 1            #9
3, 1.0d-01, 0.0d+00, 3.0000d+05, 1, 1            #10

Desorption reaction or equilibrium constant parameters:
Type 1: Desorption:
      Form 0:     Arrehenius
      Form 1:     Constant attempt frequency
        Form 2:   Simple transition state theory
        Form 3:   Complex transition state theory
Type 2: Equilibrium:
      Form 0:     Arrehenius
        Form 1:   Immobile adsorption - simple transition state theory
        Form 2:   Immobile adsorption - complex transition state theory
        Form 3:   Mobile adsorption - simple transition state theory
        Form 4:   Mobile adsorption - complex transition state theory
Type, Form, Cf, eta, vdes, Edes
1, 1, 1.0, 0.0, 1.e12, 350000.0
1, 1, 1.0, 0.0, 1.e12, 350000.0
```

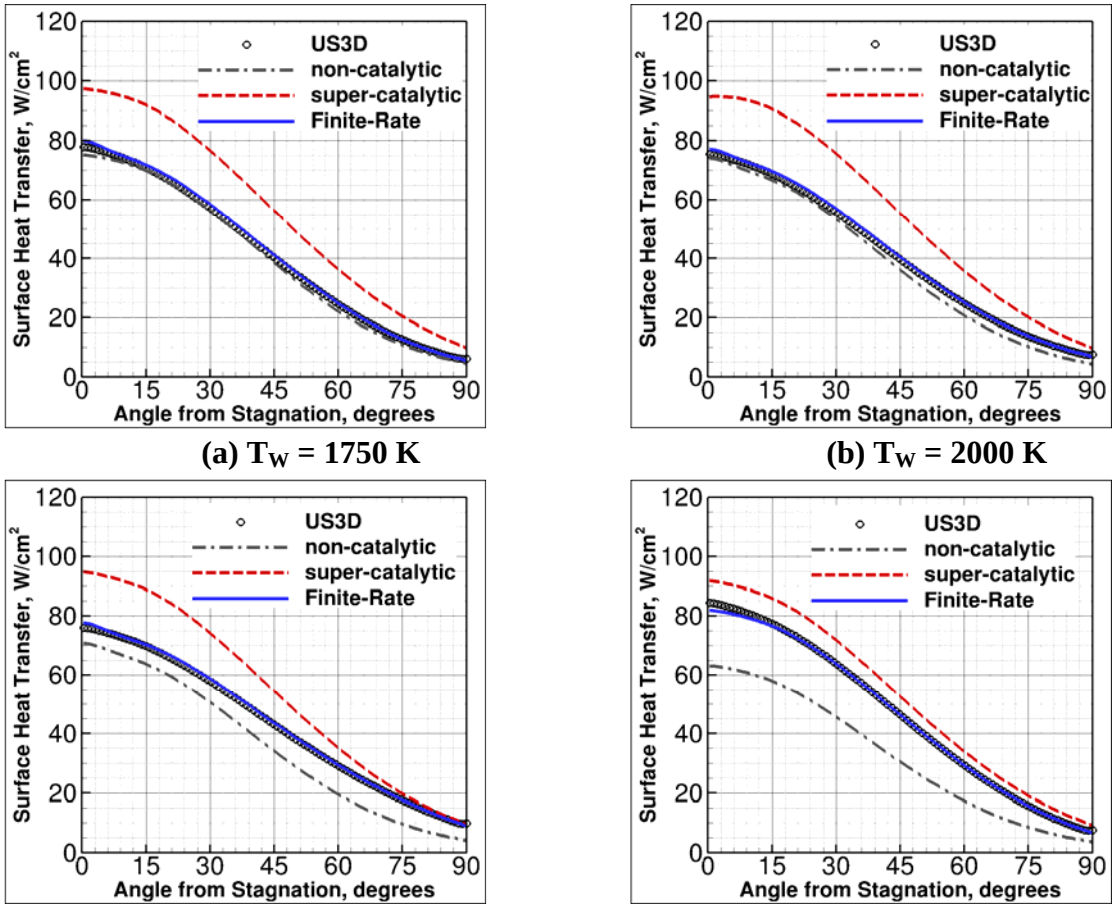

(a) T_W = 1750 K **(b) T_W = 2000 K**

(c) T_W = 2250 K **(d) T_W = 2750 K**

Figure 7.1.1. Comparison of Predicted Heat Transfer Profile Using DPLR and US3D for a Silica Cylinder at Four Different Surface Temperatures.

The comparison of the heat transfer predicted by DPLR and by US3D is shown for the four wall temperatures in Fig. 7.1.1. For all cases, the comparison is excellent–we note again these results have been obtained with two independent chemically reacting flow solvers and two independent implementations of fully coupled finite-rate surface catalysis. At the lowest surface temperatures shown, the effect of the finite-rate reactions at the surface are benign, as the net heating rate is near the non-catalytic limit. As surface temperature increases, the surface becomes more reactive as the heat transfer is observed to increase relative to the non-catalytic wall solution and toward the super-catalytic wall solution (indicative of non-physical full recombination to the lowest energy state). At the surface temperature in the intermediate range, it seems apparent the reaction rates are more efficient near the shoulder of the model than at the stagnation point where surface pressure (and hence concentration) is significantly higher.

Reaction efficiency may be more readily demonstrated by looking at the effective loss efficiency of the atoms in this system at each position on the cylinder. The loss efficiency is defined as the fraction of atom collisions with the surface that result in loss of the reactant from the gas phase. In the finite-rate surface model framework, in which reactants are lost and gained through

multiple processes simultaneously, the effective loss efficiency will be a net composite of the interacting processes, defined using Eq. (1.10.1).

The effective loss efficiency is a post-processed quantity, so it varies naturally with the reaction kinetics at different points on the surface in response to changes in surface pressure, surface temperature, or diffusion of species into the gas interior. The effective loss efficiencies for N and O atoms are shown in Fig. 7.1.2, which demonstrates that the loss efficiencies are significantly higher near the shoulders than at the stagnation point for the cases in question. If the effective loss efficiencies predicted for this case were entered as constants on a cell-by-cell basis into the commonly employed SRE catalysis -boundary condition, the same heat-transfer profile would be obtained, but the physical distribution of adsorbed surface coverage would be lost.

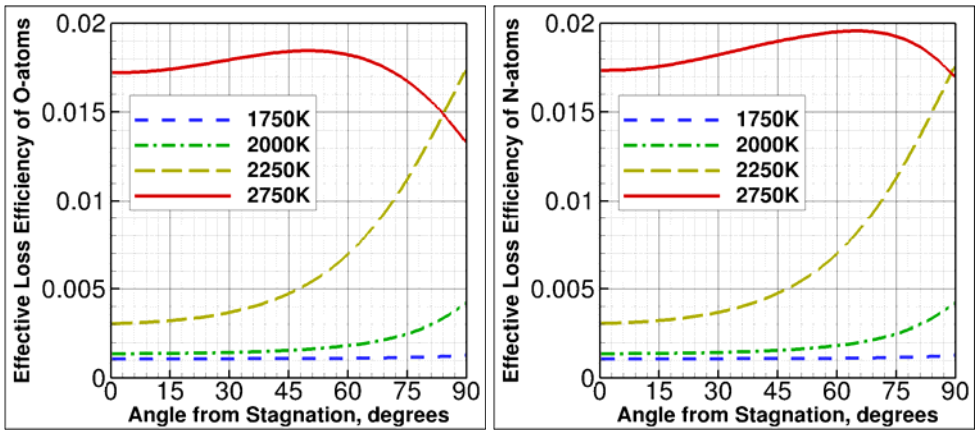

(a) O-atom **(b) N-atom**

Figure 7.1.2. Effective Atom Loss Efficiencies on a Silica Cylinder at Four Surface Temperatures.

The distribution of adsorbed species predicted at all four surface temperatures is shown in Fig. 7.1.3. The US3D results shown as discrete points have been coarsened to include every fifth surface cell purely for visual benefit. In all cases, the surface coverage is dominated by oxygen atoms, which, at the lower surface temperatures, occupy nearly every available surface site. As the temperature increases, so does desorption mobility; thus, fewer sites are observed to be occupied by atoms. The coverage at steady state decreases in general at higher temperatures, but the effective loss (catalytic recombination) efficiency of the atoms is observed to generally increase, so the effect of surface coverage on the gas-phase species is nontrivial.

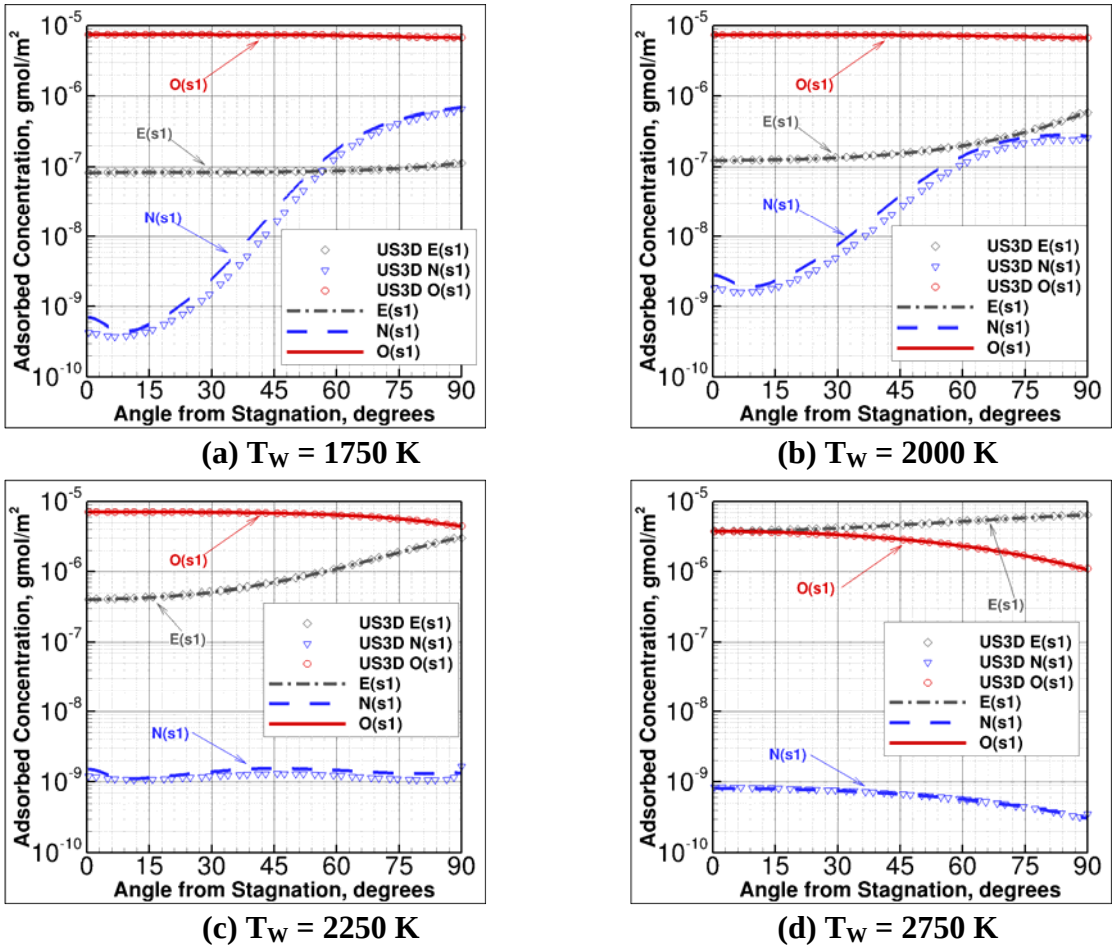

(a) T_W = 1750 K **(b) T_W = 2000 K**

(c) T_W = 2250 K **(d) T_W = 2750 K**

Figure 7.1.3. Comparison of Predicted Steady-State Surface Coverage for a Silica Cylinder at Four Different Surface Temperatures.

The surface-normal profiles of gaseous reactant species within the boundary layer along the stagnation streamline are shown in Fig. 7.1.4. The boundary layer profiles show that significant recombination does occur inside the gaseous boundary layer itself before the chemical reactants get close to the surface. For nitrogen atoms, nearly complete recombination occurs in the interior of the boundary layer, so few N atoms reach the surface. This fact helps, in part, to explain the previous observations that the steady-state surface coverage of N atoms is quite low (shown in Fig. 7.1.3), while the effective loss efficiency of nitrogen atoms is as high as the atomic oxygen loss efficiency (shown in Fig. 7.1.2(b)). This makes sense, as the reaction efficiency is a measure of the fraction of the impinging reactants for which a reaction occurs. For low concentrations of atoms, the loss efficiency can be quite high, since the absolute reaction rate required does not need to be large. Although it is a marginal effect that may be difficult to see in Fig. 7.1.4(a), the O-atom solution for the T_W = 1750 K near the surface actually predicts a slightly lower mass fraction than the T_W = 2000 K solution. This effect was verified and can be attributed to the fact that the gaseous temperature in the near-wall region for the T_W = 2000 K case is slightly higher (thus promoting less gas-phase recombination), while the increase in O-atom loss efficiency predicted by the production rates at the surface is not sufficiently higher to compensate, as observed in Fig. 7.1.2(a). The trend reverses starting with the T_W = 2250K

condition. This is just one example of the non linearity that is possible for gas/surface interaction models.

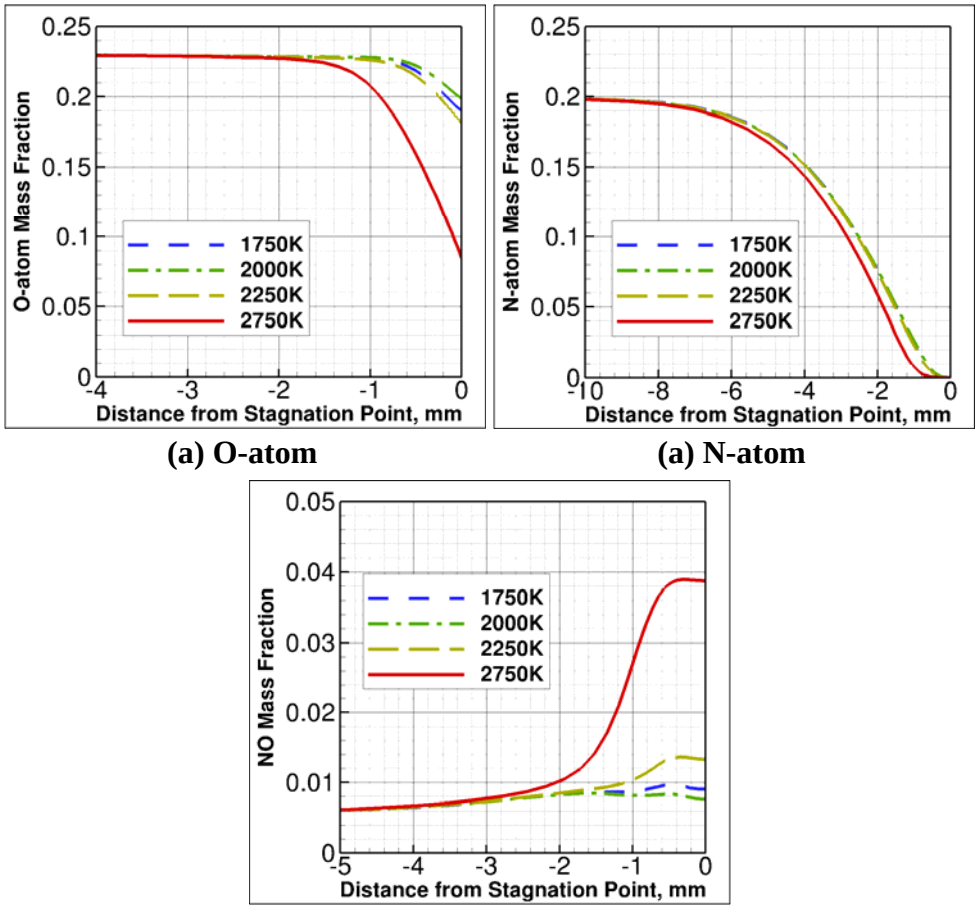

(a) O-atom **(a) N-atom**

(b) NO

Figure 7.1.4. Stagnation Line Boundary Layer Profiles for a Silica Cylinder at Four Different Surface Temperatures.

Finally, the convergence properties of these cases are addressed. Since the finite-rate surface model is implicitly coupled, the surface and the interior flow evolve together to maintain stability and good convergence properties. As the evolution of the surface affects the boundary condition to the flow field, we may expect residuals of the CFD solver to reach machine zero only when both the surface and the flow field are fully converged. However, one additional way to measure convergence with a boundary condition of this type is to monitor the molar production rates of the adsorbed surface species. When the calculation reaches steady state, these production rates should also approach machine zero as implied by Eq. (3.2.9).

The absolute value of the production rates for the two adsorbed atoms and the empty surface sites (which must total 7.5×10^{-6} gmol/m^2) at the stagnation point for the $T_W = 2750$ K case are shown against the CFD solver iteration number in Fig. 7.1.5. In addition, the normalized CFD solver residual, defined as the global L_2 norm of the continuity equation (the sum of all species equation residuals) and normalized by its initial value, is shown on the same scale. The absolute

values of the production rates are shown so that they can be plotted on a log scale together, but the production rates of the empty surface sites must obviously be the negative of the production rates of the two adsorbed atoms at any iteration. As expected, the surface and the flow field evolve together, reaching machine zero levels after nominally the same number of iterations in this case.

The absolute production rate of N atoms reaches a somewhat smaller magnitude because of the smaller final reactant concentration. As observed earlier, oxygen atom adsorption is the dominant process in the steady-state surface coverage, so the production rates of adsorbed oxygen atoms and empty surface sites are approximately equal and opposite (the same magnitude) during the evolution of the flow.

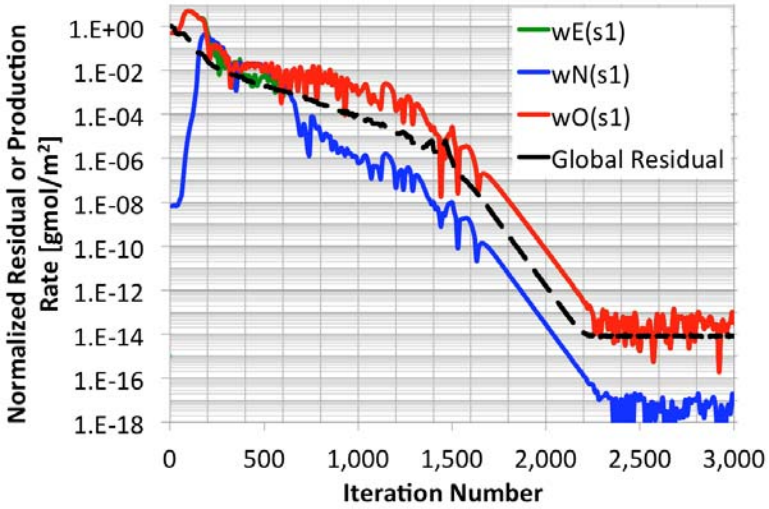

Figure 7.1.5. Molar Production Rates (Absolute Value) at Stagnation Point and L_2-Norm of Continuity Equation Residual for a Silica Cylinder at T_W = 2750 K.

7.2 Catalytic Recombination of Reacting Carbon Dioxide on a Platinum Surface

The flow of dissociated carbon dioxide over a 9-cm diameter platinum cylinder, previously considered by Valentini et al.,[32] has been used as a second test case of pure catalysis. The conditions for the test case come from measurements in a shock tunnel described by MacLean, et al,[33] in which heat transfer levels consistent with very high levels of recombination were measured in dissociated carbon dioxide environments.

Free stream conditions for this case are U = 2772 m/s, $\rho = 0.0154$ kg/m^3, T = 712 K, $y_{CO2} = 0.939$, $y_{CO} = 0.0389$, $y_{O2} = 0.0221$. The surface is considered isothermal at T_W = 500 K with 1.85 x 10^{-5} gmol/m^2 of empty active surface sites. The reaction rates of Thömel, et al.[5] were used to model catalysis on the surface of the platinum. These rates were obtained by the original authors in the form of curve-fits into an Arrhenius format from a kinetic Monte-Carlo simulation. The surface reaction input file is shown below:

File *THOEMEL_CO2PT_Model3.v1.surf*:

```
CO2-Pt Cat. V1: 4 gas species, 10 surf. reactions (Thoemel 2007-4399)
-------------------------------------------------------------------------
Number of surface and bulk phases (gas phase=1 by definition)
nsp, nbp
1    0

Blowing/pyrolyzing gas flows?(0=NO, 1=Yes) Initialization(0=empty sites, 1=QSS)
nblwflag     initsurf
0            0

Number of gas phase species participating in surface reactions
Name      ngps  #Phase
CO24s     4       1

For each surface phase: list  name, surface fraction,
number of active site sets, thermo availability (0=NO, 1=YES)
Name      sfrc         nspas      iThermo    #Phase
Platinum    1.0          1         0          2

For each surface phase with1 or more sets of active sites, list
the site density and number of species for each active site set
sdensas     nspass
1.85d-05    3

Order of gas species
Name      Molar mass  Ediss     #Species
CO2       0.04401100  1597000.01
CO        0.02801100  1071000.02
O2        0.03200000   498000.03
O         0.01600000        0.04

Order of surface species (number each consecutively)
Name      Molar mass  Edes      #Species
E(s1)     0.00000000       0.0  5
CO(s1)    0.02801100  170000.0 6
O(s1)     0.01600000  250000.0  7

Total number of surface reactions
nsrt
10

Reactant/product species for each forward surface reaction
3, 5, 0, 7, 0, 0               #1   O2 + 2(s1) <---> 2O(s1)
2, 5, 0, 6, 0, 0               #2   CO + (s1) <---> CO(s1)
4, 5, 0, 7, 0, 0               #3   O + (s1) <--->  O(s1)
6, 0, 0, 2, 5, 0               #4   CO(s1) <---> CO + (s1)
7, 0, 0, 4, 5, 0               #5   O(s1) <---> O + (s1)
4, 6, 0, 1, 5, 0               #6   O + CO(s1) <---> CO2 + (s1)
2, 7, 0, 1, 5, 0               #7   CO + O(s1) <---> CO2 + (s1)
```

```
4, 7, 0, 3, 5, 0              #8   O + O(s1) <---> O2 + (s1)
6, 7, 0, 1, 5, 0              #9   CO(s1) +O(s1) <---> CO2 + 2(s1)
7, 0, 0, 3, 5, 0              #10  2O(s1) <---> O2 + 2(s1)

Stoichiometric coefficients for each surface reaction
1, 2, 0, 2, 0, 0              #1   O2 + 2(s1) <---> 2O(s1)
1, 1, 0, 1, 0, 0              #2   CO + (s1) <---> CO(s1)
1, 1, 0, 1, 0, 0              #3   O + (s1) <--->  O(s1)
1, 0, 0, 1, 1, 0              #4   CO(s1) <---> CO + (s1)
1, 0, 0, 1, 1, 0              #5   O(s1) <---> O + (s1)
1, 1, 0, 1, 1, 0              #6   O + CO(s1) <---> CO2 + (s1)
1, 1, 0, 1, 1, 0              #7   CO + O(s1) <---> CO2 + (s1)
1, 1, 0, 1, 1, 0              #8   O + O(s1) <---> O2 + (s1)
1, 1, 0, 1, 2, 0              #9   CO(s1) +O(s1) <---> CO2 + 2(s1)
2, 0, 0, 1, 2, 0              #10  2O(s1) <---> O2 + 2(s1)

Reaction parameters for each type of reaction:
Type 0: Arrhenius:            0, Cf,         beta, Ea,   isrfon, isrbon
Type 1: Adsorption:                 1, S0(0 to 1), beta, Eads, isrfon, isrbon
Type 2: Eley-Rideal:          2, Ger(0 to 1),beta, Eer,  isrfon, isrbon
Type 3: Langmuir-Hinschelwood:      3, Clh(0 to 1),beta, Em,   isrfon, isrbon
Type 4: Sublimation                 4, a0Pv,       beta, Esub, isrfon, isrbon
Type 5: Arrhenius Adsorption: 5, Cf,         beta, Ea,   isrfon, isrbon

0, 5.65d+11, 0.0d+00, 3.3900d+03, 1, 0                #1
0, 1.36d+07, 0.0d+00, 3.8000d+03, 1, 0                #2
0, 1.79d+09, 0.0d+00, 3.7800d+03, 1, 0                #3
0, 7.57d+14, 0.0d+00, 1.7000d+05, 1, 0                #4
0, 5.12d+12, 0.0d+00, 2.5000d+05, 1, 0                #5
0, 2.13d+07, 0.0d+00, 5.6400d+03, 1, 0                #6
0, 1.15d+07, 0.0d+00, 3.7200d+03, 1, 0                #7
0, 1.52d+07, 0.0d+00, 3.7200d+03, 1, 0                #8
0, 2.89d+15, 0.0d+00, 8.4200d+04, 1, 0                #9
0, 1.16d+15, 0.0d+00, 1.4500d+05, 1, 0                #10

Desorption reaction or equilibrium constant parameters:
Type 1: Desorption:
      Form 0:     Arrhenius
      Form 1:     Constant attempt frequency
        Form 2:   Simple transition state theory
        Form 3:   Complex transition state theory
Type 2: Equilibrium:
      Form 0:     Arrhenius
        Form 1:   Immobile adsorption - simple transition state theory
        Form 2:   Immobile adsorption - complex transition state theory
        Form 3:   Mobile adsorption - simple transition state theory
        Form 4:   Mobile adsorption - complex transition state theory
Type, Form, Cf, eta, vdes, Edes
```

Here, the original reaction model of Thömel, et al.[5] has been used with the 10 forward reaction rates specified as Arrhenius functions without reverse reactions (the backward reactions have been turned off in the file by setting all *isrbon* = 0). However, we note that the reaction set

includes both adsorption and desorption processes for both O(s1) and CO(s1) species, so the surface coverage model is implicitly thermodynamically constrained (e.g., there is a path to equilibrium). These pairs of reactions can be combined in the finite-rate surface model framework to provide Gibbs energy data for the surface species so that both forward and reverse rates can be included for all reactions; this model is labeled as "modified" or "thermodynamically balanced" in several of the graphics below. The combination of rates reduces the system to 7 independent reactions listed and numbered in Table 7.2.1.

Table 7.2.1. Reactions and Numbering Nomenclature for the Modified (Thermodynamically Balanced) CO2-Platinum System.

	Reaction
1	$CO + E(s1) \leftrightarrow CO(s1)$
2	$O + E(s1) \leftrightarrow O(s1)$
3	$O + CO(s1) \leftrightarrow CO_2 + E(s1)$
4	$CO + O(s1) \leftrightarrow CO_2 + E(s1)$
5	$O + O(s1) \leftrightarrow O_2 + E(s1)$
6	$CO(s1) + O(s1) \leftrightarrow CO_2 + 2E(s1)$
7	$2O(s1) \leftrightarrow O_2 + 2E(s1)$

The surface-reaction input file for the modified system is given below:

File *THOEMEL_CO2PT_Model3.v2.surf*:

```
CO2-Pt Cat. V2: 4 gas species, 7 surf. reactions (Thoemel 2007-4399)
-------------------------------------------------------------------------
Number of surface and bulk phases (gas phase=1 by definition)
nsp, nbp
1    0

Blowing/pyrolyzing gas flows?(0=NO, 1=Yes) Initialization(0=empty sites, 1=QSS)
nblwflag     initsurf
0            0

Number of gas phase species participating in surface reactions
Name      ngps  #Phase
CO24s     4       1

For each surface phase: list  name, surface fraction,
number of active site sets, thermo availability (0=NO, 1=Yes)
Name      sfrc         nspas      iThermo    #Phase
Platinum    1.0          1         0          2

For each surface phase with 1 or more sets of active sites, list
the site density and number of species for each active site set
sdenas       nspass
1.85d-05      3
```

```
Order of gas species
Name      Molar mass  Ediss     #Species
CO2       0.04401100  1597000.01
CO        0.02801100  1071000.02
O2        0.03200000   498000.03
O         0.01600000        0.04

Order of surface species (number each consecutively)
Name      Molar mass  Edes      #Species
E(s1)     0.00000000       0.0  5
CO(s1)    0.02801100  170000.0 6
O(s1)     0.01600000  250000.0  7

Total number of surface reactions
nsrt
7

Reactant/product species for each forward surface reaction
2, 5, 0, 6, 0, 0               #1   CO + (s1) <---> CO(s1)
4, 5, 0, 7, 0, 0               #2   O + (s1) <--->  O(s1)
4, 6, 0, 1, 5, 0               #3   O + CO(s1) <---> CO2 + (s1)
2, 7, 0, 1, 5, 0               #4   CO + O(s1) <---> CO2 + (s1)
4, 7, 0, 3, 5, 0               #5   O + O(s1) <---> O2 + (s1)
6, 7, 0, 1, 5, 0               #6   CO(s1) +O(s1) <---> CO2 + 2(s1)
7, 0, 0, 3, 5, 0               #7   2O(s1) <---> O2 + 2(s1)

Stoichiometric coefficients for each surface reaction
1, 1, 0, 1, 0, 0               #1   CO + (s1) <---> CO(s1)
1, 1, 0, 1, 0, 0               #2   O + (s1) <--->  O(s1)
1, 1, 0, 1, 1, 0               #3   O + CO(s1) <---> CO2 + (s1)
1, 1, 0, 1, 1, 0               #4   CO + O(s1) <---> CO2 + (s1)
1, 1, 0, 1, 1, 0               #5   O + O(s1) <---> O2 + (s1)
1, 1, 0, 1, 2, 0               #6   CO(s1) +O(s1) <---> CO2 + 2(s1)
2, 0, 0, 1, 2, 0               #7   2O(s1) <---> O2 + 2(s1)

Reaction parameters for each type of reaction:
Type 0: Arrhenius:             0, Cf,         beta, Ea,   isrfon, isrbon
Type 1: Adsorption:                  1, S0(0 to 1), beta, Eads, isrfon, isrbon
Type 2: Eley-Rideal:           2, Ger(0 to 1),beta, Eer,  isrfon, isrbon
Type 3: Langmuir-Hinschelwood:       3, Clh(0 to 1),beta, Em,   isrfon, isrbon
Type 4: Sublimation                  4, a0Pv,       beta, Esub, isrfon, isrbon
Type 5: Arrhenius Adsorption:  5, Cf,         beta, Ea,   isrfon, isrbon

5, 1.36d+07, 0.0d+00, 3.8000d+03, 1, 1                 #1
5, 1.79d+09, 0.0d+00, 3.7800d+03, 1, 1                 #2
0, 2.13d+07, 0.0d+00, 5.6400d+03, 1, 1                 #3
0, 1.15d+07, 0.0d+00, 3.7200d+03, 1, 1                 #4
0, 1.52d+07, 0.0d+00, 3.7200d+03, 1, 1                 #5
0, 2.89d+15, 0.0d+00, 8.4200d+04, 1, 1                 #6
0, 1.16d+15, 0.0d+00, 1.4500d+05, 1, 1                 #7
```

```
Desorption reaction or equilibrium constant parameters:
Type 1: Desorption:
      Form 0:     Arrhenius
      Form 1:     Constant attempt frequency
        Form 2:   Simple transition state theory
        Form 3:   Complex transition state theory
Type 2: Equilibrium:
      Form 0:     Arrhenius
        Form 1:   Immobile adsorption - simple transition state theory
        Form 2:   Immobile adsorption - complex transition state theory
        Form 3:   Mobile adsorption - simple transition state theory
        Form 4:   Mobile adsorption - complex transition state theory
Type, Form, Cf, eta, vdes, Edes
1, 0, 7.57d+14, 0.0d+00, 1.0d+00, 1.70d+05
1, 0, 5.12d+12, 0.0d+00, 1.0d+00, 2.50d+05
```

Further, Valentini, et al.[32] made adjustments to two of the original published Thömel rates to prevent the reaction probabilities from exceeding 1.0 for certain conditions. The reaction input file for this modification to the original rates is given below:

File *Valentini_CO2PT_Model3.v1.surf*:

```
CO2-Pt Cat. V1: 4 gas species, 10 surf. reactions (Valentini 2009-3935)
---------------------------------------------------------------------------
Number of surface and bulk phases (gas phase=1 by definition)
nsp, nbp
1    0

Blowing/pyrolyzing gas flows?(0=NO, 1=Yes) Initialization(0=empty sites, 1=QSS)
nblwflag     initsurf
0            0

Number of gas phase species participating in surface reactions
Name      ngps  #Phase
CO24s     4       1

For each surface phase: list  name, surface fraction,
number of active site sets, thermo availability (0=NO, 1=YES)
Name      sfrc         nspas      iThermo    #Phase
Platinum    1.0          1         0          2

For each surface phase with1 or more sets of active sites, list
the site density and number of species for each active site set
sdensas     nspass
1.85d-05    3

Order of gas species
Name      Molar mass  Ediss     #Species
CO2       0.04401100  1597000.01
CO        0.02801100  1071000.02
```

```
O2        0.03200000   498000.03
O         0.01600000        0.04

Order of surface species (number each consecutively)
Name      Molar mass  Edes      #Species
E(s1)     0.00000000       0.0  5
CO(s1)    0.02801100  170000.0 6
O(s1)     0.01600000  250000.0  7

Total number of surface reactions
nsrt
10

Reactant/product species for each forward surface reaction
3, 5, 0, 7, 0, 0               #1   O2 + 2(s1) <---> 2O(s1)
2, 5, 0, 6, 0, 0               #2   CO + (s1) <---> CO(s1)
4, 5, 0, 7, 0, 0               #3   O + (s1) <--->  O(s1)
6, 0, 0, 2, 5, 0               #4   CO(s1) <---> CO + (s1)
7, 0, 0, 4, 5, 0               #5   O(s1) <---> O + (s1)
4, 6, 0, 1, 5, 0               #6   O + CO(s1) <---> CO2 + (s1)
2, 7, 0, 1, 5, 0               #7   CO + O(s1) <---> CO2 + (s1)
4, 7, 0, 3, 5, 0               #8   O + O(s1) <---> O2 + (s1)
6, 7, 0, 1, 5, 0               #9   CO(s1) +O(s1) <---> CO2 + 2(s1)
7, 0, 0, 3, 5, 0               #10  2O(s1) <---> O2 + 2(s1)

Stoichiometric coefficients for each surface reaction
1, 2, 0, 2, 0, 0               #1   O2 + 2(s1) <---> 2O(s1)
1, 1, 0, 1, 0, 0               #2   CO + (s1) <---> CO(s1)
1, 1, 0, 1, 0, 0               #3   O + (s1) <--->  O(s1)
1, 0, 0, 1, 1, 0               #4   CO(s1) <---> CO + (s1)
1, 0, 0, 1, 1, 0               #5   O(s1) <---> O + (s1)
1, 1, 0, 1, 1, 0               #6   O + CO(s1) <---> CO2 + (s1)
1, 1, 0, 1, 1, 0               #7   CO + O(s1) <---> CO2 + (s1)
1, 1, 0, 1, 1, 0               #8   O + O(s1) <---> O2 + (s1)
1, 1, 0, 1, 2, 0               #9   CO(s1) +O(s1) <---> CO2 + 2(s1)
2, 0, 0, 1, 2, 0               #10  2O(s1) <---> O2 + 2(s1)

Reaction parameters for each type of reaction:
Type 0: Arrhenius:             0, Cf,         beta, Ea,   isrfon, isrbon
Type 1: Adsorption:                  1, S0(0 to 1), beta, Eads, isrfon, isrbon
Type 2: Eley-Rideal:           2, Ger(0 to 1),beta, Eer,  isrfon, isrbon
Type 3: Langmuir-Hinschelwood:       3, Clh(0 to 1),beta, Em,   isrfon, isrbon
Type 4: Sublimation                  4, a0Pv,       beta, Esub, isrfon, isrbon
Type 5: Arrhenius Adsorption:  5, Cf,         beta, Ea,   isrfon, isrbon

0, 5.65d+11, 0.0d+00, 3.3900d+03, 1, 0                #1
0, 1.36d+07, 0.0d+00, 3.8000d+03, 1, 0                #2
0, 1.79d+07, 0.0d+00, 3.7800d+03, 1, 0                #3
0, 7.57d+14, 0.0d+00, 1.7000d+05, 1, 0                #4
0, 5.12d+12, 0.0d+00, 2.5000d+05, 1, 0                #5
0, 2.13d+07, 0.0d+00, 5.6400d+03, 1, 0                #6
0, 1.15d+07, 0.0d+00, 3.7200d+03, 1, 0                #7
```

```
0, 6.00d+04, 0.0d+00, 3.7200d+03, 1, 0                    #8
0, 2.89d+15, 0.0d+00, 8.4200d+04, 1, 0                    #9
0, 1.16d+15, 0.0d+00, 1.4500d+05, 1, 0                    #10

Desorption reaction or equilibrium constant parameters:
Type 1: Desorption:
      Form 0:     Arrhenius
      Form 1:     Constant attempt frequency
        Form 2:   Simple transition state theory
        Form 3:   Complex transition state theory
Type 2: Equilibrium:
      Form 0:     Arrhenius
        Form 1:   Immobile adsorption - simple transition state theory
        Form 2:   Immobile adsorption - complex transition state theory
        Form 3:   Mobile adsorption - simple transition state theory
        Form 4:   Mobile adsorption - complex transition state theory
Type, Form, Cf, eta, vdes, Edes
```

Valentini, et al.[32] studied this same test case using a fixed surface temperature of 500 K. In addition, a higher surface temperature fixed at 1300 K has also been considered here. The heat transfer profile on the cylinder is shown in Fig. 7.2.1 for these two cases. Because a different diffusion model convention has been used here than was used in Valentini's FRC/US3D model at that time, it is impossible to make a precise comparison with the results presented by Valentini et al. from their US3D simulation, but the general agreement with their results is good for the 500 K surface. For the lower surface temperature, the three model variations agree exactly and predict a level of heat transfer that is just greater than the non-catalytic limit.

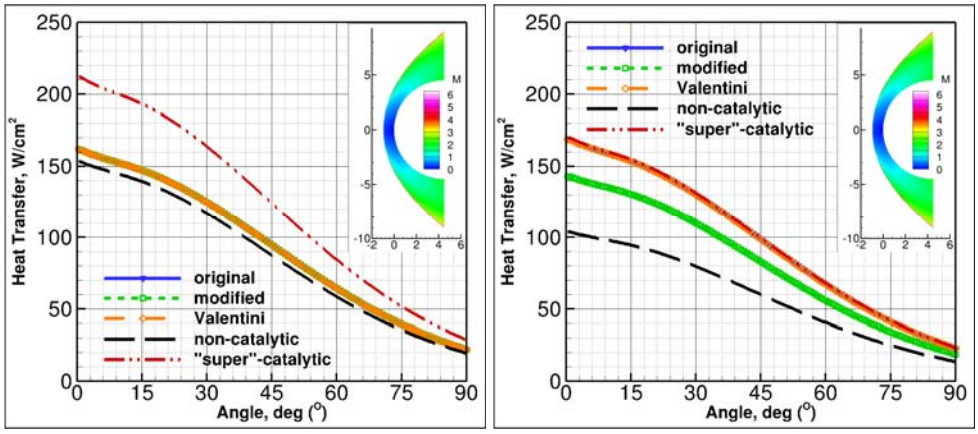

(a) T_W = 500 K **(b) T_W = 1300 K**

Figure 7.2.1. Predicted Heat Transfer Profile on a Platinum Cylinder for Various Surface Boundary Conditions at Two Fixed Wall Temperatures.

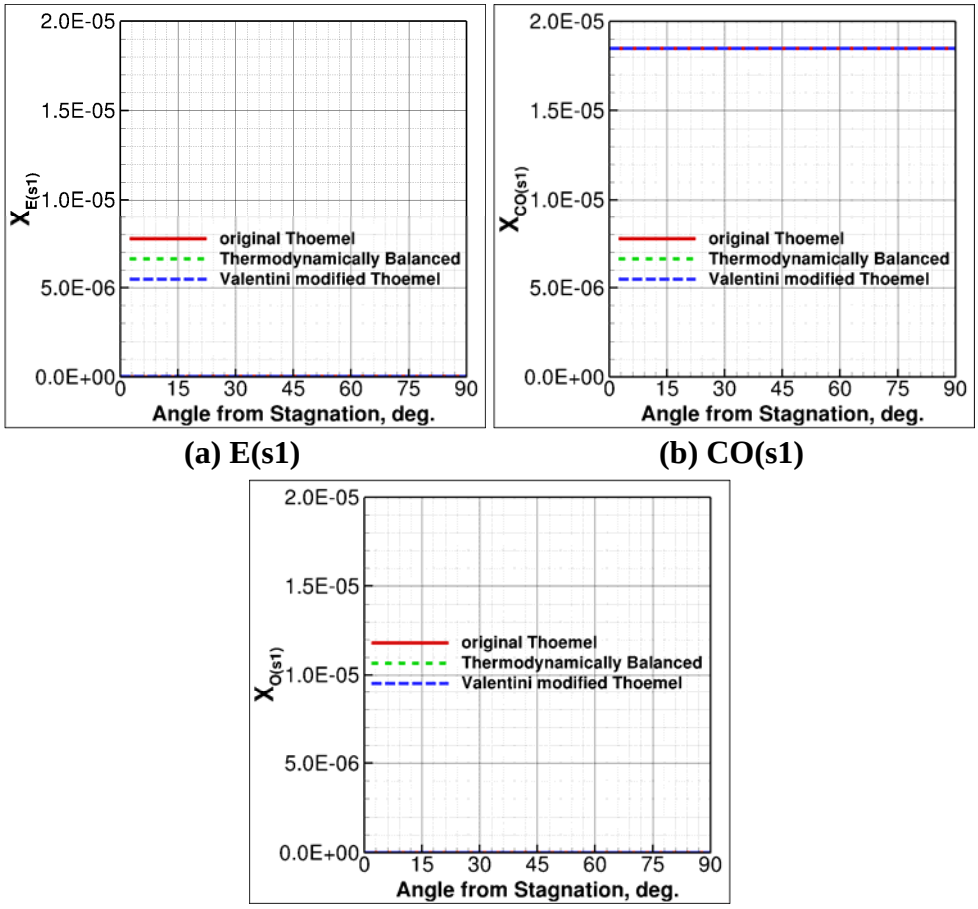

(a) E(s1) **(b) CO(s1)**

(c) O(s1)

Figure 7.2.2. Steady-State Surface Coverage Predicted for All Reaction Rate Models at a Surface Temperature of 500 K.

At the higher temperatures, a significant discrepancy is observed, with the modified model predicting a level of heat transfer significantly lower than both Thömel's original model and the Valentini model.

At 500 K, the same steady-state surface coverage is obtained for all three reaction systems as shown in Fig. 7.2.2. At steady state, the surface is filled almost exclusively by CO(s1), which occupies 99.9% of the available surface sites at the surface temperature of 500 K.

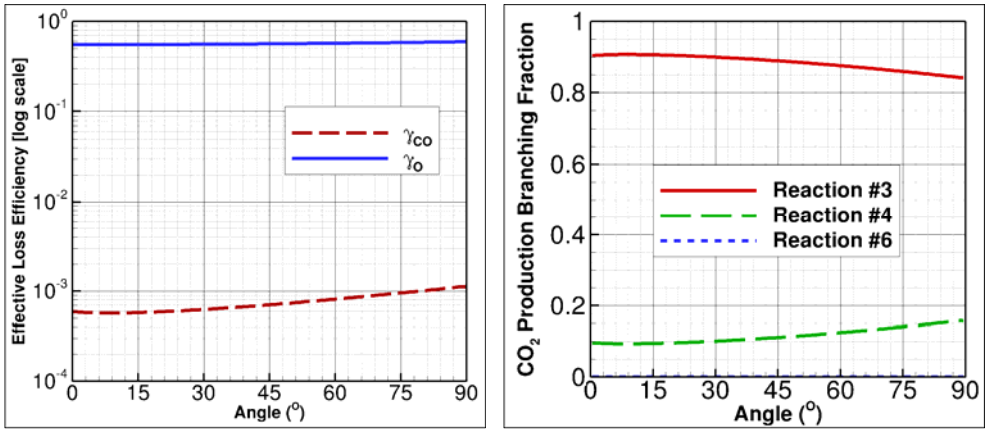

(a) γ_O and γ_{CO} **(b) branching fractions**

Figure 7.2.3. Effective Reactant Efficiencies and CO_2 Branching Fractions for Platinum Cylinder Case with 500 K Surface Temperature.

The effective loss efficiencies of both atomic oxygen and carbon monoxide are shown in Fig. 7.2.3(a). The small loss efficiency of gaseous carbon monoxide suggests that Modified Reaction #4 (Table 7.2.1) may not be promoting much catalysis. This implication is verified by plotting the branching fractions of CO_2 –the fraction of the total production rate from each reaction–in Fig. 7.2.3(b), which shows that CO_2 is being dominantly formed by Modified Reaction #3 through the reaction of an adsorbed CO(s1) molecule and a gas-phase O atom under these particular conditions.

At the higher surface temperature of 1300 K, it is clear from the heat transfer that the behavior in the three model variations is quite different. The effective loss efficiency of the atomic oxygen reactant plotted in Fig. 7.2.4 shows that the effective loss efficiency is far greater than 1.0 for both the original and the modified (thermodynamically balanced) model as Valentini, et al.[32] noted in their previous work. The changes to the reaction rates made by Valentini do indeed keep the loss efficiency at least within a scale of 0.0 to 1.0.

This is an inherent danger in using generic Arrhenius expressions rather than gas-kinetic formulations to describe gas-surface reaction-rate coefficients, as Arrhenius expressions are not explicitly constrained by the impingement rate of the gas-phase reactant.

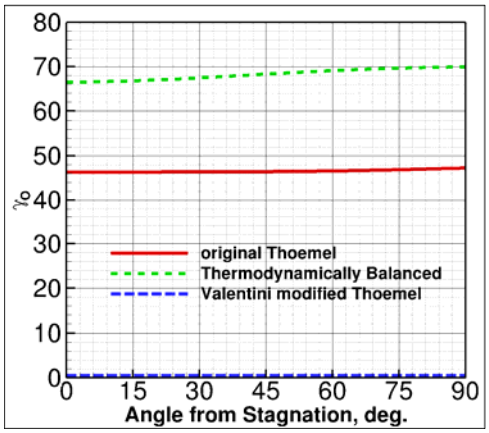

Figure 7.2.4. Effective Reactant Efficiency for Atomic Oxygen at a Surface Temperature of 1300 K.

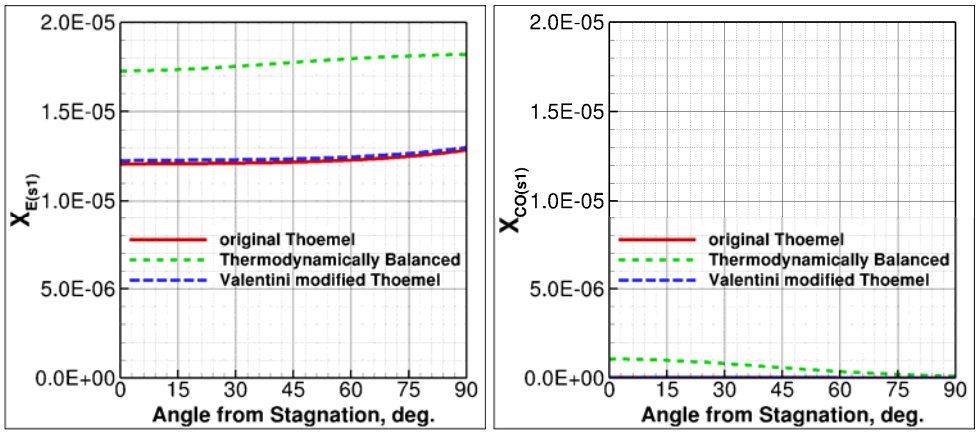

(a) E(s1) **(b) CO(s1)**

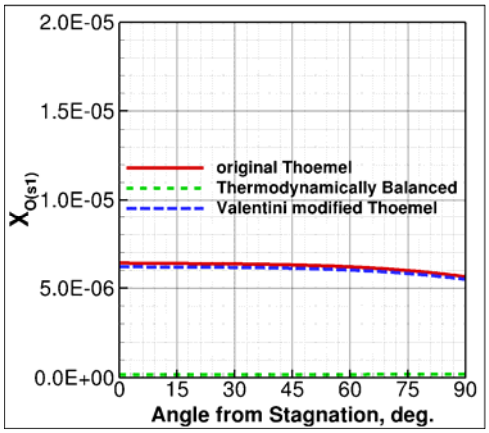

(c) O(s1)

Figure 7.2.5. Steady-State Surface Coverage Predicted for All Reaction Rate Models at a Surface Temperature of 1300 K.

One reason that a discrepancy in oxygen atom consumption is observed at the 1300 K surface temperature and not the 500 K surface temperature is that, at 500 K, the surface coverage is completely dominated by adsorbed carbon monoxide (as noted previously in Fig. 7.2.2(b)). At the higher surface temperature of 1300 K, the surface coverage shown in Fig. 7.2.5 demonstrates that adsorbed atomic oxygen is now the most significant surface reactant.

An additional diagnostic for the system is to employ the stand-alone code as a tool to assess the behaviors of the three sets of surface reaction rates. To do this, an approximate condition at the stagnation point was extracted and used in the stand-alone code as a fixed-gas composition model at the two surface temperatures. A stand-alone code input file for this test case is given here, where the two surface temperatures of 500 K and 1300 K were sequentially tested for each of the three reaction models.

File *input.inp*:

```
[surface file name]
'THOEMEL_CO2PT_Model3.v1.surf'

output conv freq,  file save freq,   [output file name]
           100,              5,      'fixed-1300-v1.dat'

Tw (K),     Ptotal (Pa),    gas phase model,      scan mode
 1300.,          113536.,                  1,              0

 dt(s),     num steps,   time order,    diagnostic,      equilibrium
2.0d-10,       7500,         2,              2,               -1

[num gas phase species]
4

[name and mole fraction of each species]
'CO2',   0.813583
'CO',    0.124349
'O2',    0.061971
 'O',    0.000097
=====================================================================

Pressure & Temperature Scan (-1.0 to end)
Ptotal(Pa)  Tw (K)
    -1.,     -1.

Mole Fraction Scan (-1.0 to end)
  yO2    yO
  -1.,   -1.

=====================================================================
```

The stand-alone code is a valuable tool for understanding the behavior of surface reaction systems in cases like this, where the CFD results are complex and difficult to interpret. The forward and backward reaction rates for steady-state surface coverage are listed for all 7 of the

independent reactions listed from Table 7.2.1 for each of the three rate models in Tables 7.2.2 and 7.2.3 for the two surface temperatures. Several differences in the rates between the models are evident and have been highlighted in the tables.

First, shown in blue in the tables, the four dissociative and partial dissociation adsorption mechanisms of Reactions #3 through #6 are not significant for the 500 K surface temperature as was previously presumed, since the backward reaction rate is at minimum 10^{15} times less than the corresponding forward rates. At the higher surface temperature, the difference has decreased to a minimum of 10^{6} times less. This is still insignificant enough that the backward rates can be neglected, but it does emphasize the need to be careful with systems such as this for conditions in which backward rates are not negligible or impact the overall thermodynamic behavior of the system.

Table 7.2.2. Individual reaction rates at steady-state coverage for 500 k surface temperature case from stand-alone code.

Reaction	Original Thömel Rates		Modified Rates		Valentini Rates	
	kf	kb	kf	kb	kf	kb
CO+E(s1)<-->CO(s1)	5.452E+06	1.318E-03	5.452E+06	1.318E-03	5.452E+06	1.318E-03
O+ E(s1)<-->O(s1)	7.211E+08	3.914E-14	7.211E+08	3.914E-14	7.211E+06	3.914E-14
O+CO(s1)<-->CO_2+E(s1)	5.485E+06	-	5.485E+06	6.044E-31	5.485E+06	-
CO+O(s1)<-->CO_2+E(s1)	4.700E+06	-	4.700E+06	2.306E-18	4.700E+06	-
O+O(s1)<-->O_2+E(s1)	6.212E+06	-	6.212E+06	3.702E-16	2.452E+04	-
CO(s1)+O(s1)<-->CO_2+2E(s1)	4.622E+06	-	4.622E+06	9.382E-09	4.622E+06	-
2O(s1)<-->O_2+2E(s1)	8.257E-01	2.500E+11	8.257E-01	9.065E-01	8.257E-01	2.500E+11

Table 7.2.3. Individual Reaction Rates at Steady-State Coverage for 1300 K Surface Temperature Case from Stand-Alone Code.

Reaction	Original Thömel Rates		Modified Rates		Valentini Rates	
	kf	kb	kf	kb	kf	kb
CO+E(s1)<-->CO(s1)	9.569E+06	1.118E+08	9.569E+06	1.118E+08	9.569E+06	1.118E+08
O+ E(s1)<-->O(s1)	1.262E+09	4.617E+02	1.262E+09	4.617E+02	1.262E+07	4.617E+02
O+CO(s1)<-->CO_2+E(s1)	1.264E+07	-	1.264E+07	2.704E-07	1.264E+07	-
CO+O(s1)<-->CO_2+E(s1)	8.151E+06	-	8.151E+06	5.569E+00	8.151E+06	-
O+O(s1)<-->O_2+E(s1)	1.077E+07	-	1.077E+07	8.528E+00	4.253E+04	-
CO(s1)+O(s1)<-->CO_2+2E(s1)	1.196E+12	-	1.196E+12	6.992E+04	1.196E+12	-
2O(s1)<-->O_2+2E(s1)	1.732E+09	4.129E+11	1.732E+09	3.745E+09	1.732E+09	4.129E+11

Second, shown in green on the tables, the reduced rates used by Valentini, et al.[32] for Reactions #2 and #5 are evident. The significantly higher rates of the original and modified models lead to the non-physical consumption rates of atomic oxygen as documented previously in Fig. 7.2.5.

Third, shown in red, we note that the explicit reaction rate given as the dissociative adsorption of molecular oxygen in the original system is not consistent with the thermodynamic constraints on the system imposed by the other reactions that were specified. For the 500 K surface temperature case, this rate is not significant since this process is effectively inactive at steady state. However, at the higher surface temperature of 1300 K, this reaction in the modified system causes significant decrease in the likelihood of dissociative oxygen adsorption and, thus, promotes a decreased likelihood of formation of CO_2 over the baseline and Valentini rates.

Finally, use of the stand-alone code to observe the unsteady time-history of the filling process for the reaction systems shown in Fig. 7.2.6, demonstrates that the filling process for even the 500 K surface temperature case varies between models. However, since the end result is the dominance of adsorbed carbon monoxide, the empty site and adsorbed oxygen concentrations asymptote to insignificant levels for all three models. For the 1300 K surface temperature case, it is clear that the three reaction systems each predict different filling and steady-state coverage, with the modified system being significantly different than the other two. The significantly lower steady-state adsorbed oxygen concentration is a result of the rate differences discussed already and leads to the reduction in exothermic energy release at the surface that was observed in the heat transfer profile.

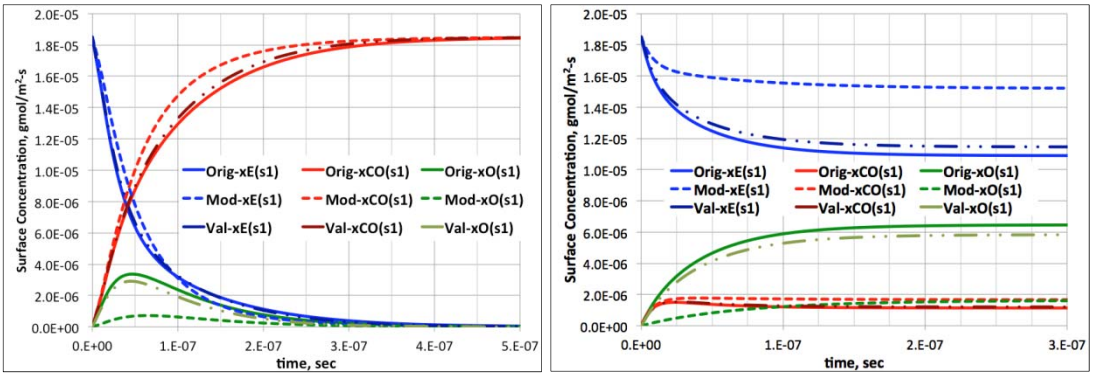

(a) T_W = 500 K **(b) T_W = 1300 K**

Figure 7.2.6. Time Accurate Surface Fill Predicted by the Stand-Alone Code for Two Surface Temperatures.

In summary, this example case has demonstrated an analysis of one of the few available sets of physics-based surface catalysis rates in the literature. The disadvantage of employing Arrhenius rates instead of the more physical kinetic formulation has been shown, as has the importance of thermodynamic constraints on the system. Furthermore, the use of the enhanced capabilities of DPLR in tandem with the stand-alone code has been demonstrated to provide physical insight and intuition into a complex set of surface reactions. Additional work needs to be done to determine the best set of rate coefficient data for the catalysis of dissociated carbon dioxide on a platinum surface.

7.3 Ablation of a FiberForm Wedge in Reacting Air

1) Specified-Reaction-Efficiency Model

The oxidation of carbon is considered by comparing to the numerical solution and the experimental data published by Driver, et al.[34] for a FiberForm sample ablated on a copper wedge model in an arc jet facility. Driver, et al.[34] employed a hard-wired version of a carbon oxidation model with a constant loss efficiency[35] to successfully model the interaction of atomic oxygen on the FiberForm substrate downstream of a cooled copper wall; they demonstrated that uncoupled material response without accounting for the interaction of the surface reactions and the gaseous boundary layer will under predict recession rates by 50% to 100%. Effects such as shape change, catalytic efficiency, and molecular versus atomic oxidation mechanisms were considered by the authors in order to best model the experimental data.

Here, the purpose of this example problem is simply to demonstrate that the finite-rate model can reproduce the same behavior as the hard-wired model and to show how the finite-rate model can be used to emulate the SRE model when no detailed rate data are available. Therefore, we have modeled the oxidation of carbon by atomic oxygen with a constant reaction probability of γ=0.9 and the simultaneous catalysis of nitrogen atoms with a constant recombination probability of γ=0.05. Driver, et al.[34] tested a range of catalytic recombination efficiencies with values as high as γ=0.5; this example has been arbitrarily selected from within their range of study.

The oxidation of bulk carbon by atomic oxygen at the wall is modeled as an irreversible ER reaction with zero activation energy and a constant reaction probability of γ=0.9. Additionally, a significantly smaller oxidation by molecular oxygen has been included for consistency with the previous results assuming a constant reaction probability of γ=0.01. As we require in the finite-rate model framework, the interaction of bulk and gaseous species must occur through a surface phase, so a single, empty surface site appears on each side of the reaction as given in Eq. (7.3.1).

$$\begin{aligned} O + (s1) + (C)_{b1} &\rightarrow CO + (s1) \qquad \gamma = 0.9 \\ O_2 + 2(s1) + 2(C)_{b1} &\rightarrow 2CO + 2(s1) \qquad \gamma = 0.01 \end{aligned} \tag{7.3.1}$$

The catalysis of nitrogen with constant atomic loss efficiency can be accomplished in the finite-rate model framework via the inclusion of a pair of reactions–an irreversible adsorption reaction with a constant sticking coefficient and zero adsorption energy followed by an irreversible Eley-Rideal reaction with zero activation energy and constant reaction efficiency. For this system, the net reactant loss efficiency for steady-state coverage can be shown to follow the relationship in Eq. (7.3.2) as a function of the constant sticking coefficient and constant Eley-Rideal reaction probability.

$$\gamma = \frac{2 S_0 \gamma_{ER}}{S_0 + \gamma_{ER}} \tag{7.3.2}$$

To achieve a net reactant loss efficiency, γ_N=0.05, both the reaction coefficients are selected as S_0=0.05 and γ_{ER}=0.05. This reaction system is given by Eq. (7.3.3).

$$\begin{aligned} N + (s2) &\rightarrow (N)_{s2} \qquad S_0 = 0.05 \\ N + (N)_{s2} &\rightarrow N_2 + (s2) \qquad \gamma_{ER} = 0.05 \end{aligned} \tag{7.3.3}$$

It is also essential to note that the surface is modeled with two independent active site sets, in which one active site set is dedicated to the oxidation reaction, Eq. (7.3.1), and the second is dedicated to the nitrogen catalysis reactions, Eq. (7.3.3). Two active site sets are necessary, because the desired approximation is that the reaction efficiencies of the two processes are independent. If only one active site set were used, the adsorption of nitrogen atoms onto the surface partially fills up the available empty surface sites and reduces the observed reaction probability of the oxidation process. In some situations, such an interaction may be desirable and physically meaningful, but here we neglect it to match the behavior of the previous simulations.

For the finite-rate model, the effective atomic loss efficiency can be post-processed from the converged solution using the relationship given in Eq. (1.10.1) to verify that it is the same as for the SRE formulation. The surface reaction input file for this model is given below:

File *ConstantGamma_Fiberform.surf*:

```
Fiberform Oxidation v1: 5 gas species, 4 surf. reac. (Driver, et al. 2010-1177)
-------------------------------------------------------------------------------
Number of surface and bulk phases (gas phase=1 by definition)
nsp, nbp
2    1

Blowing/pyrolyzing gas flows?(0=NO, 1=Yes) Initialization(0=empty sites, 1=QSS)
nblwflag     initsurf
0                 0

Number of gas phase species in surface reaction and blowing model
Name      ngps  #Phase
Air6s     5      1

For each surface phase: list  name, surface fraction,
number of active site sets, thermo availability (0=No, 1=Yes)
Name      sfrc       nspas     iThermo    #Phase
Carbon1   1.0        1         0          2
Carbon2   1.0        1         0          2

For each surface phase with 1 or more sets of active sites, list
the site density and number of species for each active site set
sdenas (mol/m2)      nspass
1.0d-5               2
1.0d-5               1
```

```
For each bulk phase: list  name, mass density, porosity,
phase volume fraction and number of bulk species
Name      density      porosity     vol. frac.    nbps
Carbon     175.0       0.0          1.0           1

Order of gas species
Name      Molar mass  Ediss     #Species  Dissociation Reaction
O2        0.03200000  493440.0   1          O2=>O+O
N2        0.02801600  945000.0   2              N2=>N+N
O         0.01600000  0.0        3
N         0.01400800  0.0        4
CO        0.02801100  1071726.0  5          CO=>C+O

Order of surface species (number each consecutively)
Name      Molar mass  Ed              #Species
E(s1)     0.00000000  0.0                 6
N(s1)     0.01400800  350000.0       7
E(s2)     0.00000000  0.0                 8

Order of bulk species (number each consecutively)
Name      Molar mass  Mole fraction     #Species
C(b1)      0.01201100  1.0                9

Total number of surface reactions
nsrt
4

Reactant/product species for each forward surface reaction
3, 8, 9, 5, 8, 0         #1   O + (s1) + C(b1) <---> CO + (s1)
1, 8, 9, 5, 8, 0         #2   O2 + 2(s1) +2C(b1) <---> 2CO + 2(s1)
4, 6, 0, 7, 0, 0                #3   N + (s1) <---> N(s1)
4, 7, 0, 2, 6, 0         #4   N + N(s1) <---> N2 + (s1)

Stoichiometric coefficients for each surface reaction
1, 1, 1, 1, 1, 0         #1   O + (s1) + C(b1) <---> CO + (s1)
1, 2, 2, 2, 2, 0         #2   O2 + 2(s1) +2C(b1) <---> 2CO + 2(s1)
1, 1, 0, 1, 0, 0         #3   N + (s1) <---> N(s1)
1, 1, 0, 1, 1, 0         #4   N + N(s1) <---> N2 + (s1)

Reaction parameters for each type of reaction:
Type 0: Arrhenius:       0, Cf,         beta, Ea,   isrfon, isrbon
Type 1: Adsorption:            1, S0(0 to 1), beta, Eads, isrfon, isrbon
Type 2: Eley-Rideal:           2, Ger(0 to 1),beta, Eer,  isrfon, isrbon
Type 3: Langmuir-Hinschelwood: 3, Clh(0 to 1),beta, Em,   isrfon, isrbon
Type 4: Sublimation   a0Pv(T)  4, a0Pv0,      beta, Esub, isrfon, isrbon
Type 5: Arrhenius Adsorption:  5, Cf,         beta, Ea,   isrfon, isrbon
Type, A, beta, Ea, isrfon, isrbo
2, 0.90d+00, 0.0d+00, 0.0000d+00, 1, 0      #1 O + (s1) + C(b1) <---> CO + (s1)
2, 0.01d+00, 0.0d+00, 0.0000d+00, 1, 0      #2 O2 + 2(s1) +2C(b1) <---> 2CO +
2(s1)
1, 0.05d+00, 0.0d+00, 0.0000d+00, 1, 0      #3 N + (s1) <---> N(s1)
```

```
2, 0.05d+00, 0.0d+00, 0.0000d+00, 1, 0      #4 N + N(s1) <---> N2 + (s1)

Desorption reaction or equilibrium constant parameters:
Type 1: Desorption:
      Form 0:     Arrhenius
      Form 1:     Constant attempt frequency
        Form 2:   Simple transition state theory
        Form 3:   Complex transition state theory
Type 2: Equilibrium:
      Form 0:     Arrhenius
        Form 1:   Immobile adsorption - simple transition state theory
        Form 2:   Immobile adsorption - complex transition state theory
        Form 3:   Mobile adsorption - simple transition state theory
        Form 4:   Mobile adsorption - complex transition state theory
Type, Form, Cf, eta, vdes, Edes
1, 1, 1.0, 0.0, 1.e12, 350000.0
```

The density of available surface sites for both active site sets was taken as 1 x 10^{-5} gmol/m^2. This selection is arbitrary for this particular case since we note that, for this simple set of reactions replicating the constant loss efficiency, both the steady-state and time-accurate response of the gas phase is independent of the site density. The only effect of the surface site density is to control the non-dimensional fill rate of adsorbed nitrogen atoms. This may potentially be a means to control numerical stability issues in certain situations, but no issues were observed in this case.

It should also be noted that, in the above reaction input file, Reaction #3 is a reaction of the "Adsorption" type. This reaction is defined to be irreversible, but the code still expects that a corresponding desorption reaction be specified in the last block of text and the line of data below. Since a desorption rate is not needed, these data are not actually used, but placeholder parameters must still be listed to avoid an error in the input routines.

The CFD flow field of the model is shown in Fig. 7.3.1. Driver et al. considered effects, such as shape change, point wise specification of the free stream, and three-dimensional flow in order to obtain better agreement with the measured recession distribution. Here, only the initial (flat) shape of the wedge model was used, and shape change effects were neglected.

We assume that the free stream is uniform at the following conditions: U = 4818 m/s, ρ = 0.00671 kg/m^3, T = 4744 K, T_V = 4535 K, y_{N2} = 0.5107, y_{NO} = 0.0006, y_N = 0.2079, y_O = 0.2172, and y_{Ar} = 0.0636.

The nose piece and lower side of the flow field have a cold, copper wall (350 K) considered to be fully catalytic to atoms, while the back of the upper side is modeled with the finite-rate boundary condition and radiative equilibrium with an emissivity ε = 0.90. The formation of CO as the gas hits the carbon surface is evident in the flow in Fig. 7.3.1(b).

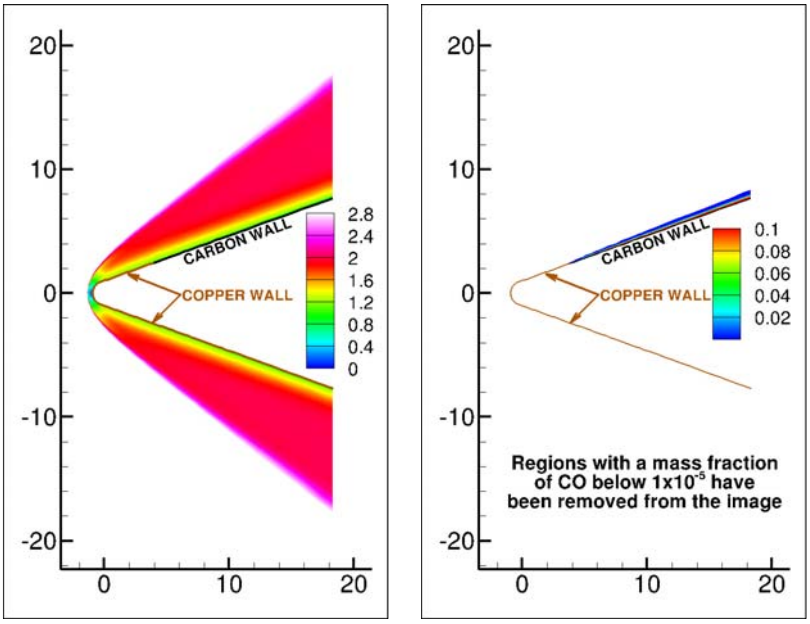

(a) Mach Number **(b) CO Mass Fraction**

Figure 7.3.1. Mach Number and CO Mass Fraction Contours of Wedge Flowfield.

The calculated recession rate on the carbon surface is shown in Fig. 7.3.2(a), which comes from oxidation by atomic oxygen. The blowing rate for this case is compared to the existing hard-wired model that was used by Driver et al.[34] The agreement between the two formulations is exact, since the finite-rate model has been set to replicate the loss efficiencies of all of the reaction processes. Further, we observe that catalysis of nitrogen has only a negligibly small effect on the overall blowing rate, essentially due to the change to the diffusive capacity of the gas at the wall with the change in composition. However, the effect on surface temperature in Fig. 7.3.2(b) is significantly larger, because the catalytic recombination increases it by nominally 200 K along the surface.

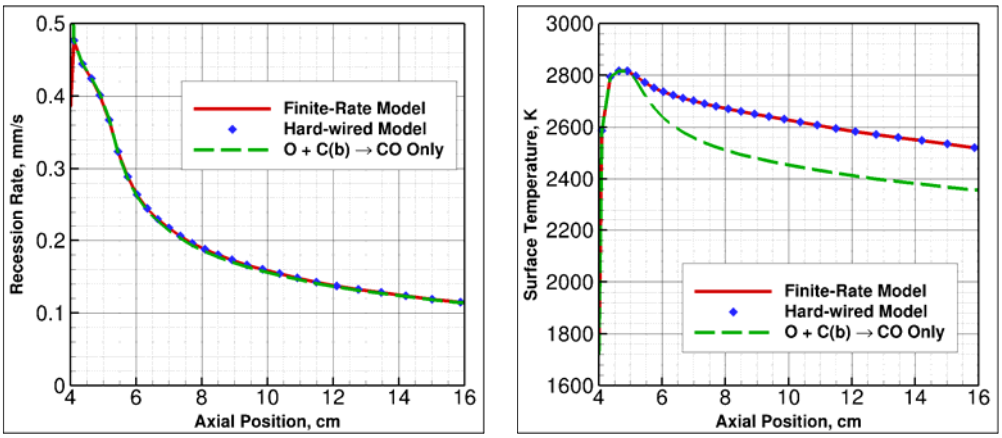

(a) Recession rate **(b) Temperature**

Figure 7.3.2. Surface Recession Rate and Surface Temperature on Carbon Surface.

The atomic mass fractions of oxygen and nitrogen are plotted in Figs. 7.3.3(a) and 7.3.3(b) along the carbon surface, and the effective loss rates have been computed by Eq. (20). As expected, the loss rates are the exact values of 0.9 and 0.05 required from the model. The upstream copper surface has been modeled as fully catalytic to nitrogen, while the carbon surface is only partially catalytic; thus, there is a slight increase in the population of nitrogen atoms as the boundary layer moves onto the carbon wall. The same is true for oxygen atoms, which are fully consumed at the copper wall, but 10% of the diffusing atoms remain on the carbon surface.

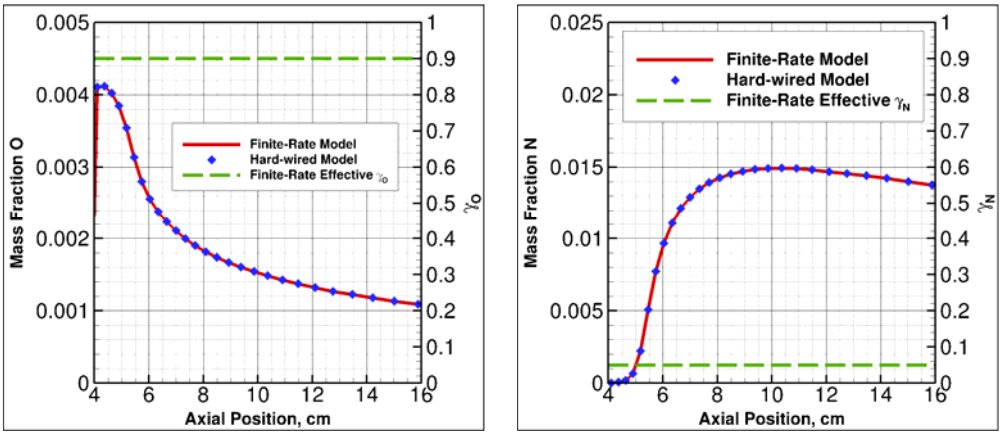

(a) O-atom **(b) N-atom**

Figure 7.3.3. Atom Mass Fraction and Effective Loss Rate.

2) Models of Increased Complexity

Although the model of carbon oxidation assuming a constant loss efficiency of atomic oxygen is simplistic, it has been shown to be effective for this case[34] and in other applications.[36] However, since the finite-rate model that has been implemented in DPLR is capable of modeling more complex surface systems, we have chosen to include results using several popular carbon oxidation models from the literature including the Park model and the Zhluktov and Abe model.[37] Beerman, et al.[38] compare these two models in great detail. The Park model is an extended version of the baseline oxidation model that includes irreversible oxidation by both atomic and molecular oxygen, irreversible nitridation by atomic nitrogen, and C_3-sublimation. The four-reaction model and the associated rates actually come from Chen and Milos,[39] who suggested a model that was loosely inspired by some earlier work of Park;[40] however, this four-reaction model continues to be commonly called "the Park model" in the literature despite the fact that it is not really directly attributable to Park's published work, and we will continue that convention here. The earliest oxidation model actually published by Park[41] is also implemented and will be referred to as the "Park(1976) model." The Zhluktov and Abe model takes full advantage of the new features now in DPLR for modeling finite rate surface chemistry. It makes use of ER, LH, sublimation, adsorption and desorption reactions on the surface and includes a number of adsorbed surface species. The Zhluktov and Abe model is a finite-rate model with 12 defined forward and reverse rates for each process that are thermodynamically constrained. The reaction input files for all three of these models are given below:

File *Park_Carbon_Model3_FF.surf*:

```
  Park Carbon Model with Fiberform Bulk Density
-------------------------------------------------------------------------
Number of surface and bulk phases (gas phase=1 by definition)
nsp, nbp
1    1

Blowing/pyrolyzing gas flows?(0=NO, 1=Yes) Initialization(0=empty sites, 1=QSS)
nblwflag     initsurf
0            0

Number of gas phase species in surface reaction and blowing model
Name      ngps  #Phase
Air6s     6      1

For each surface phase: list  name, surface fraction,
number of active site sets, thermo availability (0=No, 1=Yes)
Name      sfrc       nspas     iThermo    #Phase
Carbon    1.0        1         0          2

For each surface phase with 1 or more sets of active sites, list
the site density and number of species for each active site set
sdenas (mol/m2)      nspass       #phase#sites
7.5d-06              1             2/1

For each bulk phase: list  name, mass density, porosity,
phase volume fraction and number of bulk species
Name      density      porosity     vol. frac.    nbps      #Phase
Carbon     175.0       0.0          1.0           1         5

Order of gas species
Name      Molar mass  Ediss     #Species  Dissociation Reaction
O2        0.03200000  493440.0   1          O2=>O+O
O         0.01600000  0.0        2
N         0.01400800  0.0        3
CO        0.02801100  1071726.0  4          CO=>C+O
CN        0.02601900  745166.0   5          CN=>C+N
C3        0.03603300  1302582.0  6          C3=>C+C+C

Order of surface species (number each consecutively)
Name      Molar mass  Ed              #Species
E(s1)     0.00000000  0.0                 7

Order of bulk species (number each consecutively)
Name      Molar mass  Mole fraction     #Species
C(b1)      0.01201100  1.0                8

Total number of surface reactions
nsrt
5
```

```
Reactant/product species for each forward surface reaction
2, 7, 8, 4, 7, 0         #1   O + (s1) + C(b1) <---> CO + (s1)
1, 7, 8, 4, 7, 0         #2   O2 + 2(s1) +2C(b1) <---> 2CO + 2(s1)
3, 7, 8, 5, 7, 0         #3   N + (s1) +C(b1) <---> CN + (s1)
7, 8, 0, 6, 7, 0         #4   3(s1) + 3C(b1) <---> C3 + 3(s1)
6, 7, 0, 7, 8, 0         #5   C3 + 3(s1) <---> 3(s1) + 3C(b1)

Stoichiometric coefficients for each surface reaction
1, 1, 1, 1, 1, 0         #1   O + (s1) + C(b1) <---> CO + (s1)
1, 2, 2, 2, 2, 0         #2   O2 + 2(s1) +2C(b1) <---> 2CO + 2(s1)
1, 1, 1, 1, 1, 0         #3   N + (s1) +C(b1) <---> CN + (s1)
3, 3, 0, 1, 3, 0         #4   3(s1) + 3C(b1) <---> C3 + 3(s1)
1, 3, 0, 3, 3, 0         #5   C3 + 3(s1) <---> 3(s1) + 3C(b1)

Reaction parameters for each type of reaction:
Type 0: Arrhenius:       0, Cf,         beta, Ea,   isrfon, isrbon
Type 1: Adsorption:            1, S0(0 to 1), beta, Eads, isrfon, isrbon
Type 2: Eley-Rideal:           2, Ger(0 to 1),beta, Eer,  isrfon, isrbon
Type 3: Langmuir-Hinschelwood: 3, Clh(0 to 1),beta, Em,   isrfon, isrbon
Type 4: Sublimation   a0Pv(T)  4, a0Pv0,      beta, Esub, isrfon, isrbon
Type 5: Arrhenius Adsorption:  5, Cf,         beta, Ea,   isrfon, isrbon

2, 0.63d+00, 0.0d+00, 9.6440d+03, 1, 0      #1 O + (s1) + C(b1) <---> CO + (s1)
2, 0.5d+00, 0.0d+00, 0.0000d+00, 1, 0 #2 O2 + 2(s1) +2C(b1) <---> 2CO + 2(s1)
2, 0.3d+00, 0.0d+00, 0.0000d+00, 1, 0 #3 N + (s1) +C(b1) <---> CN + (s1)
4, 5.19d+13, 0.0d+00, 7.7581d+05, 1, 0      #4 3(s1) + 3C(b1) <---> C3 + 3(s1)
2, 1.0d-01, 0.0d+00, 0.0000d+00, 1, 0 #5 C3 + 3(s1) <---> 3(s1) + 3C(b1)

Desorption reaction or equilibrium constant parameters:
Type 1: Desorption:
      Form 0:     Arrhenius
      Form 1:     Constant attempt frequency
        Form 2:   Simple transition state theory
        Form 3:   Complex transition state theory
Type 2: Equilibrium:
      Form 0:     Arrhenius
        Form 1:   Immobile adsorption - simple transition state theory
        Form 2:   Immobile adsorption - complex transition state theory
        Form 3:   Mobile adsorption - simple transition state theory
        Form 4:   Mobile adsorption - complex transition state theory
Type, Form, Cf, eta, vdes, Edes
```

File *Park1976_Carbon_Model3_FF.surf*:

```
  Park(1976) Carbon Model adapted for Fiberform
-------------------------------------------------------------------------
Number of surface and bulk phases (gas phase=1 by definition)
nsp, nbp
2    1

Blowing/pyrolyzing gas flows?(0=NO, 1=Yes) Initialization(0=empty sites, 1=QSS)
nblwflag     initsurf
```

```
0            0

Number of gas phase species in surface reaction and blowing model
Name      ngps  #Phase
Air3s     3      1

For each surface phase: list  name, surface fraction,
number of active site sets, thermo availability (0=No, 1=Yes)
Name      sfrc       nspas     iThermo    #Phase
Carbon1   1.0        1         0          2
Carbon2   1.0        1         0          3

For each surface phase with 1 or more sets of active sites, list
the site density and number of species for each active site set
sdenas (mol/m2)      nspass       #phase#sites
7.5d-06              2             2/1
7.5d-06              1             3/1

For each bulk phase: list  name, mass density, porosity,
phase volume fraction and number of bulk species
Name      density      porosity     vol. frac.    nbps      #Phase
Carbon     175.0       0.0          1.0           1         4

Order of gas species
Name      Molar mass  Ediss     #Species  Dissociation Reaction
O2        0.03200000  493440.0   1          O2=>O+O
O         0.01600000  0.0        2
CO        0.02801100  1071726.0  3          CO=>C+O

Order of surface species (number each consecutively)
Name      Molar mass  Ed              #Species
E(s1)     0.00000000  0.0                 4
O(s1)     0.01600000  350000.0            5
E(s2)     0.00000000  0.0                 6

Order of bulk species (number each consecutively)
Name      Molar mass  Mole fraction     #Species
C(b1)     0.01201100  1.0                7

Total number of surface reactions
nsrt
4

Reactant/product species for each forward surface reaction
1, 6, 7, 3, 2, 6         #1   O2 + (s2) + C(b1) <---> CO + O + (s2)
2, 6, 7, 3, 6, 0         #2   O + (s2) + C(b1) <--->  CO + (s2)
2, 4, 0, 5, 0, 0         #3   O + (s1)  <---> O(s1)
2, 5, 0, 1, 4, 0         #4   O + O(s1) <---> O2 + (s1)

Stoichiometric coefficients for each surface reaction
1, 1, 1, 1, 1, 1         #1   O2 + (s2) + C(b1) <---> CO + O + (s2)
1, 1, 1, 1, 1, 0         #2   O + (s2) + C(b1) <--->  CO + (s2)
```

```
1, 1, 0, 1, 0, 0         #3   O + (s1)  <---> O(s1)
1, 1, 0, 1, 1, 0         #4   O + O(s1) <---> O2 + (s1)

Reaction parameters for each type of reaction:
Type 0: Arrhenius:       0, Cf,         beta, Ea,   isrfon, isrbon
Type 1: Adsorption:            1, S0(0 to 1), beta, Eads, isrfon, isrbon
Type 2: Eley-Rideal:           2, Ger(0 to 1),beta, Eer,  isrfon, isrbon
Type 3: Langmuir-Hinschelwood: 3, Clh(0 to 1),beta, Em,   isrfon, isrbon
Type 4: Sublimation   a0Pv(T)  4, a0Pv0,      beta, Esub, isrfon, isrbon
Type 5: Arrhenius Adsorption:  5, Cf,         beta, Ea,   isrfon, isrbon
Type, Param, beta, E, isrfon, isrbon
2, 0.01d+00,  0.0d+00, 0.0000d+00,  1, 0    #1   O2 + (s2) + C(b1) <---> CO + O +
(s2)
2, 0.63d+00,  0.0d+00, 9.6440d+03,  1, 0    #2   O + (s2) + C(b1) <--->  CO +
(s2)
1, 0.63d+00,  0.0d+00, 9.6440d+03,  1, 0    #3   O + (s1)  <---> O(s1)
2, 0.63d+00,  0.0d+00, 9.6440d+03,  1, 0    #4   O + O(s1) <---> O2 + (s1)

Desorption reaction or equilibrium constant parameters:
Type 1: Desorption:
      Form 0:     Arrhenius
      Form 1:     Constant attempt frequency
        Form 2:   Simple transition state theory
        Form 3:   Complex transition state theory
Type 2: Equilibrium:
      Form 0:     Arrhenius
        Form 1:   Immobile adsorption - simple transition state theory
        Form 2:   Immobile adsorption - complex transition state theory
        Form 3:   Mobile adsorption - simple transition state theory
        Form 4:   Mobile adsorption - complex transition state theory
Type, Form, Cf, eta, vdes, Edes
1, 1, 1.0, 0.0, 1.e12, 350000.0
```

File *ZA_Carbon_Model3_FF.surf*:

```
Z&A Carbon Model with Fiberform Density
-------------------------------------------------------------------------
Number of surface and bulk phases (gas phase=1 by definition)
nsp, nbp
1    1

Blowing/pyrolyzing gas flows?(0=NO, 1=Yes) Initialization(0=empty sites, 1=QSS)
nblwflag     initsurf
0            0

Number of gas phase species participating in surface reactions
Name      ngps  #Phase
CAblZA9s     9      1

For each surface phase: list  name, surface fraction,
number of active site sets, thermo availability (0=NO, 1=YES)
Name      sfrc         nspas      iThermo    #Phase
```

```
CarbonS1    1.0          1         0          2

For each surface phase with 1 or more sets of active sites, list
the site density and number of species for each active site set
sdenas         nspass         #phase/#site
5.812d-05      3                2/1

For each bulk phase: list  name, mass density, porosity,
phase volume fraction and number of bulk species
Name      density       porosity     vol. frac.     nbps      #Phase
CarbonB     175.0          0         1.0             1          3

Order of gas species
Name      Molar mass  Ediss     #Species  Dissociation Reaction
O         0.01600000  0.0        1
N         0.01400800  0.0        2
O2        0.03200000  493440.0   3          O2=>O+O
N2        0.02801600  945000.0   4          N2=>N+N
C         0.01201100  0.0        5
C2        0.02402200  600000.0   6          C=>C+C
C3        0.03603300  1302582.0  7          C3=>C+C+C
CO        0.02801100  1071726.0  8          CO=>C+O
CO2       0.04401100  1600374.0  9          CO2=>C+O+O

Order of surface species (number each consecutively)
Name      Molar mass  Ed              #Species
E(s1)     0.00000000  0.0                10
O(s1)     0.01600000  3.7413d5           11
N(s1)     0.01400800  3.0429d5           12

Order of bulk species (number each consecutively)
Name      Molar mass  Mole fraction     #Species
C(b)      0.01201100  1.0                13

Total number of surface reactions
nsrt
12

Reactant/product species for each forward surface reaction
1, 10, 0, 11, 0, 0             #1   O + E(s1) <---> O(s1)
11, 0, 0, 3, 10, 0             #2   2O(s1) <---> O2 + 2E(s1)
3, 10, 0, 1, 11, 0       #3   O2 + E(s1) <---> O + O(s1)
9, 10, 0, 8, 11, 0       #4   CO2 + E(s1) <---> CO + O(s1)
11, 13, 0, 8, 10, 0            #5   O(s1) + C(b) <---> CO + E(s1)
1, 11, 13, 9, 10, 0            #6   O + O(s1) + C(b) <---> CO2 + E(s1)
11, 13, 0, 9, 10, 0            #7   2O(s1) + C(b) <---> CO2 + 2E(s1)
5, 10, 0, 10, 13, 0            #8   C + E(s1) <---> E(s1) + C(b)
6, 10, 0, 10, 13, 0            #9   C2 + 2E(s1) <---> 2E(s1) + 2C(b)
7, 10, 0, 10, 13, 0            #10  C3 + 3E(s1) <---> 3E(s1) + 3C(b)
2, 10, 0, 12, 0, 0             #11  N + E(s1) <---> N(s1)
4, 10, 0, 2, 12, 0             #12  N2 + E(s1) <---> N + N(s1)
```

```
Stoichiometric coefficients for each surface reaction
1, 1, 0, 1, 0, 0         #1   O + E(s1) <---> O(s1)
2, 0, 0, 1, 2, 0         #2   2O(s1) <---> O2 + 2E(s1)
1, 1, 0, 1, 1, 0         #3   O2 + E(s1) <---> O + O(s1)
1, 1, 0, 1, 1, 0         #4   CO2 + E(s1) <---> CO + O(s1)
1, 1, 0, 1, 1, 0         #5   O(s1) + C(b) <---> CO + E(s1)
1, 1, 1, 1, 1, 0         #6   O + O(s1) + C(b) <---> CO2 + E(s1)
2, 1, 0, 1, 2, 0         #7   2O(s1) + C(b) <---> CO2 + 2E(s1)
1, 1, 0, 1, 1, 0         #8   C + E(s1) <---> E(s1) + C(b)
1, 2, 0, 2, 2, 0         #9   C2 + 2E(s1) <---> 2E(s1) + 2C(b)
1, 3, 0, 3, 3, 0         #10  C3 + 3E(s1) <---> 3E(s1) + 3C(b)
1, 1, 0, 1, 0, 0         #11  N + E(s1) <---> N(s1)
1, 1, 0, 1, 1, 0         #12  N2 + E(s1) <---> N + N(s1)

Reaction parameters for each type of reaction:
Type 0: Arrhenius:       0, Cf,         beta, Ea,   isrfon, isrbon
Type 1: Adsorption:            1, S0(0 to 1), beta, Eads, isrfon, isrbon
Type 2: Eley-Rideal:           2, Ger(0 to 1),beta, Eer,  isrfon, isrbon
Type 3: Langmuir-Hinschelwood:  3, Clh(0 to 1),beta, Em,   isrfon, isrbon
Type 4: Sublimation   a0Pv(T)  4, a0Pv0,      beta, Esub, isrfon, isrbon
Type 5: Arrhenius Adsorption:  5, Cf,         beta, Ea,   isrfon, isrbon

1, 1.d0,      0.0d0, 0.0d0,     1, 1  #1   O + E(s1) <---> O(s1)
0, 3.583d+10, 1.0d0, 2.5607d+5, 1, 1  #2   2O(s1) <---> O2 + 2E(s1)
2, 1.0d0,     0.0d0, 1.1806d+5, 1, 1  #3   O2 + E(s1) <---> O + O(s1)
2, 0.9d0,     0.0d0, 0.0d0,     1, 1  #4   CO2 + E(s1) <---> CO + O(s1)
0, 2.082d+9,  1.0d0, 3.3256d+5, 1, 1  #5   O(s1) + C(b) <---> CO + E(s1)
2, 0.8d0,     0.0d0, 1.663d+4,  1, 1  #6   O + O(s1) + C(b) <-> CO2 + E(s1)
0, 3.583d+14, 1.0d0, 3.3256d+5, 1, 1  #7   2O(s1) + C(b) <---> CO2 + 2E(s1)
2, 0.24d0,    0.0d0, 0.0d0,     1, 1  #8   C + E(s1) <---> E(s1) + C(b)
2, 0.5d0,     0.0d0, 0.0d0,     1, 1  #9   C2 + 2E(s1) <---> 2E(s1) + 2C(b)
2, 0.023d0,   0.0d0, 0.0d0,     1, 1  #10  C3 + 3E(s1) <---> 3E(s1) + 3C(b)
1, 1.0d0,     0.d0,  0.0d0,     1, 1  #11  N + E(s1) <---> N(s1)
2, 1.0d0,     0.d0,  6.3685d+5, 1, 1  #12  N2 + E(s1) <---> N + N(s1)

Desorption reaction or equilibrium constant parameters:
Type 1: Desorption:
      Form 0:     Arrhenius
      Form 1:     Constant attempt frequency
      Form 2:     Simple transition state theory
      Form 3:     Complex transition state theory
Type 2: Equilibrium:
      Form 0:     Arrhenius
      Form 1:     Immobile adsorption - simple transition state theory
      Form 2:     Immobile adsorption - complex transition state theory
      Form 3:     Mobile adsorption - simple transition state theory
      Form 4:     Mobile adsorption - complex transition state theory
Type, Form, Cf, eta, vdes, Edes
2, 3, 1.7206d+4, 0.0d0, 0.d0, 3.7413d+5
2, 3, 1.7206d+4, 0.0d0, 0.d0, 3.0429d+5
```

The recession rate predicted by these three models is compared to the baseline model in Fig. 7.3.4. The Park model predicts a significantly higher recession rate than the baseline model, while the Zhluktov and Abe model predicts a significantly lower recession rate. Noting again that the baseline model accurately predicted the measured recession rate of the experiment when accounting for an accurate free stream distribution and shape change, the differences predicted by the other two models are not desirable.

The Park (1976) model accurately matches the baseline model recession rate in the downstream portion of the surface, but it is more limited upstream by availability of atomic oxygen immediately following the fully catalytic copper surface, as demonstrated by the effective atomic loss efficiency of this model shown in Fig 7.3.5(a). This effect was forecasted to possibly occur downstream of a highly catalytic surface in this situation by Driver, et al.[34]

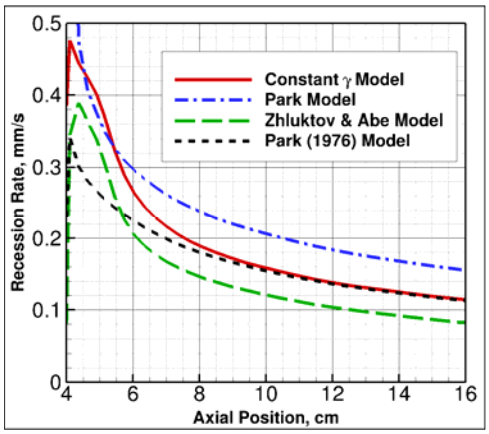

Figure 7.3.4. Surface Recession Rates for Baseline, Park, Park(1976) and Zhluktov and Abe Models.

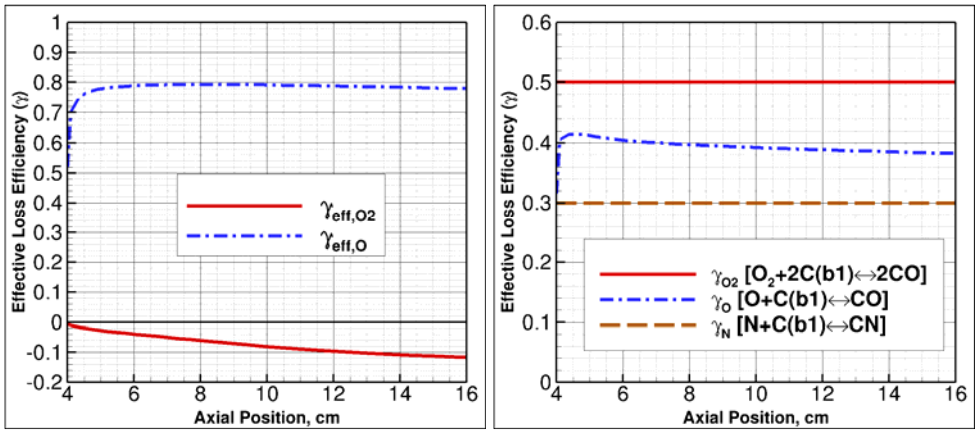

(a) Park(1976) Model **(b) Park Model**

Figure 7.3.5. Effective Loss Efficiencies for the Park(1976) and Park Models.

The reasons for the differences in predicted recession rates between the other models may be more closely examined by looking at the distribution of several gaseous species at the surface.

The effective loss efficiencies for the Park model are shown in Fig. 7.3.5(b). The loss efficiency of molecular oxygen and atomic nitrogen are fixed at 0.5 and 0.3 respectively. In addition, the loss efficiency of atomic oxygen is shown to vary because of the temperature dependence of the expression, but the average is approximately 0.4.

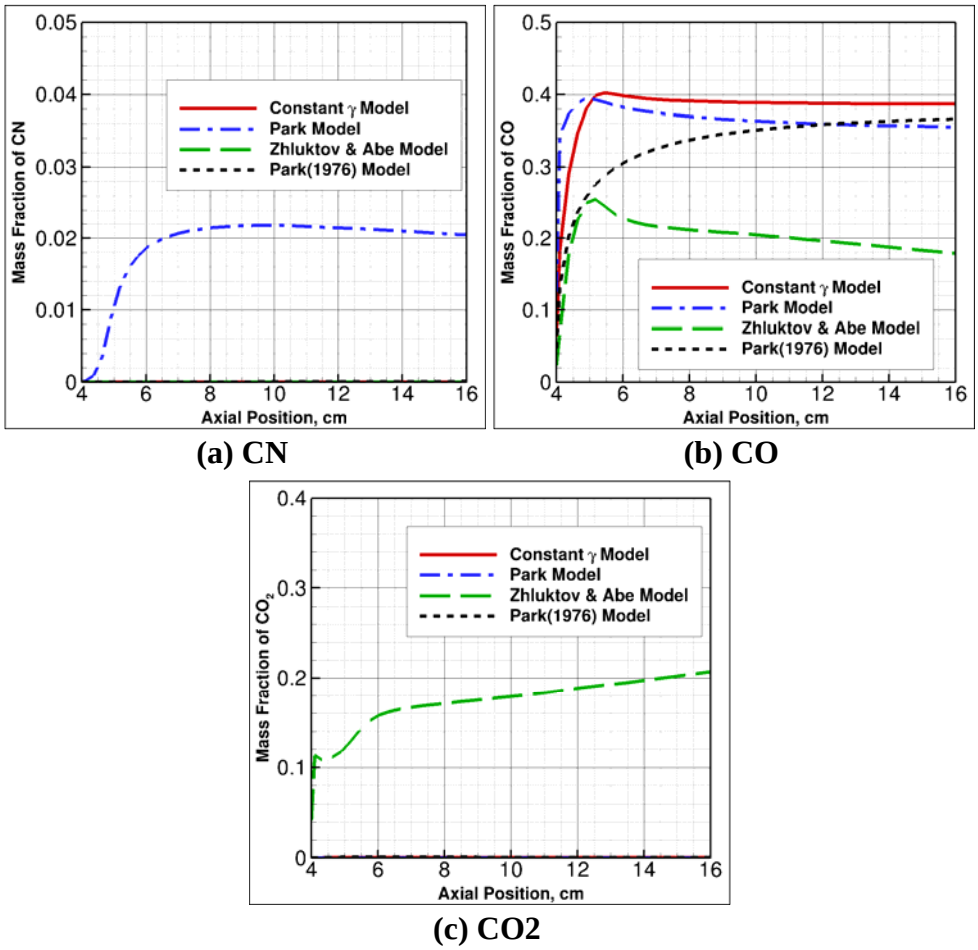

Figure 7.3.6. Surface Mass Fraction Distribution for Baseline, Park, Park(1976) and Zhluktov and Abe Models.

The production of the CN species is shown in Fig. 7.3.6(a). The Park model produces a significant amount of CN, while the other three models do not. Driver, et al.[34] noted as part of their analysis that the production of CN predicted with the nitrogen atomic loss rate of 0.3 from the Park model did not correlate well with similar measurements of recession rate in a pure nitrogen gas. The mass fraction of carbon monoxide shown in Fig. 7.3.6(b) is similar for both the Park and the baseline models, although the Park model produces carbon monoxide through both molecular and atomic oxidation. The total fraction of the diffusing oxygen that is consumed is similar to the baseline model, and it was verified that the change in recession rate is caused primarily by the CN formation reaction through testing the Park model with that reaction turned off.

The production of CO from the Zhluktov and Abe model is significantly lower than the others. The same calculation shows a significant production of carbon dioxide in Fig. 7.3.6(c). Simple stoichiometry dictates that the creation of CO_2 will consume half as much carbon per reacting oxygen atom as the creation of CO. This fact explains why the overall predicted recession rate of the Zhluktov and Abe model is lower than the baseline model. Given the good agreement with arc jet data using the baseline model, it seems that a significant production of either CN or CO_2 is not likely.

The finite-rate model formulation provides a powerful framework to test potential systems to help improve the accuracy of surface reaction rates for applications such as this.

7.4 Ablation of Phenolic Impregnated Carbon Ablator (PICA) in Reacting Air

To demonstrate the addition of pyrolysis gas products to the finite-rate surface model system, a test case published by Driver and MacLean[42] is considered that models reacting air ablating a phenolic impregnated carbon ablator (PICA) surface. The shape that has been considered is a 4-inch diameter "Iso-Q" shape, thus named because it exhibits approximately uniform heat flux and recession rate across the surface.

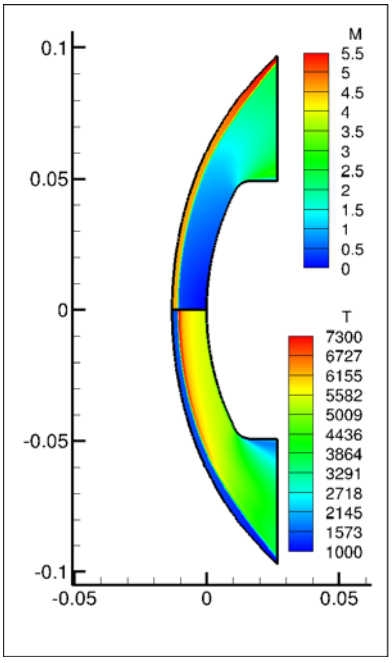

Figure 7.4.1. Mach Number and Temperature Contours of Iso-Q Flowfield.

The predicted recession rates were successfully compared to measurements made in an arcjet facility at nominal free stream conditions of: U = 3860 m/s, ρ = 0.00345 kg/m^3, T = 1470 K, T_V = 1787 K, y_{N2} = 0.7096, y_{O2} = 0.0242, y_{NO} = 0.0202, y_O = 0.1824, y_{Ar} = 0.0636. The flow field

is given in Fig. 7.4.1, in which Mach number contours are shown on the upper half of the figure, and temperature contours are shown on the lower half of the figure.

The surface reaction model is the same as the one used in the previous example of flow over the wedge given in Eq. (7.3.1) and Eq. (7.3.3). In addition to the surface reactions, pyrolysis is modeled via the steady-state pyrolysis approximation, in which the mass of the pyrolysis gas injected from the surface is proportional to the bulk-phase (carbon) loss rate governed by Eq. (1.11.1). The blowing file used to control the steady-state pyrolysis is activated by changing the flag *nblwflag=1* in the *Fiberform_ConstantGamma.surf* file (which was renamed *PICA1506_ConstantGamma.surf* for this purpose), and the associated blowing file is given below.

File *PICA1506_ConstantGamma.blw*:

```
Blowing gas file for PICA1506 (Driver & MacLean 2011-0141)
-----------------------------------------------------------
1     EBC type (0: mdotg (kg/s)) (1: cyield) (2: cyield, ha (J/kg))
0.83682  0.0d0
0.0   O2     <= begin mole fractions for steady state pyrolysis
0.0   N2
0.0   O
0.0   N
0.2   CO      mg(CO) = 0.051*(wB)
0.6   H2      mg(H2) = 0.153*(wB)
0.2   C       mg(C)  = 0.051*(wB)
```

The surface temperature is assumed to be in radiative equilibrium. Driver and MacLean[42] performed a detailed analysis and determined that the char yield for the PICA sample is C_y = 0.83683 with a pyrolysis gas molar composition that is 60% H_2, 20% CO, and 20% C. The use of atomic carbon here is consistent with the approximation made by Driver and MacLean, who noted that after injection C_3 is sufficiently unstable and immediately decomposes in the boundary layer. Thus, atomic carbon is used for simplicity both here and in the referenced analysis.

The predicted unit mass blowing rate from the surface is shown in Fig. 7.4.2. The figure shows multiple solutions. One is without pyrolysis injection, so the blown mass comes purely from the bulk-phase loss rate at the surface. When the pyrolysis injection is included, the overall blowing rate increases as it should. However, the magnitude is somewhat less than the 19.5% increase that might be expected if the pyrolysis is uncoupled by applying Eq. (1.11.3) to the production rate from the bulk-phase-only case. Because additional products are injected into the near-wall boundary layer region, the amount of atomic oxygen that can diffuse to the surface to oxidize the bulk is diluted. The reduction in bulk oxidation, of course, affects the rate of pyrolysis in the steady-state pyrolysis approximation, and the overall effect is non-linear.

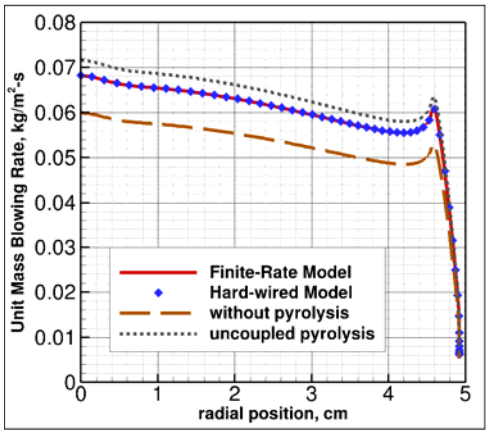

Figure 7.4.2. Unit Blowing Rate Along Iso-Q Surface with Coupled and Uncoupled Pyrolysis Addition.

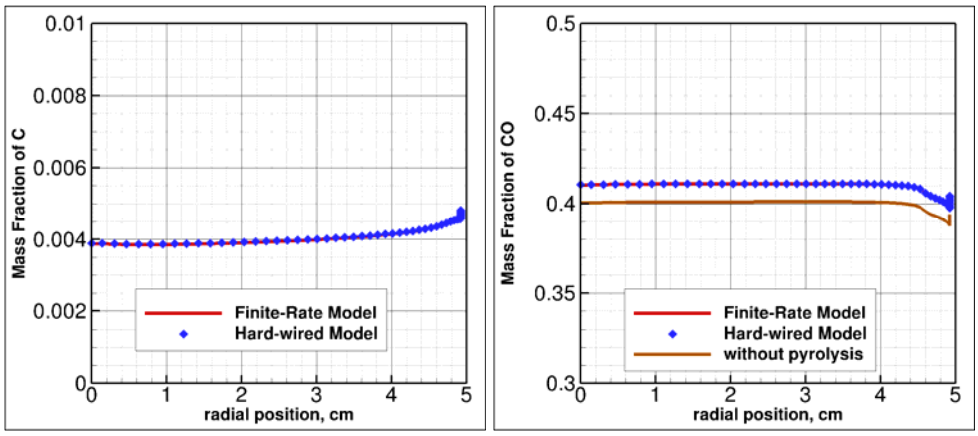

(a) C **(b) CO**

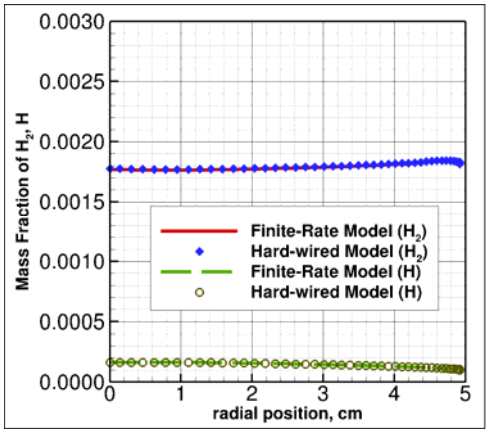

(c) H2 and H

Figure 7.4.3. Unit Blowing Rate Along Iso-Q Surface with Coupled and Uncoupled Pyrolysis Addition.

The mass fractions of the pyrolysis species at the surface are shown in Fig. 7.4.3. Again, the results are compared with the results obtained by Driver and MacLean[42] with the hard-wired surface model. The agreement is also observed to be exact since the generalized finite-rate surface model has been fixed to produce the same result. The relative fractions of the pyrolysis products are not equal to the specified steady-state pyrolysis mass proportionality constants, because the model enforces the ratio of the production rates and not the species concentrations themselves. The production rate controls the mass balance at the surface, but diffusion and convection play a role also. With unequal diffusion of the gaseous species, the effect is somewhat unintuitive.

Table 7.4.1. Terms Computed for Mass Balance at Stagnation Point of Iso-Q Solution

[kgmol/m^2-s] ➔	$+J_k/M_k$	$-\rho_W v_W y_{k,W}/M_k$	$\dot{w}_k$	sum
O	.00476	-.00001	-.00475	$4.52\text{x}10^{-16}$
C(b1)	-	-	-.00475	$-4.75\text{x}10^{-3}$
CO	-.00399	-.00100	.00499	$4.34\text{x}10^{-18}$
C	-.00022	-.00002	.00024	$-3.11\text{x}10^{-16}$
H_2	-.00066	-.00006	.00072	$-1.14\text{x}10^{-16}$

The terms of the mass balance of the converged solution at the stagnation point are given in Table 7.4.1. In addition to showing that mass is properly conserved at the surface for all participating species, the ratio of the molar production rates, $\dot{w}_k$, of the pyrolysis participants should follow the target proportionality assumed for the steady-state pyrolysis model. With the prescribed char yield and pyrolysis gas mole fractions, 1.051 moles of CO, 0.051 moles of C, and 0.153 moles of H_2 are expected for each 1.0 mole of bulk carbon loss. The molar production rates of the participant species are observed to follow exactly these proportions.

The response of the surface with time at the stagnation point has been considered as part of the finite-rate solution. As noted in previous examples, it is useful to monitor the surface coverage while the flow evolves as one metric of convergence. The evolution of the adsorbed nitrogen species concentration is shown in Fig. 7.4.4(a), and its production rate is shown in Fig. 7.4.4(b). The production rate of the surface species decreases to machine zero as the empty surface fills via Eq. (7.3.3). The loss rate of the bulk-phase carbon is shown in Fig. 7.4.4(c). Unlike the surface phase, the production or loss rate of the bulk phase constituents do not tend to zero since the bulk loss rate determines the blowing mass rate in to the gas. However, it does reach a steady-state value, indicating convergence of the solution. The overall convergence of the CFD solver is plotted in Fig. 7.4.4(d) as measured by the L_2-norm of the continuity equation residual. This again emphasizes that the flow and the surface evolve together. The change in the density residual slope after approximately 1,100 iterations indicates the surface has reached a steady-state coverage, and the shock-layer convergence proceeds at a different rate at which the number of nitrogen atoms adsorbing to the surface is equal to the number of those lost due to ER recombination as the interior of the flow finishes its evolution.

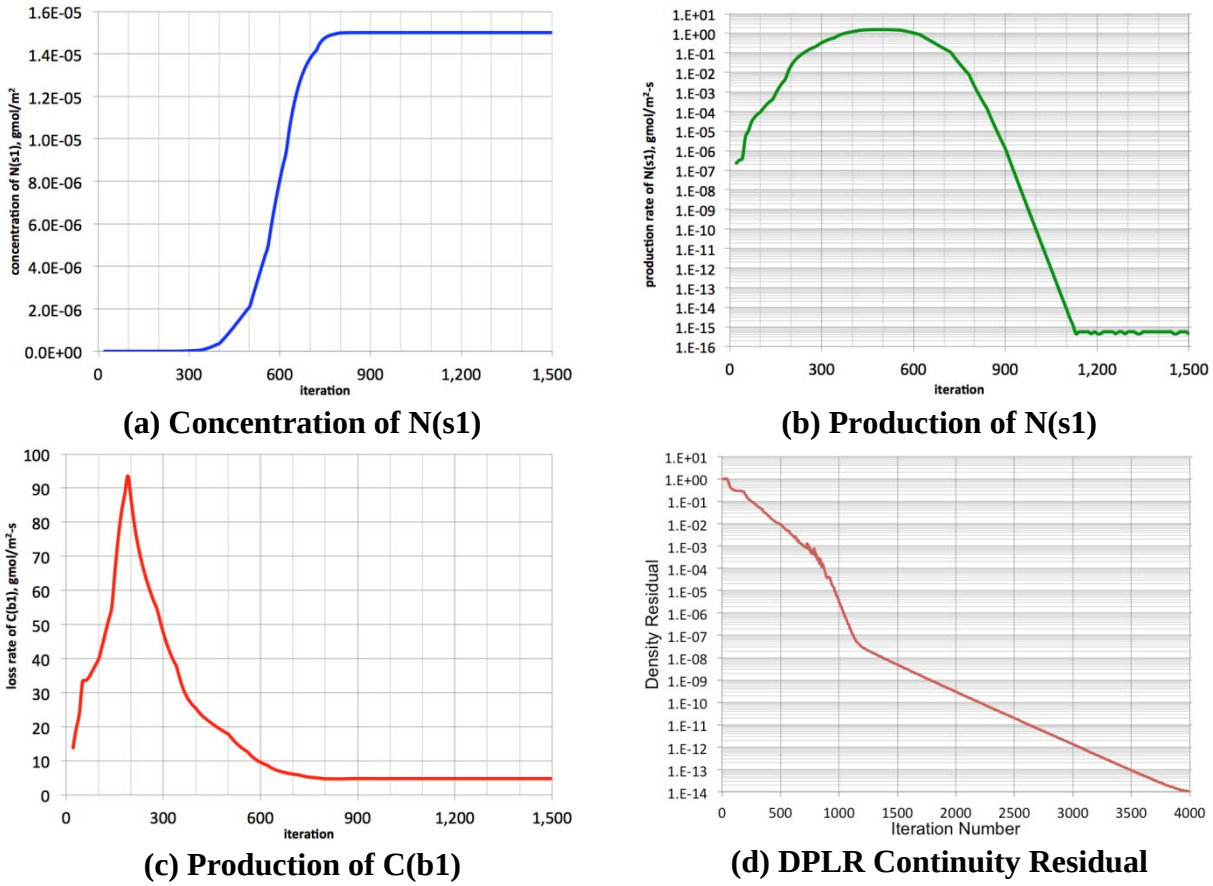

Figure 7.4.4. Surface and Bulk Species Convergence and CFD Continuity Equation Residual.

Finally, the effect of the inclusion of the steady-state energy balance as derived in Eq. (3.1.9) is shown in Fig. 7.4.5. The SSEB is an extension of the common radiative equilibrium boundary condition that accounts for conduction into the ablating surface under the steady-state ablation approximation. The use of the radiative equilibrium boundary condition is the same as a situation in which the virgin enthalpy is equal to the enthalpy of the gas mixture at the wall (and thus the extra term is zero). In this case, the mixture enthalpy blown from the surface using radiative equilibrium is approximately 2.2 MJ/kg as an average.

The surface temperature for the SSEB boundary condition using this value for the virgin enthalpy is shown in Fig. 7.4.5(a) along with the surface temperature from the radiative equilibrium case. The match is excellent, as expected. In addition, several other solutions are shown for virgin enthalpy increments spanning likely values for this type of ablator. Control of the SSEB boundary condition is through a simple modification to the third line of the blowing file as shown below with several increments of the virgin enthalpy by modifying the associated parameter in the fourth line of the file, highlighted in red.

File *PICA1506_ConstantGamma.blw* (modified for SSEB):

```
Blowing gas file for PICA1506 (Driver & MacLean 2011-0141)
-----------------------------------------------------------
2     EBC type (0: mdotg (kg/s)) (1: cyield) (2: cyield, ha (J/kg))
0.83682  -4.4d6
0.0   O2     <= begin mole fractions for steady state pyrolysis
0.0   N2
0.0   O
0.0   N
0.2   CO      mg(CO) = 0.051*(wB)
0.6   H2      mg(H2) = 0.153*(wB)
0.2   C       mg(C)  = 0.051*(wB)
```

The solution with a virgin enthalpy of 0.0 MJ/kg is shown simply as a reminder that, when using the SSEB boundary condition, this choice of virgin material enthalpy does not mean that the term is not active. An ablator with a negative absolute enthalpy results in a decrease in surface temperature relative to radiative equilibrium because of the implied surface conduction. However, all of the predictions for surface blowing rate are shown in Fig. 7.4.5(b), and it is observed that the change in energy balance has no discernable effect on the blowing rate for this model since the oxidation rate chosen for this case is not a function of temperature. For a general finite-rate model with reaction rates that depend on surface temperature, we might expect to see a coupling from this additional term. The use of the steady-state pyrolysis and the steady-state energy balance boundary conditions should result in a solution that is close to a detailed material response analysis undergoing steady-state ablation.

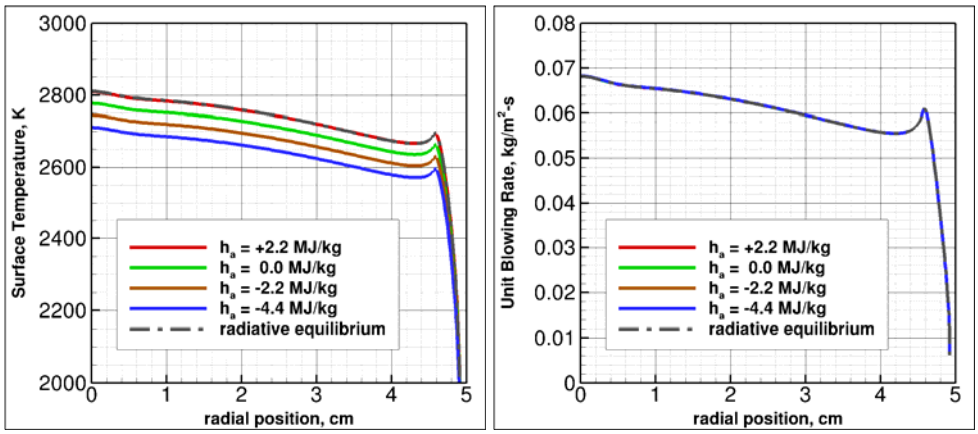

(a) Surface temperature **(b) Surface blowing rate**

Figure 7.4.5. Surface Temperature and Surface Blowing Rate for Iso-Q Case using SSEB Model for Various Virgin Enthalpy Values.

References

[1]Anon., "Surface Chemkin: A Software Package for the Analysis of Heterogeneous Chemical Kinetics at a Solid-Surface - Gas-Phase Interface," SUR-036-1, Reaction Design, San Diego, September 2000.

[2]Coltrin, M., Kee, R.J., and Rupley, F.M., "Surface Chemkin: A Generalized Formalism and Software for Analyzing Heterogeneous Chemical Kinetics at a Gas-Surface Interface," *International Journal of Chemical Kinetics*, Vol. 23, 1991, pp. 1111-1128.

[3]Lefèvre, L., Belmonte, T., and Michel, H., "Modeling of Nitrogen Atom Recombination on Pyrex: Influence of the Vibrationally Excited N_2 Molecules on the Loss Propability of N," *Journal of Applied Physics*, Vol. 87, No. 10, 2000, pp. 7497-7507.

[4]Guerra, V., "Analytical Model of Heterogeneous Atomic Recombination on Silicalike Surface," *IEEE Transactions On Plasma Science*, Vol. 35, No. 5, 2007, pp. 1397-1412.

[5]Thömel, J., Lukkien, J.J., and Chazot, O., "A Multiscale Approach for Building a Mechanism Based Catalysis Model for High Enthalpy CO_2 Flow," AIAA Paper 2007-4399, June 2007.

[6]Christmann, K., *Introduction to Surface Physical Chemistry*, Springer-Verlag, New York, 1991.

[7]Glasstone, S., Laidler, K.J., and Eyring, H., *The Theory of Rate Processes*, McGraw-Hill Book Company, New York, 1941.

[8]Jumper, E.J. and Seward, W.A., "Model of Oxygen Recombination on Reaction-Cured Glass," *Journal of Thermophysics and Heat Transfer*, Vol. 8, 1994, pp. 460-465.

[9]Nasuti, F., Barbato, M., and Bruno, C., "Material-Dependent Catalytic Recombination Modeling for Hypersonic Flows," *Journal of Thermophysics and Heat Transfer*, Vol. 10, No. 1, 1996, pp. 131-136.

[10]Armenise, I., Barbato, M., Capitelli, M., and Kustova, E., "State-to-State Catalytic Models, Kinetics, and Transport in Hypersonic Boundary Layers," *Journal of Thermophysics and Heat Transfer*, Vol. 20, No. 3, 2006, pp. 465-476.

[11]Daiß, A., Frühauf, H.-H., and Messerschmid, E.W., "Chemical Reactions and Thermal Nonequilibrium on Silica Surfaces," in *Molecular Physics and Hypersonic Flows*, edited by M. Capitelli, (Kluwer Academic, Boston, 1996), p. 203-218.

[12]Daiß, A., Frühauf, H.-H., and Messerschmid, E.W., "Modeling of Catalytic Reactions on Silica Surfaces with Consideration of Slip Effects," *Journal of Thermophysics and Heat Transfer*, Vol. 11, No. 3, 1997, pp. 346-352.

[13]Tannehill, J.C., Anderson, D.A., and Pletcher, R.H., *Computational Fluid Mechanics and Heat Transfer, 2nd Edition*, Taylor & Francis, Washington DC, 1997.

[14]Gordon, S. and McBride, B.J., "Computer Program for Calculation of Complex Chemical Equilibrium Compositions and Applications I. Analysis," NASA RP-1311, NASA Lewis Research Center, Cleveland, Ohio, October 1994.

[15]McBride, B.J., Zehe, M.J., and Gordon, S., "NASA Glenn Coefficients for Calculating Thermodynamic Properties of Individual Species," NASA/TP—2002-211556, NASA Glenn Research Center, Cleveland, OH, September 2002.

[16]Wright, M.J., Candler, G.V., and Bose, D., "Data-Parallel Line Relaxation Method for the Navier-Stokes Equations," *AIAA Journal*, Vol. 36, No. 9, 1998, pp. 1603-1609.

[17]Rindal, R.A., Flood, D.T., and Kendall, R.M., "Analytical and Experimental Study of Ablation Materials for Rocket-Engine Application," NASA CR-54757, ITEK Corporation, Palo Alto, May 1966.

[18]Ramshaw, J.D., "Self-Consistent Effective Binary Diffusion in Multicomponent Gas Mixtures," *Journal of Non-Equilibrium Thermodynamics*, Vol. 15, No. 3, 1990, pp. 295-300.

[19]Ramshaw, J.D. and Chang, C.H., "Friction-Weighted Self-Consistent Effective Binary Diffusion Approximation," *Journal of Non-Equilibrium Thermodynamics*, Vol. 21, No. 3, 1996, pp. 223-232.

[20]Sutton, K. and Gnoffo, P.A., "Multi-Component Diffusion with Application to Computational Aerothermodynamics," AIAA Paper 98-2575, June 1998.

[21]Gosse, R. and Candler, G., "Diffusion Flux Modeling: Application to Direct Entry Problems," AIAA Paper 2005-389, January 2005.

[22]Stewart, D.A., "Surface Catalytic Efficiency of Advanced Carbon Carbon Candidate Thermal Protection Materials for SSTO Vehicles," NASA TM-110383, February 1996.

[23]Stewart, D.A., "Surface Catalysis and Characterization of Proposed Candidate TPS for Access-to-Space Vehicles," NASA TM-112206, July 1997.

[24]Gupta, R.N., Lee, K.P., and Scott, C.D., "Aerothermal Study of Mars Pathfinder Aeroshell " *Journal of Spacecraft and Rockets*, Vol. 33, No. 1, 1996, pp. 61-69.

[25]Mitcheltree, R.A. and Gnoffo, P.A., "Wake Flow about the Mars Pathfinder Entry Vehicle," *Journal of Spacecraft and Rockets*, Vol. 32, No. 5, 1995, pp. 771-776.

[26]Afonina, N.E., Gromov, V.G., and Kovalev, V.L., "Catalysis Modeling for Thermal Protection Systems of Vehicles Entering into Martian Atmosphere," AIAA Paper 2001-2832, June 2001.

[27]Marschall, J., Copeland, R.A., Hwang, H.H., and Wright, M.J., "Surface Catalysis Experiments on Metal Surfaces in Oxygen and Carbon Monoxide Mixtures," AIAA Paper 2006-181, January 2006.

[28]Sepka, S., Chen, Y.-K., Marschall, J., and Copeland, R.A., "Experimental Investigation of Surface Reactions in Carbon Monoxide and Oxygen Mixtures," *Journal of Thermophysics and Heat Transfer*, Vol. 14, No. 1, 2000, pp. 45-52.

[29]Sorensen, C. and Schwartzentruber, T., "Sensitivity Analysis of Reaction Rates in a Finite Rate Surface Catalysis Model," AIAA Paper accepted to the 42nd AIAA Thermophysics Conference, Honolulu, HI, June 2011.

[30]Nompelis, I., Drayna, T., and Candler, G., "Development of a Hybrid Unstructured Implicit Solver for the Simulation of Reacting Flows over Complex Geometries," AIAA Paper 2004-2227, July 2004.

[31]Nompelis, I., Drayna, T., and Candler, G., "A Parallel Unstructured Implicit Solver for Hypersonic Reacting Flow Simulation," AIAA Paper 2005-4867, June 2005.

[32]Valentini, P., Schwartzentruber, T.E., and Cozmuta, I., "A Mechanism-Based Finite-Rate Surface Catalysis Model for Simulating Reacting Flows," AIAA Paper 2009-3935, June 2009

[33]MacLean, M., Wadhams, T., Holden, M., and Hollis, B., "Investigation of Blunt Bodies with CO_2 Test Gas including Catalytic Effects," AIAA Paper 2005–4693, June 2005.

[34]Driver, D., Olsen, M., Barnhardt, M., and MacLean, M., "Understanding High Recession Rates of Carbon Ablators Seen in Shear Tests in an Arc Jet," AIAA Paper 2010–1177, January 2010.

[35]MacLean, M., Barnhardt, M., and Wright, M., “Implicit Surface Boundary Conditions for Blowing, Equilibrium Composition, and Diffusion-Limited Oxidation,” AIAA Paper 2010–1179, January 2010.

[36]Titov, E.V., Levin, D.A., Anderson, B.P., Rodriguez, A., and Picetti, D.J., "Simulation of the Stagnation Region Microcrack Growth During Space Shuttle Reentry," *Journal of Thermophysics and Heat Transfer*, Vol. 25, No. 1, 2011, pp. 48-54.

[37]Zhluktov, S.V. and Abe, T., "Viscous Shock-Layer Simulation of Airflow Past Ablating Blunt Body with Carbon Surface," *Journal of Thermophysics and Heat Transfer*, Vol. 13, No. 1, 1999, pp. 50-59.

[38]Beerman, A.F., Lewis, M.J., Starkey, R.P., and Cybyk, B.Z., “Nonequilibrium Surface Interactions Ablation Modeling with the Fully Implicit Ablation and Thermal Response Program,” AIAA Paper 2008-1224, January 2008.

[39]Chen, Y.-K. and Milos, F.S., "Navier-Stokes Solutions with Finite Rate Ablation for Planetary Mission Earth Reentries," *Journal of Spacecraft and Rockets*, Vol. 42, No. 6, 2005, pp. 961-970.

[40]Park, C., "Stagnation-Point Ablation of Carbonaceous Flat Disks - Part I: Theory," *AIAA Journal*, Vol. 21, No. 11, 1983, pp. 1588-1594.

[41]Park, C., "Effects of Atomic Oxygen on Graphite Ablation," *AIAA Journal*, Vol. 14, 1976, pp. 1640-1642.

[42]Driver, D. and MacLean, M., “Improved Predictions of PICA Recession in Arc Jet Shear Tests,” AIAA Paper 2011–0141, January 2011.